Numerical Investigation of the Effect of Vertical Load on the Lateral capacity of Pile in layered Soil

Teressa Chala Hunde

A Thesis Submitted to the Department of Civil Engineering
School of Civil Engineering and Architecture

Presented in Partial Fulfillment of the Requirement for the award of Degree of Masters in Civil Engineering (Geotechnical Engineering).

Office of Graduate Studies
Adama Science and Technology University

November, 2024
Adama, Ethiopia

Numerical Investigation of the Effect of Vertical Load on the Lateral capacity of Pile in layered Soil

Teressa Chala Hunde

Advisor: Argaw Asha (PhD)

A Thesis Submitted to the Department of Civil Engineering
School of Civil Engineering and Architecture

Presented in Partial Fulfillment of the Requirement for the award of Degree of Masters in Civil Engineering (Geotechnical Engineering).

Office of Graduate Studies
Adama Science and Technology University

November, 2024
Adama, Ethiopia

Declaration

I declare that this MSc Thesis entitled "Numerical Investigation of the Effect of Vertical Load on the Lateral capacity of Pile in layered Soil" is my original work and has not been presented for a degree in any other University to any university for similar purpose. The references used in this thesis are duly recognized by proper citations.

Teressa Chala Hunde	______________________	____________________
Name of Student	Signature	Date

Recommendation of Advisors

I, the major advisor of this thesis, hereby certify that I have read the revised version of the thesis entitled "Numerical Investigation of the Effect of Vertical Load on the Lateral capacity of Pile in layered Soil" prepared under my guidance by Teressa Chala submitted in partial fulfillment of the requirement for the award of degree of Master of Science in Civil Engineering (Geotechnical Engineering).Therefore, I recommend the submission of the revised version of the thesis to the department following the applicable procedures.

Argaw Asha (PhD)	________________________	______________________
Major-Advisor	Signature	Date
________________________	________________________	______________________
Co-advisor	Signature	Date

Approval Page of M.Sc. Thesis

I/we, the advisors of the thesis "Numerical Investigation of the Effect of Vertical Load on the Lateral capacity of Pile in layered Soil" developed by Teressa Chala, hereby certify that the recommendation and suggestions made by the board of examiners are appropriately incorporated into the final version of the thesis.

Argaw Asha (PhD)	____________________	_______________
Major-Advisor	Signature	Date

We, the undersigned, members of the Board of Examiners of the thesis by Teressa Chala have read and evaluated the thesis entitled "Numerical Investigation of the Effect of Vertical Load on the Lateral capacity of Pile in layered Soil" and examined the candidate during open defense. This is, therefore, to certify that the thesis is accepted for partial fulfillment of the requirement of the degree of Master of Science in Civil Engineering (Specialization in Geotechnical Engineering).

____________________	____________________	__________________
Chairperson	Signature	Date
____________________	____________________	__________________
Internal -Examiner	Signature	Date
Biruk Gissila (PhD)	____________________	11/11/2024
External -Examiner	Signature	Date

Finally, approval and acceptance of the thesis proposal are contingent upon submission of its final copy to the Office of Postgraduate Studies (OPGS) through the Department Graduate Council (DGC) and School Graduate Committee (SGC).

________________________	____________________	________________
Department Head	Signature	Date
_______________________	____________________	_________________
School Dean	Signature	Date
__________________________	__________________	_______________
Office of Postgraduate Studies, Dean	Signature	Date

Table of Contents

Lists of Figures

Lists of Tables

Abbrevations and Symbols

	Boundary element method,
FEM	Finite Element Method
3D	Three Dimensional
2D	Two Dimensional
P-Y	Horizontal Load verses Deflection
L_C	Critical embedded pile length
LLP	laterally loaded piles
ULS	ultimate limit state method
Es	soil modulus of elasticity
μ_s	Poisson’s ratio of the soil
u	Lateral deflection of pile at point z along the length of the pile
Ep	Pile modulus of elasticity
k_h	horizontal coefficient of subgrade reaction
P	Soil pressure over the pile
D	Pile diameter
Ip	Pile cross section moment of Inertia
Q	Axial load on pile
SPTN	Standard Penetration Test Number
Gc	characteristic soil stiffness
Vult	Vertical Ultimate Capacity

Abstract

The piles in general are designed for vertical and lateral loads acting simultaneously on them. According to the literature, the effects of vertical loads are not so clear on the lateral behaviour of piles due to the scarcity of investigations. In this paper, an attempt has been made to study the effects of vertical loading on the lateral response of a single vertical pile by conducting a series of three-dimensional finite element analyses in Plaxis 3D. The pile was modelled with a linearly elastic material whereas the soil using Mohr-Coulomb constitutive framework. It is seen that for vertical loads larger than 75% of the vertical capacity, both the lateral load and bending moment capacities are reduced. It is observed from analysis result that, for the pile with L/D = 12, the application of vertical load of 75% and 100% reduces the lateral response by 3.3% and 7.2%, respectively, while for an L/D of 30, the application of vertical loading is seen to increase the lateral capacity slightly. The most important result coming out from the interpretation is that a three-dimensional, complete-length finite element analysis is necessary to obtain an appropriate evaluation of the coupled vertical and lateral loading on the lateral response of the piles. This study will prove to be helpful in developing a better insight into the behavior of single pile foundations and will go a long way in assisting the design and analysis of such a structure.

Key Words: Single pile, Finite Element Plaxis 3D, Combined load, Axial pile loading, Mohr Coulomb

5. INTRODUCTION

1.1. Background of the study

Pile foundations are employed for carrying civil engineering structures such as bridges and multistoried buildings when the superficial soil strata are highly compressive and of inadequate strength to carry the load of superstructure; the bed rock is not met at a depth that is considered reasonable below the ground surface; and when the structures are subjected to horizontal forces and need to counteract bending moments in addition to vertical loads. Normally, piles are used where the shallow foundations are believed to show considerable settlement or shear failure. These piles can be designed to carry vertical loading, lateral loading, or any combination of vertical and lateral loading. Due to the complications in examining a pile under combined loading conditions, however, most analyses in today's perspective involve independent analysis of piles for vertical loads in their determination of deformations and settlements, while for their lateral loads, determination of flexural response is applied.

The interaction of the mechanisms of vertical loads on the lateral capacity of piles under combined loadings has not been studied in-depth, and there is scanty literature on this subject. Very little information concerning the subject is available which is obtained from analytical studies, experimental research, and field investigations. If the observation made by (Davisson MT and Robinson KE, 1965), and also by (Goryunov.BF, 1975) is analyzed, at a constant lateral load, lateral deflection of piles shows an increase in their values for the application of vertical loads. This was further expounded upon by (Anagnostopoulos, C., & Georgiadis, M., 1993), who, applying an experimentally validated model tested through two-dimensional finite-element analysis, showed that a state of modified soil stresses and only local volume changes in the soil continuum due to the action of vertical and lateral loads is what is not taken into consideration by the conventional subgrade-reaction models, theories based on elastic half-space, and other two-dimensional techniques. Hence, nonlinear three-dimensional finite-element analysis can be recommended as the most appropriate approach in such analyses. Three-dimensional finite-element analysis for the axial response of piles subjected to lateral loads has been considered by (Trochanis et al., 1991). The behavior of the piles, which are too often poorly designed for lateral loads, under both lateral and vertical loads will thus become more important and relevant to the design engineers. This thesis therefore concentrated on piles under vertical and lateral loads by 3D finite-element analyses. The details related to the numerical model, the validation of the developed model with field test cases, and the results from the analysis will be presented in the paper.

1.2. Statement of the Problem

Addis Ababa is a fast-growing city in number and construction activities, which aimed at providing accessible roads, transportation, and construction of multi-story buildings for residence and business purposes. This increase the need for piles foundation, which is used to support combined loads that result effect the settlement and deflection of pile. The lateral resistance of piles under combined load has been studied numerically by several researchers. They have revealed contradictory findings, which is very likely to be caused by soil type, modelling assumptions, constitutive laws, relative load magnitude, pile slenderness, boundary conditions, and other considerations such as load application sequence. No general agreement has been drawn on whether vertical load increases or reduces subsequent lateral displacement under lateral load.

The behavior of piles especially installed in silty-clay geologic deposits in the study area under combined load needs to be clarified. To see the influence of vertical load on the soil-pile interaction, analysis, and parametric study is important. Therefore, these significance needs to be carried out in study.

1.3. Research questions

- What is the impact of vertical load on the lateral load capacity of a single pile?
- How do vertical and horizontal deformations, as well as bending moments, vary in a pile subjected to combined vertical and lateral loads?
- How does the pile slenderness ratio affect the performance of a single pile under combined vertical and lateral loading?

1.4. Objective

1.4.1. General Objective

The general objective of this study is to investigate the effect of vertical load on the lateral capacity of a single pile by analyzing soil-pile interaction in layered soils using Plaxis 3D finite element software.

1.4.2. Specific Objective

The specific objectives of this research work are:

- ❖ To evaluate the effects of vertical load on the lateral load capacity of a single pile.
- ❖ To analyze vertical and horizontal deformations, as well as bending moments in a pile under combined loading.
- ❖ To investigate the influence of the pile slenderness ratio on the behavior of a single pile subjected to combined vertical and lateral loads.

1.5. Significance of The Study

The results of this study will have a great importance on ever-growing building infrastructures and high-rise buildings in Ethiopia, especially for those constructed in Addis Ababa. This study presents the three-dimensional finite element analysis and provides an interaction-based design method for the analysis and design of pile foundation. Numerical investigation of the effect of vertical load on the lateral capacity of single pile is nice approach for checking the stability of soil and structures in short time by software. These will reduce costs used in field test and uses for preliminary designs.

1.6. Limitation and Scope of the Study

The subsurface profile of the site and the engineering properties of the layered soil of Addis Ababa, Kirkos sub city around Mexico Square specific for Bank of Abyssinia Mexico Square Branch Building 3B+G+20 project was constructed was used.

For the case of study, only the parametric study for proposed was taken, and the finite element modeling and analyzing soil-structure interaction will be investigated the effect of vertical load on lateral capacity of single pile. The effect of lateral load eccentricity, effect of water, the effect of dynamic loads are not in this scope.

The scope of this thesis work is limited to the following features:

- ❖ In all cases considered, the pile was embedded in non-homogeneous dry Silt-clay and was assumed to be fully drained
- ❖ The nature of loading considered is only static loading.
- ❖ Pile slender ration is used as parametric study.

1.7. Organization of the Thesis

The thesis has six chapters. The first chapter describes some information on the title and the main task of this work. A literature review would be presented in chapter two. Chapter three labels research methodology. The fourth chapter outlines the different parameters and numerical modeling validation analysis done. Chapter 5 outlines the results and discussion from parametric study. Moreover, chapter six summarizes the work of previous chapters and gives general conclusion and recommendation for possible future work.

6. Review of Related Literatures

2.1. Introduction

Deep foundations become necessary when the soil from shallow depth is not adequate to take up the structural loads. The main purposes of pile foundations are to transfer superstructure loads on deeper load-bearing strata, resist lateral, vertical, and uplift loads, and minimize settlement. The ground beneath a structure's base seldom has adequate bearing capacity to resist the designed structural load; hence, the structure can be founded on piles. Where site investigation results reveal that unstable soil is at a shallow depth or the calculated settlement exceeds the acceptable limits, a pile foundation shall be adopted.

Pile analysis under lateral and vertical loading becomes really complicated because the soil reaction depends upon the pile movement, whereas it is again related to the soil response and superstructure load. Thus, the problem becomes one of the soil-structure interactions. The introduction of other piles in the neighborhood, or stated otherwise, making a pile group consideration introduces additional complexity due to pile-soil interaction, along with the physical implications of the group geometry. Further modification may be done for construction issues, like the actual conduction process, not to mention other factors that could affect the lateral capacity of the pile, such as pile head fixity (Basu et al., 2008).

In response to these varied issues, a fundamental framework of mathematical models augmented by empirical rules has developed (Fleming et al., 2009) and (Basu et al., 2008). Single pile behavior has made a fundamental contribution to the above understanding, with the latter helping point out general problems of pile-soil interaction, while providing a benchmark from which group behavior can be evaluated. Single pile behavior and load transfer to it will be reviewed in this section. Proper understanding of the load transfer mechanisms for piles is essential for analysis and design. Piles transfer axial and lateral loads by different mechanisms. In the case of axial (vertical) loads, piles may be looked upon as axially loaded columns; they transfer loads to the ground by shaft friction and base resistance Figure 2.1. As a pile is axially loaded it settles somewhat, and the soil mass surrounding the pile resists the downward movement. Because soil is a frictional material frictional forces develop at the interface of the pile shaft and the surrounding soil that oppose the downward pile movement. Normally, engineers would prefer to design end-bearing piles since the base resistance is more reliable compared to shaft friction. But where such a layer is not available at a particular site, engineers have to rely on only shaft friction in which case the pile is known as a floating pile.

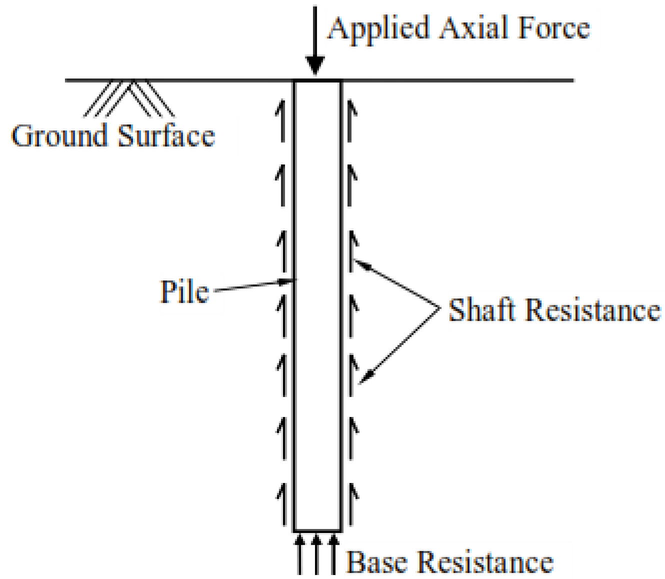

Figure 6.1: Load Transfer Mechanism of Axially Loaded Piles after (Basu et al., 2008).

In the case of lateral loads, piles are said to act as beams under transverse loading. The piles transfer the lateral load to the surrounding soil mass using the lateral resistance of the soil Figure 2.2. When a pile is loaded laterally, a part or whole of the pile tries to shift horizontally in the direction of the applied load, causing bending, rotation, or translation of the pile (Fleming et al., 2009) and (Basu et al., 2008). It tends to push the soil in front of it or the soil mass lying in the direction of the applied load, thus developing compressive and shear stresses and strains in the soil opposing the pile movement-this is the primary mechanism of load transfer for lateral loads.

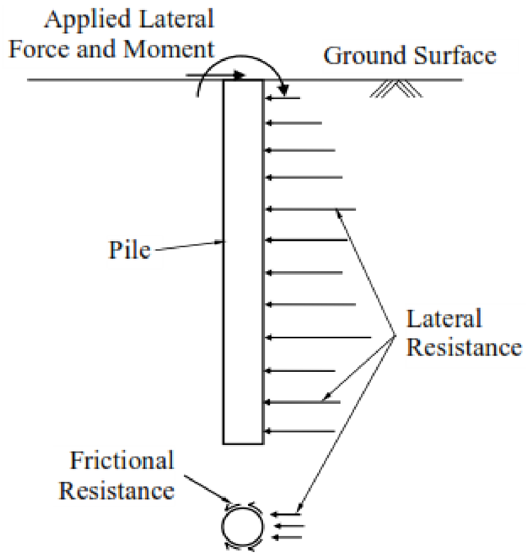

Figure 6.2: Load Transfer Mechanism of Laterally Loaded Piles (Basu et al., 2008)

In many instances, the load acting on a superstructure exceeds the capacity of a single pile. Quite many research studies can be found in the literature that present several different methods of analyzing the laterally loaded piles. These may be presented, in general, under the following broad categories: (a) the ultimate limit state method (ULS); (b) the subgrade reaction approach; (c) the continuum method; and (d) the finite element method, FEM. Methods associated with the ultimate limit state, ULS, provide the maximum lateral load a pile can carry. Approaches in the subgrade reaction approach are utilized to calculate the allowable lateral pile deflection, i.e. serviceability limit states, assuming that the soil is represented by a series of linear or nonlinear springs. On the other hand, continuum approach is also used to obtain the allowable lateral displacement, however, idealization of the soil is presented as a linear elastic infinite stratum. Basically, the two major ways in continuum approach include the boundary element method, BEM, and the simplified continuum models; finite element method, FEM is a numerical technique which is based on a continuum approach concept. Generally, it can handle the complication brought about by the loading as well as the soil boundary conditions. This paper has presented a critical review of the research dealing with the analysis methods of laterally loaded single piles under vertical loading.

2.2. p-y Curve Method

The p-y curve method relates the nonlinear behavior between the soil resistance *(p)* and the lateral pile deflection *(y)*. The plot of the *p* and *y* variables at depth is called the p-y curve, (Haiderali and Madabhushi, 2016). The *p-y* curves are derived and validated by performing field tests on fully instrumented piles. In 1950s, the full-scale testing for laterally loaded piles was possible because of two main developments at that time: (a) the availability of digital computers and, (b) the ability for remotely reading the strain gauges to obtain the soil response, (Lymon C.Reese and William F.Van Impe, 2011). The method implicitly accounted for the soil continuity and the nonlinearity of the pile-soil system; however, its main shortcoming is that the p-y curve is unique for a particular soil and pile properties, (Horvath and Colasanti, 2011). Owing to the popularity of the p-y curve method and its reasonable results, it was suggested to be used in engineering practice by (API, 1987 and 2007). Furthermore, (FHWA, 2011) recommended the use of LPILE or FBPIER software that use the p-y curve method, in the analysis of laterally loaded piles, (Favaretti et al., 2015).

2.3. Continuum Method

In the continuum approach, the assumption of modeling the soil by linear or nonlinear springs is replaced by a more appealing and realistic representation. The soil is represented by an infinite, linear and elastic medium and its behavior is described by the deflection along the vertical soil profile, (P.Kavitha, K.Beena and K.Narayanan, 2016). However, this approach is hard to be used by the engineers in practice due to its mathematical complication. The works in this field and they are grouped in two main categories: (a) the boundary element method (BEM), and (b) the simplified continuum models.

2.3.1. Boundary Element Method (BEM)

The early work on BEM for laterally loaded piles goes back to (D.Douglas and E.Davis, 1964) who introduced a simple theory for a laterally applied load and a moment on the top of a thin vertical plate buried in elastic media. The mathematical theory for the proposed method included two steps: (a) the integration of the (R.D.Mindlin, 1936) equation for a horizontal displacement induced by a lateral point load within a semi-infinite mass, and (b) the calculation of the distributed normal stress by employing a numerical solution. In addition, it was assumed that the plate is perfectly smooth and the adhesion between the plate and the soil is neglected. Similarly, (W.R.Spillers and R.D.Stoll, 1964) proposed a simplified theoretical solution based on BEM by introducing a limiting lateral pressure value for the soil-pile interaction to account for the soil nonlinearity for a pile in both elastic half-space and plastic half space.

(H.G.Poulos, 1971a,b), utilized the previous work and contributed significantly in this field. The author introduced the stress for single and group pile-soil system using the BEM with various boundary conditions at the top and bottom of the pile. The pile was modelled as a thin rectangular strip, which interacted with an ideal linearly elastic media. As shown in Fig. 2.3, the pile was divided into equal segment lengths, except at the top and bottom of the pile. The response of the soil-pile interaction system was calculated by considering an applied normal uniformly distributed load on each pile segment, whereas, the shear stress at the interface of the pile sides was neglected. Further, the horizontal displacement at each segment can be calculated by equating the displacements of the pile and soil at the center of each segment. In this process, the soil horizontal displacement was calculated through the (R.D.Mindlin, 1936) equation, while the pile deflection was calculated by the differential equation, which is expressed as a finite difference expression for bending of a thin beam. (H.G.Poulos, 1973), had improved his model by considering the soil yielding and nonlinearity, i.e. the elastic-perfectly plastic soil behavior.

Moreover, (P.K.Banerjee and T.G Davis, 1978) used the BEM to analyze the laterally loaded piles in a two-layered elastic half space system with soil modulus that is linearly increasing with depth. The results of the proposed theory were compared with the behavior from full-scale tests; they showed that their method could provide a more rigorous prediction of the response, due to the linear variation of soil modulus. Thereafter, (T.Davies and M.Budhu, 1986), (M.Budhu and T.G.Davies, 1987,1988) extended the linear algorithm of (P.K.Banerjee and T.G Davis, 1978) to account for the nonlinear behavior of laterally loaded piles embedded in over consolidated clays, cohesion less soils and soft clays. The soils were modelled as linear elastic at small strains, while the soil plastic behavior was considered when the soil pressure at the pile surface was equal to certain values.

(M.F.Randolph, 1981) Introduced the concept of characteristic soil stiffness (Gc) which the average of soil stiffness over the critical length of the pile. In his parametric study, the deflection, moment and shear for laterally loaded piles were insignificant after certain depth, which was smaller than the actual pile length, measured from the pile head. Therefore, in his analysis, he considered the use of critical depth (lc) for a pile embedded in ideal elastic half-space.

2.3.2. Finite Element Method (FEM)

The FEM method is a mathematical technique used to calculate an approximate solution to the partial differential equations based on the continuum theory. (C.Desai and G.Appel, 1976) Started the early work on the 3D FEM by proposing a general finite element procedure to study the behavior of laterally loaded piles and their interaction with the soil. The soil behavior was assumed to be linear-elastic and the pile was modelled as a 1D beam element. The interaction between the pile and the soil was modelled using a thin-layer element, which was capable to consider different modes of deformations, e.g. stick mode, gapping or slippage. It was found that the use of the interface element considerably affected the pile-head displacements. (M.Faruque and C.Desai, 1982) Included the material and geometric nonlinearity in their 3D finite element model for axially and laterally loaded piles. The soil nonlinear stress-strain relation was modelled with the Drucker Prager plasticity theory. The authors concluded that the geometric nonlinearity had a significant effect on the analysis of pile-soil interaction.

(D.A.Brown,M. Kumar,et al., 1989)developed p-y curves by creating 3D finite element models in ABAQUS considering elastoplastic behavior for the soil. The p-y curves and the field results were not in a good agreement due to the simplicity of the soil model. However, (D.A. Brown and C.F. Shie, 1990,1991), concluded that the 3D finite element models are an effective tool to capture the 3D the interaction between the piles and the soil, the soil nonlinearity, the variation of the soil strength with depth, and the interface friction. The model for the interface frictional element accounted for two soil constitutive laws, i.e. a simple elastic-plastic model with a Von Mises yield surface and an extended Drucker-Prager model with non-associated flow. The p-y curves were in good agreement with those obtained from the COM624 program. Additionally, the authors recommended the FEM for the evaluation of the factors influencing the behavior of the laterally loaded piles.

(A.M.Trochanis, J.Bielak and P.Christiano, 1991), who studied the nonlinearity in pile-soil interaction for axially and laterally loaded piles presented another important work. Their soil constitutive models included a linear elastic and a Drucker–Prager model. The pile was modelled as a 1D-beam element and a special 2D interface element was used to capture the pile-soil interaction. The interface element was characterized by a friction coefficient, its geometry and an elastic stiffness. The main findings of this study were the factors that affect significantly the axially and laterally loaded piles which are the interface slippage and gap formation, respectively.

(J.R.Peng, M.Rouainia,and B.Clarke, 2010), investigated the effect of fin dimensions on the lateral capacity of the pile in sand. The Mohr-Coulomb constitutive model was used in the numerical analysis using the software PLAXIS-3D. The sand was assumed to be a linear elastic perfectly plastic and the soil Young’s modulus was assumed to increase linearly.

2.4. Ultimate Lateral Resistance

Structures on pile foundations may be subjected to lateral forces and movements because of ship impact and wave action in harbor and offshore structures, retaining walls, high wind forces in transmission-tower foundations, and lateral accelerations acting on structures in earthquake zones. Therefore, one key issue for pile design may be estimation of the ultimate lateral resistance. Various methods have been proposed to estimate the ultimate lateral load capacity Hu ((B.Hansen, 1961), (B.B.Broms, 1964a, b, 1965). One of the most popular methods for estimating Hu is Broms' method (Lee et al., 2010). For unrestrained or free-headed piles, (B.B.Broms, 1964a, b, 1965) assumed that the ultimate soil resistance is equal to three times the passive Rankine earth pressure (H.G.Poulos and E.H.Davis, 1980).

A horizontal load test was carried out on a pile consists of placing two piles at some distance from each other and either pulling them toward each other or pushing them apart. The resulting load displacement curve for one pile gives the horizontal load Ho versus the horizontal displacement y_o (Figure 2.3). From this curve, an ultimate load can be defined as the horizontal load Ho corresponding to a displacement equal to one-tenth of the pile diameter (B/10) (Briaud, 2013).

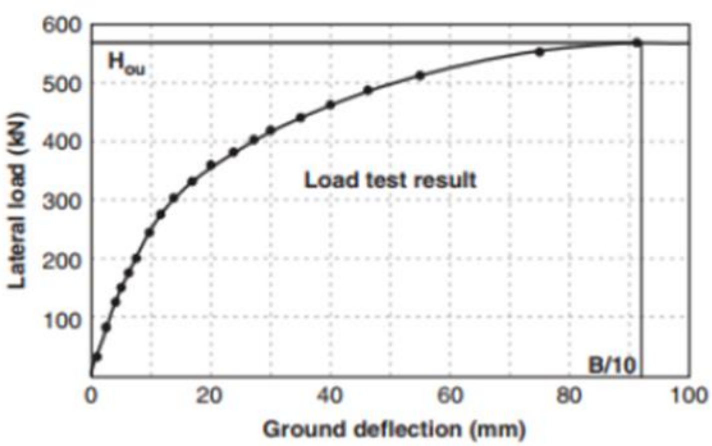

Figure 6.3: Load test result *(Briaud, 2013)*

In addition, in finite element method the control factor in evaluating the ultimate lateral load capacity of the piles is the yield of the maximum allowed lateral displacement at the pile head that is taken to be 10% of the pile diameter as it is more compliant with the design criterion (ASTM STP-835, 1983 and USACE, 1998).

According to British Standard as recommended in BS EN 1997-1:2004+A1:2013, 7.6.1.1(3), the ultimate horizontal load measured at deflection equal to 10% of the pile's diameter when it is difficult to define the ultimate limit state from the loading deflection curve.

2.5. Constitutive Models

Soil is a complicated material that behaves non-linearly and often shows anisotropic and time dependent behavior when subjected to stresses. Generally, soil behaves differently in primary loading, unloading and reloading. It exhibits non-linear behavior well below the failure condition with stress dependent stiffness. Soil undergoes plastic deformation and is inconsistent in dilatancy and experiences small strain stiffness at very low strains and upon stress reversal. In addition to soil behavior, its failure in three-dimensional state of stress is extremely complicated. Numerous criteria have been devised to explain the condition for failure of a material under such loading state.

In the finite element analysis, reliable predictions can be achieved by using an appropriate constitutive model for a particular geotechnical problem. In general, the criterion for the soil model evaluation should always be a balance between the requirements from the continuum mechanics aspect, the requirements of realistic representation of soil behavior from the laboratory testing aspect, convenience of parameter derivation and simplicity in computational application. The application of some constitutive models in Plaxis finite element model are briefly discussed below used for this study.

2.5.1. Linear Elastic Model

The use of the linear elastic model is quite common to model massive structures in the soil or bedrock layers that include piles and so on (R.B.J. Brinkgreve and W. Broere, 2006). This model represents Hooke's law of isotropic linear elasticity used for modelling the stress–strain relationship of the pile material. Linear elastic constitutive model is probably the most common model used to approximate the stress-strain relationship of materials. Linear elastic models involve two elastic stiffness parameters namely Young's modulus (E) and Poisson's ratio (ν). The linear elastic model is not suitable to model soil because soil behavior is highly nonlinear and irreversible, but it is appropriate to model stiff volumes in soil like concrete structures.

2.5.2 Mohr Coulomb Model

The Mohr Coulomb Model is a linear elastic and perfectly plastic model. It involves five parameters, both elastic and plastic behavior parameters i.e. Young's modulus (E) and Poisson's ratio (v) for soil elasticity, friction angle (ϕ) and cohesion(c), for soil plasticity and the dilatancy angle (ψ).

The stiffness behavior below the failure line is assumed to be linear elastic according to Hook's law. Hence, the model does not accurately predict deformation behavior before failure, especially in situation where the stress levels are changing or multiple different stresses paths are allowed. However, the model does not show softening behavior after peak strength. Soft soils like normally consolidated clays, generally show a decreasing mean effective stress during undrained shearing, whereas the Mohr-Coulomb's model would predict a constant mean effective stress in this case, which results in an over prediction of the shear strength (Plaxis 3D Manual,2020) (R.B.J. Brinkgreve and W. Broere, 2006).

The soil in the problems of this paper is modeled as elastic-plastic material. The basic principle of elasto-plasticity is that strains and strain rates are decomposed into an elastic part and plastic part as shown in Figure 2.4.

Hooke's law is used to relate the stress rates to the elastic strain rates. According to the classical theory of plasticity, plastic strain rates are proportional to the derivative of the yield function with respect to the stresses. This means that the plastic strain rates can be represented as vectors perpendicular to the yield surface. This classical form of the theory is referred to as associated plasticity. However, for Mohr-Coulomb type yield functions, the theory of associated plasticity overestimates dilatancy (Plaxis 3D Manual, 2020) (R.B.J. Brinkgreve and W. Broere, 2006).

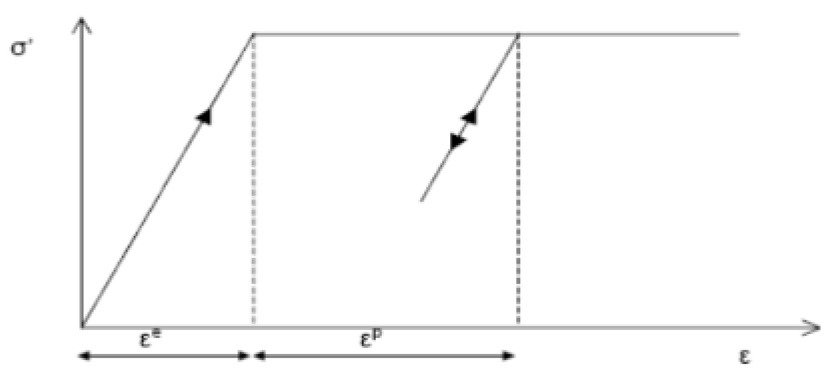

Figure 6.4: Basic idea of an elastic perfectly plastic model *(R.B.J. Brinkgreve and W. Broere, 2006)*

The Mohr-Coulomb yield condition is an extension of Coulomb's friction law to general states of stress. In fact, this condition ensures that Coulomb's friction law is obeyed in any plane within a material element. The full Mohr-Coulomb yield condition consists of six yield functions when formulated in terms of principal stresses and six plastic potential functions (Plaxis 3D Manual, 2020) (R.B.J. Brinkgreve and W. Broere, 2006).

The two plastic model parameters appearing in the yield functions are the well-known friction angle ϕ and the cohesion c. The plastic potential functions contain a third plasticity parameter, the dilatancy angle ψ. This parameter is required to model positive plastic volumetric strain increments (dilatancy) as actually observed for dense soils. For stress states within the yield surface, the behavior is elastic and obeys Hooke's law isotropic linear elasticity, as discussed above (Plaxis 3D Manual, 2020) (R.B.J. Brinkgreve and W. Broere, 2006).

2.6. The influence of vertical load on the lateral response in clay

The vertical and horizontal behavior for piles is today most often analyzed separately. Like the p-y curves for pure lateral loading of piles, the vertical displacement is characterized by t-z curves for vertical loading. Both the p-y and t-z curves are uncoupled, and therefore the soil reactions in the one direction are considered uncoupled from the other direction, and interaction effects are neglected.

As the vertical load is most often small compared to the vertical capacity, the lateral capacity is most often governing in design. Some studies have been conducted to investigate the effect the static vertical and lateral loading on the lateral pile response. (Anagnostopoulos, C., & Georgiadis, M., 1993) ; (Hazzar et.l, 2017) and (Karthigeyan et.l, 2007) have investigated this effect, and their results will be discussed.

2.6.1. Existing studies

(Anagnostopoulos, C., & Georgiadis, M., 1993) investigated effects of lateral loading on axial pile displacement and stresses experimentally, and the effects of axial loading on lateral pile response. Six model tests were performed on close ended piles with a diameter of 19mm, a wall thickness of 1.5mm, and a length of 500mm. This results in a slenderness ratio of L/D=26. The soil tested was soft laboratory-prepared clay, with su=kPa. The findings from the study concluded with a rather limited effect of axial loading on the lateral pile response. Nevertheless, conventional methods assume no interaction between the axial and lateral load, and the methods are, therefore, not able to capture the interaction between the axial and lateral pile response. Based on the study, a non-linear three-dimensional finite element method is recommended for analyzing the effect of the combined vertical and lateral loads.

(Karthigeyan et al.,2007**)** investigated the effect of piles subjected to both vertical and lateral loads through a series of 3D finite element analyses. The pile was modelled as a linear elastic material with a varying square cross-section. The Von Mises constitutive model with associated flow rule was used for analyzing homogeneous clayey soil profiles. For clayey soils, the effect of vertical loads on the lateral capacity was marginally reduced for piles with up to 60% of the vertical capacity utilized. For higher vertical loads the lateral capacities were reduced by as much as 20%. The effect of the pile slenderness ratio was also investigated by increasing the length of the pile. The results indicate that the effect of vertical load decreases for increasing slenderness ratio. For slenderness ratios larger than L/D=16, the influence of vertical load was found to be constant, and the effect of vertical loads was found to be limited. For longer piles, the reduction in lateral capacity can be expected to decrease. The findings from the study highlight the importance of the effect of vertical load on the lateral response.

(Hazzar et al., 2017) analyzed the influence of vertical loads on the lateral pile response through a series of 3D finite differences analyses. The lateral capacities and bending moments were evaluated. The models were verified with full-scale load and laboratory model testing data. The soil was idealized with the Mohr-Coulomb constitutive model with a non-associated flow rule. Three clayey soil profiles were analyzed, one with a varying shear modulus, G=300su, one with a constant shear modulus, G=38.5MPa, and one with two-layered strata. Several cases with different undrained shear strength, su, were considered for the clayey soil profile with a varying shear modulus. For an undrained shear strength below su<16kPa, there was no effect of vertical load on the lateral response. Further-more, the model with a constant undrained shear strength was compared to a model with increasing undrained shear strength. The results indicate a significant difference in lateral load-deflection between the two models, and the study indicates that the lateral load-deflection is depending on the variation of the undrained shear strength with depth. The study also indicates that for layered soil, the lateral load-deflection depends on both the characteristics of the soil surrounding the pile and the soil beneath the pile tip. The findings from the study indicate a reduced lateral capacity due vertical loading, compared to pure lateral loading in clayey soils. Based on the findings from the study, (Hazzar et al., 2017) state that it is unconservative to assume no interaction between vertical and lateral loads for the design of piles installed in clay.

7. Methodology of the Study

3.1. General description of study area

3.1.1. Location

The study was based on the findings of subsurface exploration and geotechnical engineering studies for Bank of Abyssinia Mexico Square Branch Building project which is in Addis Ababa, Kirkos sub city around Mexico Square. The proposed development consists of the construction of twenty story building with three basements and ground floor (3B+G+20).

Figure 7.1: Satellite image of the project area with borehole locations

3.1.2. Site Geology and Subsurface Condition

The geology of the project area constituted of various soil and rock formation. The top most part of the project site is covered with backfill material constituted of partly asphalt and hardcore material and partly residual soil characterized by medium stiff, dark colored, high plastic silty CLAY/ clayey SILT soil layer extending up to a maximum depth of 2.75m around BH-1. Beneath the upper most formation is weak to extremely weak, greenish gray IGNIMBRITE rock i.e 3.65m thick (max around

BH-1) and 0.25m thick (min. around BH-4). Underlying the IGNIMBRITE rock layer; stiff to hard, reddish brown to light grey, high plastic clayey SILT soil layer is found that extends to a maximum depth of 13.40m around BH-2. Beneath the clayey SILT soil layer, a stiff to hard variegated color (dominantly brown), low to high plastic, sandy SILT with variable proportion of weak core stone is found and extended up to 23.15m around BH-4. Very dense, variegated color low to high plastic silty SAND/GRAVEL soil layer is found in BH-1 from depth of 28.00m to 32.25m and in BH-4 from depth of 26.40m to 30.95m. Basaltic rock layer characterized with a wide range of degree of fracturing and intensity of weathering encountered below the soil formation which extends up to end of investigation depth in BH-3, BH-4 and BH-5 but up to 59.85m in BH-1 and 65.0 in BH-2.. Below the rock layer hard variegated color, non to high plastic clayey SILT/ gravelly SILT with sand is found.

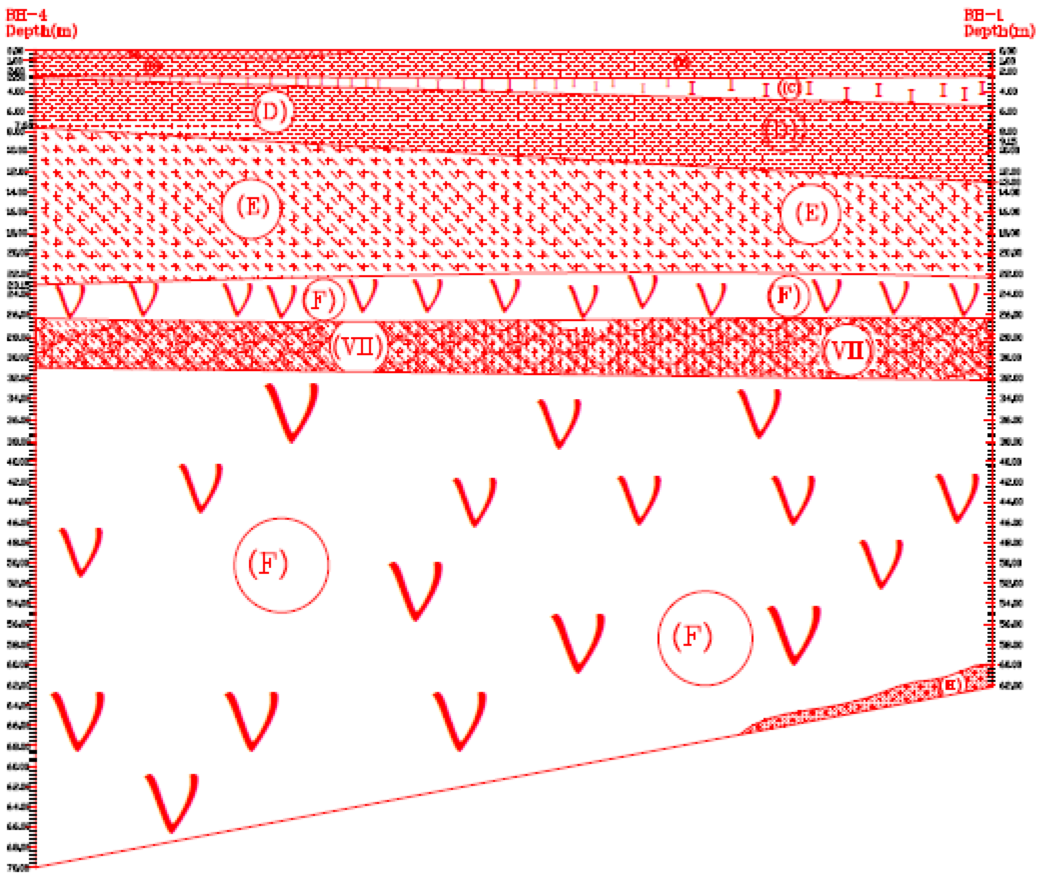

Figure a: Profile 1-4(North-South profile)

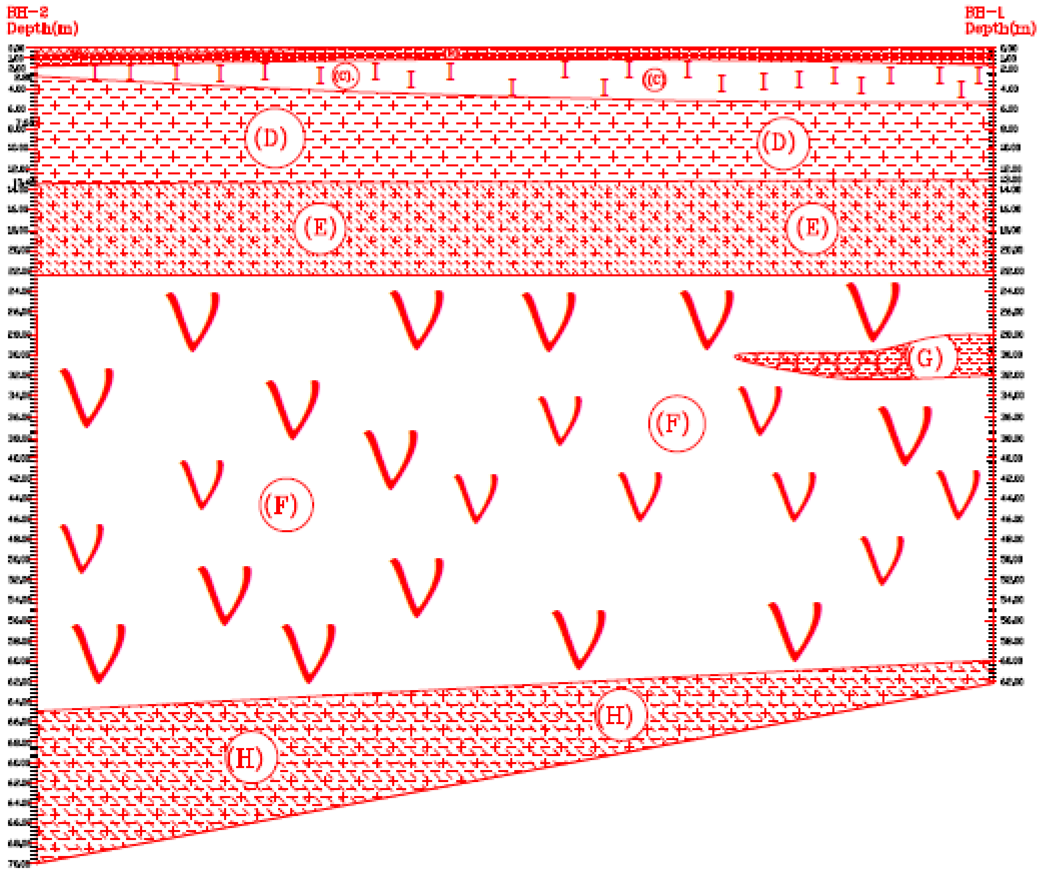

Figure b: Profile 1-2 (East-West profile)

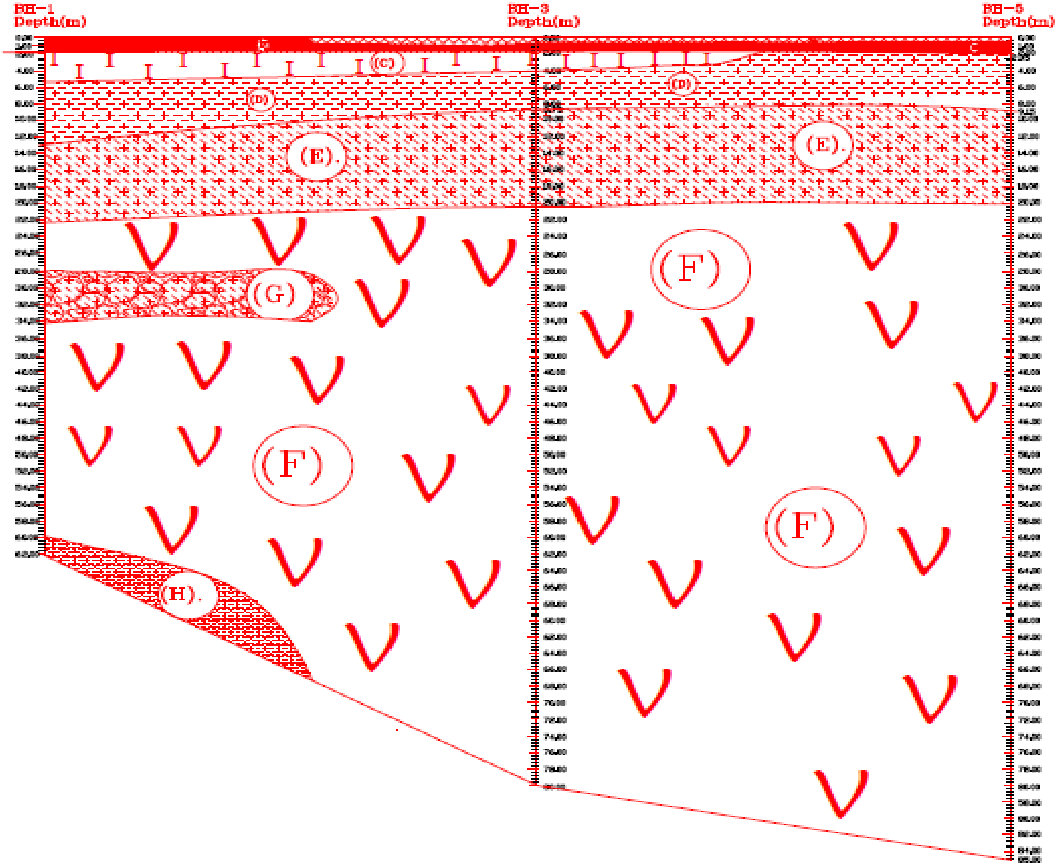

Figure c: Profile 1-3-5 (Northwest-Southeast)

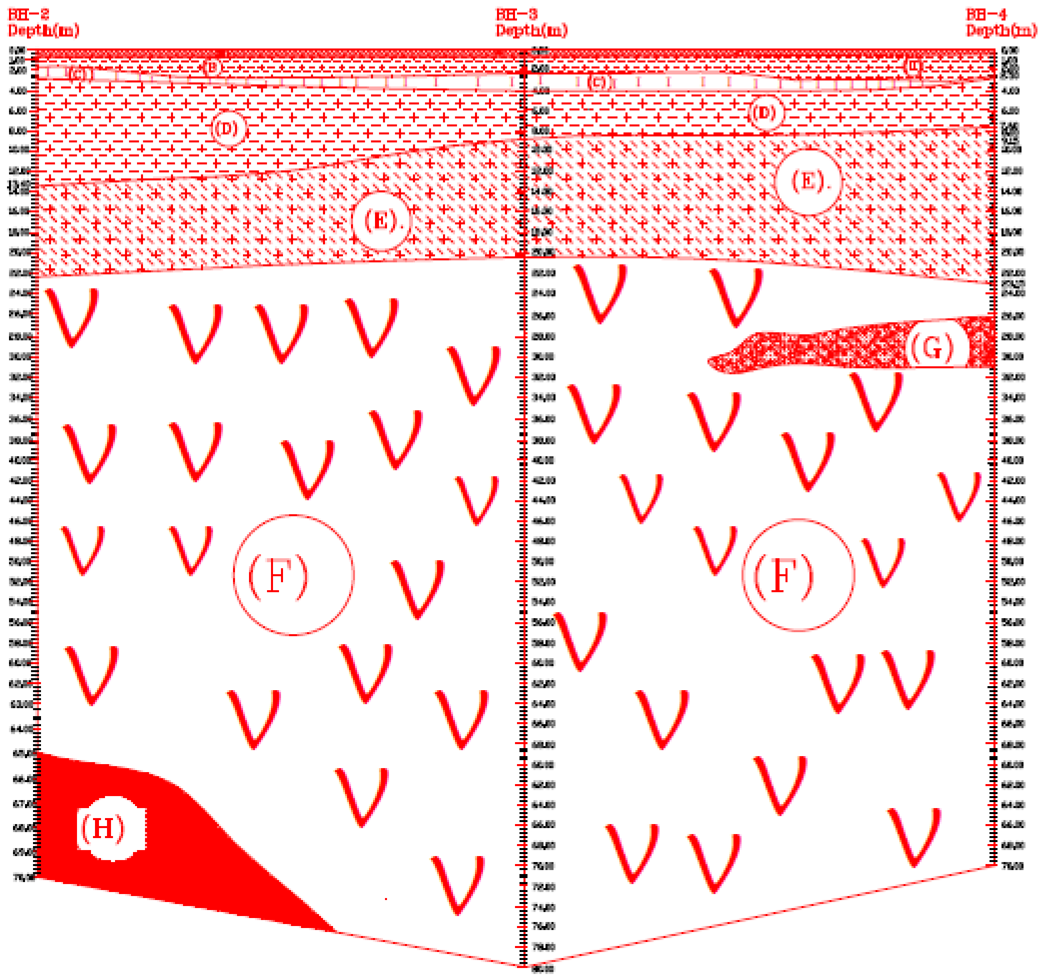

Figure d: Profile 5-3-2 (Northeast-Southwest)

Key

(A). Backfill-Asphalt followed by hard core.

(B). Medium stiff, dark brown to black high plastic silty CLAY soil layer.

(C). Weak to very weak, greenish gray, moderately weathered to decomposed and moderately jointed IGNIMBRITE rock layer.

(D). Stiff to very stiff, reddish brown to light gray, high plastic clayey SILT/ silty CLAY soil layer (weathering product of IGNIMBRITE)

(E). Stiff to hard, variegated color , low to high plastic sandy SILT with clay and weak core stone.

(F). Strong to very weak, dark gray, slightly to highly weathered moderately fractured to crushed BASALT/ vesicular BASALT rock layer.

(G). Very dense, variegated color (dominantly brown), low to high plastic silty SAND/GRAVEL soil layer.

(H). Very stiff to hard, variegated color, non high plastic sandy SILT /silty SAND with gravel.

Figure 7.2: Selected geological profiles from Fig a to d.

Ground water Observation

Measurement of ground water level was made on the borehole. Drilling operation recorded that there was no ground water within boreholes (Arcon design-built Plc, 2017).

3.2. Methodologies

The existing literatures and theories related to this study were examined to establish the proper functioning of laterally loaded single pile. The secondary soil data from the soil investigation report of Bank of Abyssinia Mexico Square Branch Building project which is in Addis Ababa, Kirkos sub city around Mexico Square area was collected and correlated to use as an input during analysis using finite element software PlAXIS 3D. Numerical models are validated and then analyses were carried out to investigate the influences of vertical loads on the lateral capacity of piles. PLAXIS 3D was then used to analyze the effect of vertical load on lateral capacity of single pile. The ultimate vertical load (Vult) capacity of a single pile was evaluated a priori by separate numerical analyses. Then the response of piles under combined loading was analyzed separately with the vertical load equal to zero (pure lateral load case), 25, 50, 75, and 100 % of the ultimate vertical load capacity of the pile, Vult. The whole process was documented in the final report together with the important conclusions and recommendations.

3.3. Parameters used for the base model

To obtain a pile head stiffness that represents a wide range of practical problems for static laterally loaded pile and soil properties are involved.

3.3.1. Soil parameters

The basic elements for analysis laterally loaded pile foundations are identifying parameters for base model, using in-situ test or correlations of parameters. Based on the investigations made by (Arcon design-built Plc, 2017) a representative value of SPT test data is chosen and required soil parameter correlations are used and selected based on data quality, soil profile, consistency, and availability. The soil types considered for this study are silty- clay underlain by weathered basalt rock investigated for Bank of Abyssinia Mexico Square Branch Building project which is in Addis Ababa, Kirkos sub city around Mexico Square. Ground water level was not found in borehole depth, which is 65m from natural ground level. Therefore, the effect of water is not considered in this thesis. The engineering design parameters were extracted from SPT N values of representative borehole log sheet, which was conducted by (Arcon design-built Plc, 2017) and considered to represent the soil in study area. The soil parameters obtained from the correlation of SPTN values and laboratory tests are used as input parameters for PLAXIS 3D. The average corrected blow count for the silty/clayey layer over all boreholes down to the depth of 10 m is about 12, whereas the average for the remaining 12 m is about 23. These parameters are shown in table in 3.2.

Undrained shear strength (Cu) of soil determined from correlation proposed by (Stroud, 1974).

$Cu = 5N, When\ 20 < PI < 30$..*(7.1)*

$Cu = 4.2N, When\ PI > 30$..*(7.2)*

Where, Cu = Cohesion in kPa and PI = Plasticity Index.

For the effective cohesion value, the method recommended by **Invalid source specified.**

$C' = 0.1 * Cu$ ....*(7.3)*

The empirical equation developed by (Peck et al., 1974) was used to estimate soil friction angle from SPT.

$\varphi = \sqrt{0.3N} + 27$ (Here N=field SPT N value) ....*(7.4)*

The effective young's modulus value is estimated by the method recommended by (Bowles, 1996)

$E' = 2G(1 + v)$..*(7.5)*

Where, $G = \frac{E_u}{3}$ and $E_u = 300 * Cu$.

Estimation of the rock mass modulus, cohesion and friction angle

A GSI of 25% and a D of 0.5 are taken for the condition of the rock under consideration, which is highly fractured and weathered. The method recommended by (Hencher, 2012) is used.

$E\_mass\ (MPa) = 10\text{^}5\ (1 - D/2)/(1 + e\text{^}(((75 + 25D - GSI)/11)\ )\ )$...............................*(7.6)*

The cohesion and friction angle are estimated using the following empirical relationship with the uniaxial loads as suggested by (Sivakugan et al., 2014).

$\varphi = sin^{-1}\left(\frac{\sigma_c - 4\sigma_t}{\sigma_c - 2\sigma_t}\right)$...*(7.7)*

$C = 1.82\sigma_t$ ....*(7.8)*

Where, $\sigma_t = 0.1 * \sigma_c$

From laboratory test result $\sigma_c = 44kPa$

Table 7.1: Lab test results on undrained for boreholes at corners of the site (Arcon design-built Plc, 2017)

Depth (m)	cu (MPa	Plasticity, index, PI				PI_{avg}	(ϕ)
		BH1	BH2	BH4	BH5		
0 - 5	50	29	27	50	45	38	28
5 – 10	50	39	26	30	37	33	29
10 - 15	115	35	27	25	18	26	30
15 - 20	115	19	30	35	23	27	30

Table 7.2: Soil Parameters for Base Model from SPT correlation.

Depth (m)	Descriptions	SPTN Value	E (MPa)	poison's ratio (v)	Unit weight (bulk)	c (MPa)	Friction angle (ϕ)	Rint
0-10	Medium to Stiff, highly plastic SILT	12	13	0.3	17	0.005	28	0.8
10-22	Stiff to Very Stiff, highly plastic SILT	23	30	0.3	17	0.0115	30	0.8
22-60	Highly to moderately weathered fractured BASALT	R	270	0.27	27	8.316	48.59	1

3.3.2. Parameters of reinforced concrete circular pile used for the model

To understand the effect of pile properties on the lateral response of single piles, an effort is made to include a wide range of piles. The parameters described in the following sections are considered based on their use in practice.

Most of the time, reinforced concrete is used in the construction of pile foundations. Due to this reason, more emphasis is given to reinforced concrete piles. So, the material properties listed below are only for reinforced concrete. However, this does not indicate that the model is not calibrated for piles made of other materials.

Pile Young's modulus ($\boldsymbol{Ep}$)

According to EN 1992.1.-2004 (Part 1.1, Table 3.1), the modulus of elasticity varies depending on the compressive strength of concrete and is given by Equation (3.3)

$$E_{cm} = 22\left(\frac{f_{cm}}{10}\right)^{0.3} \qquad (7.9)$$

Where, $f_{cm} = f_{ck} + 8MPa$ and f_{ck} is the characteristics compressive strength, and f_{cm} is in (N/mm^2).

In most pile foundation construction projects, the value of f_{ck} varies between 16 to 40 MPa (C 20 – C 50). The modulus of elasticity under consideration is selected as 31 GPa for $f_{ck} = 20MPa$ (C 30).

Pile diameter and lengths

Three length and four diameter of the piles was included in the analysis. The piles were modeled as linear elastic model and the parameters for this model is listed in table 3.3.

Table 7.3: Pile parameters used in the numerical analysis

Parameter	Symbol	Volume pile length and diameters				unit
Material		Concrete	Concrete	Concrete	Concrete	
Material model		Linear elastic	Linear elastic	Linear elastic	Linear elastic	
Drainage type		Non-porous	Non-porous	Non-porous	Non-porous	
Modulus of elasticity	E	31	31	31	31	GPa
Poisson's ratio	v	0.15	0.15	0.15	0.15	-
Unit weight	γ	25	25	25	25	k/m^3
Length	L	10	15	20		m
Diameter	D	0.5	0.75	1.0	1.25	m

Table 7.4 :Material properties of beam inside volume pile

Parameter	Symbol	Pile length and diameters				unit
Modulus of elasticity	E	31	31	31	31	kPa
Poisson's ratio	ν	0.15	0.15	0.15	0.15	-
Unit weight	γ	25	25	25	25	k/m^3
Length	L	10	15	20		m
Diameter	D	0.5	0.75	1.0	1.25	m
Cross-section area	A	0.1963	0.4416	0.785	1.2266	m^2
Inertia moment	I	0.00307	0.01552	0.04906	0.11978	m^4

8. Numerical Modeling

4.1. Introduction

In this study, numerical modelling was used to investigate the effect of vertical load on lateral response of pile in the soils of the study area. Verification of the study with full-scale load tests result from the literature was used to control the accuracy of the numerical model results. After verification of finite element analysis solution, a parametric study has been conducted (chapter-5). Variations in the factors such as the embedment depth of the pile, pile diameter, and vertical loads will be analyzed. Three-dimensional geotechnical finite element package Plaxis 3D V20 connect edition was used in all analyses. In this chapter, properties and main functions of the 3D finite element methodology were presented briefly for better understanding of the model designs.

4.2. Use of PLAXIS 3D CE V20 as Numerical modeling tool

PLAXIS 3D CE v20 is a full three-dimensional finite element program which combines an easy- to-use interface with full 3D modeling facilities. The first PLAXIS 3D program was released in 2010. It is developed for the analysis of deformation, stability and groundwater flow in geotechnical engineering and design. The modeling process in PLAXIS 3D CE v20 involves five workflow steps. These are Soil, Structures, Mesh, Flow conditions and Staged construction. These mode tabs in PLAXIS 3D used for defining soil stratigraphy, structure components, discretizing and transforming the model geometry in to finite element, water levels, and calculation settings and calculation for Soil, Structures, Mesh, Flow conditions and Staged construction respectively. Concerning constitutive models PLAXIS 3D CE v20 incorporate different types of diversified material models including user define option. These are Linear Elastic model (LE), Mohr-Coulomb model (MC), Hardening Soil model (HS), Modified Cam- Clay model (MCC), options.

Plaxis 3D provides extensive ways for the documentation of the analysis results. Output program was presented all numerical analysis results in variety of forms including curves, diagrams, and tables. It mainly consists of the results of deformations and stresses. In addition, force results are presented for structural elements. This chapter is devoted to introduce the details of constitutive models, material properties, and finite element modelling used in the performed parametric study.

4.2.1. PLAXIS volume pile

The volume pile consists of volume elements in which the interaction with surrounding soil is modelled by means of interface elements. In PLAXIS 3D, the volume pile may be created by two options. The first one relates to the use of "Insert Solid" function which allows to set up the shape and the location of volume element (see Figure 4.1). The second one relates to use the "command box" in which the volume pile is defined by the length, the radius and the numbers of segments of the pile shaft.

The properties of the volume pile are properties. For example, to assign the volume pile which has properties of the $unit\ weight\ \gamma = 25\ kN/m^3$ and the Young's modulus $E = 3.10^7\ kN/m^2$, "soil and interface" material type and "linear elastic" material model are set up. The other material parameters are shown in Table 3.2. Due to being volume element with soil material, the volume pile can't give results of Force like the embedded pile. Therefore, to investigate the results of Force, a beam element is inserted at the axial axis of the volume pile. This beam is set up with the same properties as the volume pile except for the *E* modulus which is 10^6 times lower than E modulus of the volume pile material (see Table 3.3). With the set deformations of the beam will be as similar as that of the volume pile. However, to obtain the actual result of the bending moment in the pile, the bending moment value of beam in Plaxis output has to be multiplied by the factor "10^6".

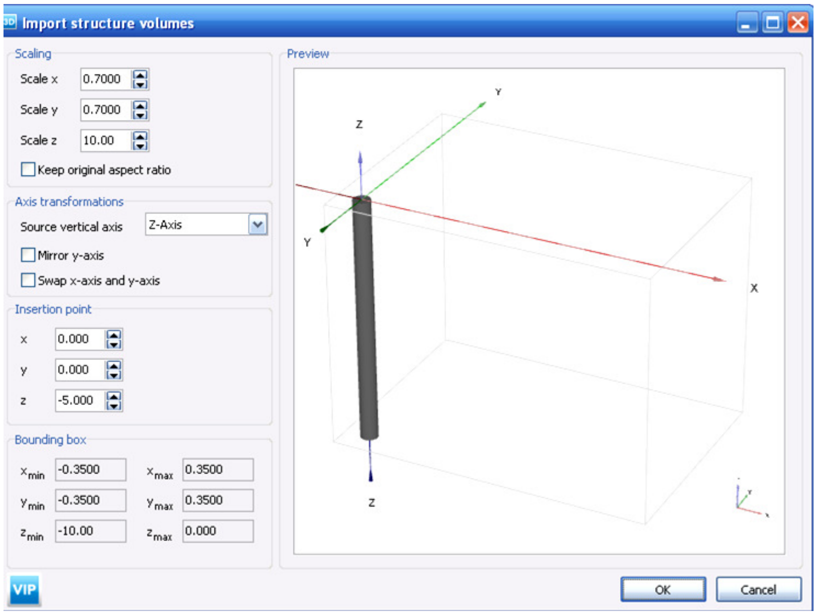

Figure 8.1: Shape and location of volume structure in Plaxis 3D

4.3. Generation of the Model

4.3.1. Model Geometry

In this part of the research, numerical modelling was conducted on a single pile in layered soil by using Plaxis 3D FEM package. The pile was modeled using a volume pile model available in Plaxis 3D. The model geometry depends on both the diameter of pile and its length. The soil is layered and the cross section of the soil block was pre-defined in the model tab on the project properties window. Based on the pile geometry, the limits of the soil contour were defined as the x_{min}, x_{max} and y_{min}, y_{max} . The depth (z-axis) was applied using the "create borehole" button, in this function groundwater table, level can also be selected. The top boundary of the soil layer is at z = 0, and the bottom boundary of the soil layer is a function of pile diameter and its length. Once the soil block was drawn, the soil properties can be assigned to it.

According to (Karthigeyan et al., 2007) for static lateral load condition, the soil mass dimension depends on the pile diameter and length. The width of soil mass was taken as 40D, in which, D is the pile diameter or pile width. The soil mass effect on the pile response is diminishing for the width more than 40D. The height of soil mass was taken as L+20D, in which, L is the length of pile as shown in Figure 4.2.

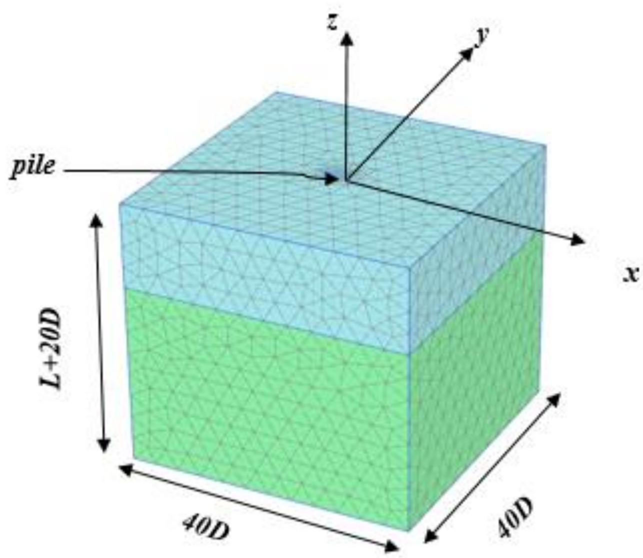

Figure 8.2: 3D finite element mesh for soil mass and location of pile.

Table 8.1: 3D FEM model dimensions (design of experiments)

Embedded pile length L(m)	Pile diameter D (m)	Width of soil mass along X (m)	Length of soil mass along Y (m)	Height of soil mass along Z (m)
10	0.5	20	20	20
	0.75	30	30	25
	1	40	40	30
	1.25	50	50	35
15	0.5	20	20	25
	0.75	30	30	30
	1	40	40	35
	1.25	50	50	40
20	0.5	20	20	30
	0.75	30	30	35
	1	40	40	40
	1.25	50	50	45

4.3.2. Model Properties

Finite element analysis software Plaxis 3D was used for the investigation of the effects of vertical load on lateral response of a pile. To carry out a parametric study, other properties should be kept constant while the effect of the change in a certain property was being investigated. Therefore, the interpretation of parametric study results can be more complex, since the effect of several factors will interfere with each other. In addition, actual laterally loaded pile model with all external boundaries will require much more 3D mesh elements, which cause longer calculation times.

Volume pile option in Plaxis 3D was used to model the vertical pile and its properties in all analyses. This option was given the opportunity of modelling piles as structural members with a definite rigidity and mechanical properties.

Before systematically investigating the factors affecting the pile-soil interaction behavior, the boundary size, surface fixity conditions, and mesh generation effects were studied, as it is necessary to establish correct geometry and model of the problem.

4.3.3. Model Boundary Fixities

The boundaries of the soil in the model must be constrained in the vertical and lateral directions where the displacement of the soil due to the lateral load is negligible. To minimize the boundary effects in the model many authors suggested different locations of these boundaries. The horizontal length extent of 40D (40 times of the pile diameter) and vertical depth extent of L+20D (length of a pile plus 20 times diameter of a pile) is enough after which no appreciable stress and strain variation effect was observed by (Karthigeyan et al., 2007).

Therefore, boundaries of the model were placed at enough distances from the pile so that the influence of the boundaries on the deformations of the pile is minimized. Three separate boundary conditions were imposed onto the model. Nodes on both lateral boundaries of the model were fixed against horizontal movement($u_x = u_y = u_z = 0$), yet free to move in the horizontal direction. Meanwhile, nodes on the bottom boundary of the model were fixed against all directions($u_x = u_y = u_z = 0$), whereas the top boundary was free to move in all directions as shown in Figure 4.2.

It is desirable to select the size/geometry of the model large enough so that boundaries are far away from the area where we are making calculations, and that stress-strain distributions in the soil are not affected from the geometrical constraints near the boundaries. However, long calculation times in three-dimensional analyses make this procedure inefficient.

Therefore, the size/geometry of the model and distance to the boundaries were studied to determine the optimum dimensions enough for an accurate model. The deflections in the soil were investigated because of pile resistance are not affected or interrupted because of the model boundaries.

4.3.4. Mesh Generation

After completing the geometry and input parameters of soil and structure model, finite element mesh generation step is proceeded. Mesh generation is the process of dividing the model consisting of soil and structural elements into the volume elements to make computations. Plaxis 3D generates 10 - node tetrahedral elements in mesh procedure of soil volume.

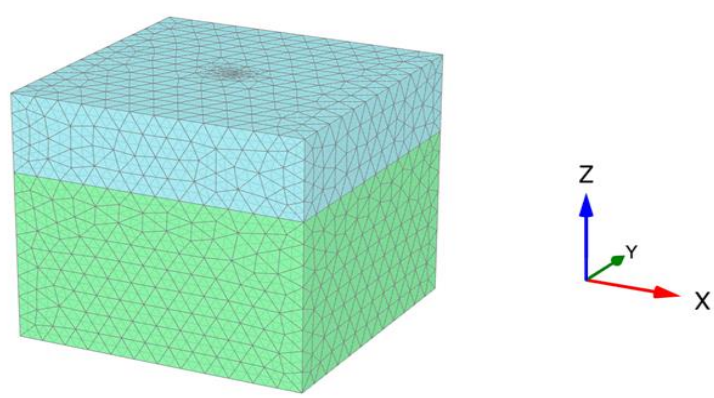

Figure 8.3: Typical mesh connectivity.

The mesh element size can be adjusted by using a general mesh size varying from very coarse to very fine and by using line, cluster, and point refinements. Very fines mesh should be avoided to reduce the number of elements, thus to reduce the memory consumption and calculation time. The program does not allow entering a new structural element or a new soil cluster after the mesh was generated. If a new element or cluster was added to the geometry model, the mesh generation should be repeated with the new input.

4.3.5. Sensitivity Analysis

As mentioned above, in the finite element calculations, the model has divided into elements, which compose the "finite element mesh". The finite element mesh size will possibly influence the results. To investigate the influence of number of elements or mesh coarseness on the behavior of laterally loaded pile foundation, five different finite element meshes were performed. These were done by varying their number and sizes keeping material properties and all other parameters constant. For this purpose, a horizontal load of 2548 kN/m^2 was applied at the pile head. The generated number of elements and the head deflection of a pile is given in Table 4.4.

Table 8.2: Influence of mesh size on head deflection

Model	Mesh Coarseness	Number of elements	Head deflection (mm)
1	Very Coarse	6062	53.2
2	Coarse	7121	52.2
3	Medium	12146	50.11
4	Fine	25071	49.31
5	Very Fine	59832	48.22

Table 4.2 shows the influence of mesh density on the head deflection of the pile. As shown from the figure head deflection decreases with increases number of elements until the number of elements reach 12146, after that an increasing in number of elements has no significant effect on the head deflection of pile. It can be said that mesh is converged with 12146 elements because there is no significant change in deflection when the number of elements increased to 59832. Therefore model 3 (medium mesh) was used to investigate the effect of vertical load on the general lateral response of the pile foundation.

4.3.6. Calculation Process

The pile is modelled with a surface at the top of the pile, with the vertical static load is applied as constant surface pressure, σ_z, on top of the pile, whereas the lateral load is applied as a prescribed displacement at the surface of the pile head. The benefit of using a prescribed displacement instead of a load is that the force and displacement can be extracted directly from the output in Plaxis 3D. The calculation stages are divided into phases, calculated with the Plastic analysis, Stage construction. As the purpose is to analyze the effect of the combined vertical and lateral load on the lateral response, a node at the top of the pile is used to investigate the lateral deflection. The force and displacement of the pile are extracted from this node, at the center of the pile head.

First vertical capacity analyses are performed. The vertical capacity is found by applying a vertical surface load at the pile head and loading until failure.

In Plaxis 3D, the construction stages of a finite element model are defined by calculation phases. The calculation phases used for creating the finite element model presented in this chapter is listed below:

- **Phase 0**: Initial phase, the K_0 calculation procedure is used to calculate the initial stress state of the soil material.
- **Phase 1**: Installation of the pile, the pile and interfaces are activated.
- **Phase 2**: Vertical loading, a vertical load is activated.
- **Phase 3**: Resetting displacements.
- **Phase 4**: Lateral loading, introduced in the model as prescribed lateral displacements.

To achieve a good relationship between the pile structure and the soil volume, an interface was created. Interfaces were joint elements to be added to the surfaces to allow for a proper modelling of soil-structure interaction. Interfaces were used to simulate the contact between a plate (from the pile structure surfaces) and the surrounding soil. An interface can be created next to the plate or geogrid elements or between two soil volumes. In the model, the interface was created next to the pile plates. The thickness of the interface was zero, which means that the pair of nodes were located with the same coordinates. The interface consists of 16 nodes quadrilateral shaped elements. Interface elements are numerically integrated using three Gauss integration points. Figure 4.4 shows the position of the nodes and integration points.

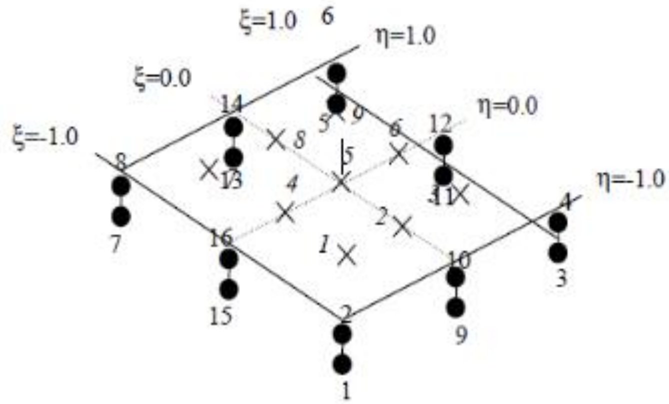

Figure 8.4: Local numbering and positioning of nodes (Ɛ) and integration points (x) of a 16-node interface element (Plaxis 3D, 2020).

The interface elements have pairs of nodes instead of single nodes. The distance between the two nodes of a node pair is zero. The aim of these interface nodes is to allow for differential displacements between the node pairs slipping and gapping.

The interface stiffness and strength can be defined depending on the kind of analysis, and it is controlled by the parameter R*inter*. A rigid interface, perfectly rough soil-structure, is used when the interface should not have a reduced strength with respect to the strength of the surrounding soil. The strength of these interfaces was assigned as rigid (which corresponds to R*inter* = 1.0). It behaves as an element with the same material properties as the adjacent soil element. In thin layer element method, the contact between structure and soil was described as perfectly rough. The material behaviors in the contact area (the thin element) were simulated by the material behavior of the soil (Table 3.1, Table 3.2, and Table 3.3).

The following rules are applied to calculate the interface properties from the soil properties in the related data set and value of *Rinter*.

$c_{inter} = c_{soil}$ .... *(8.1)*

$tan\phi_{inter} = tan\phi_{soil}$ .... *(8.2)*

Where: c_{inter} –Cohesion of the interface

c_{soil} -Cohesion of the soil

$tan\phi_{inter}$ –Interface friction angle

$tan\phi_{soil}$ –Soil friction angle

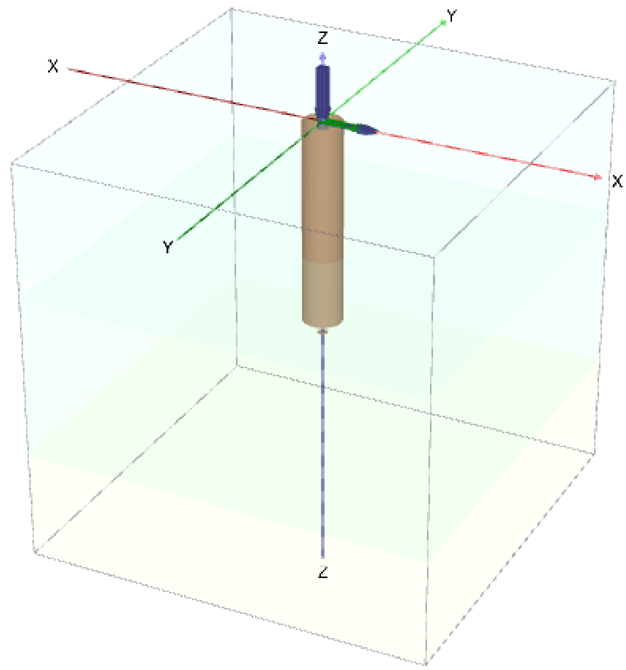

Figure 8.5: Creation of Pile structure and Loads.

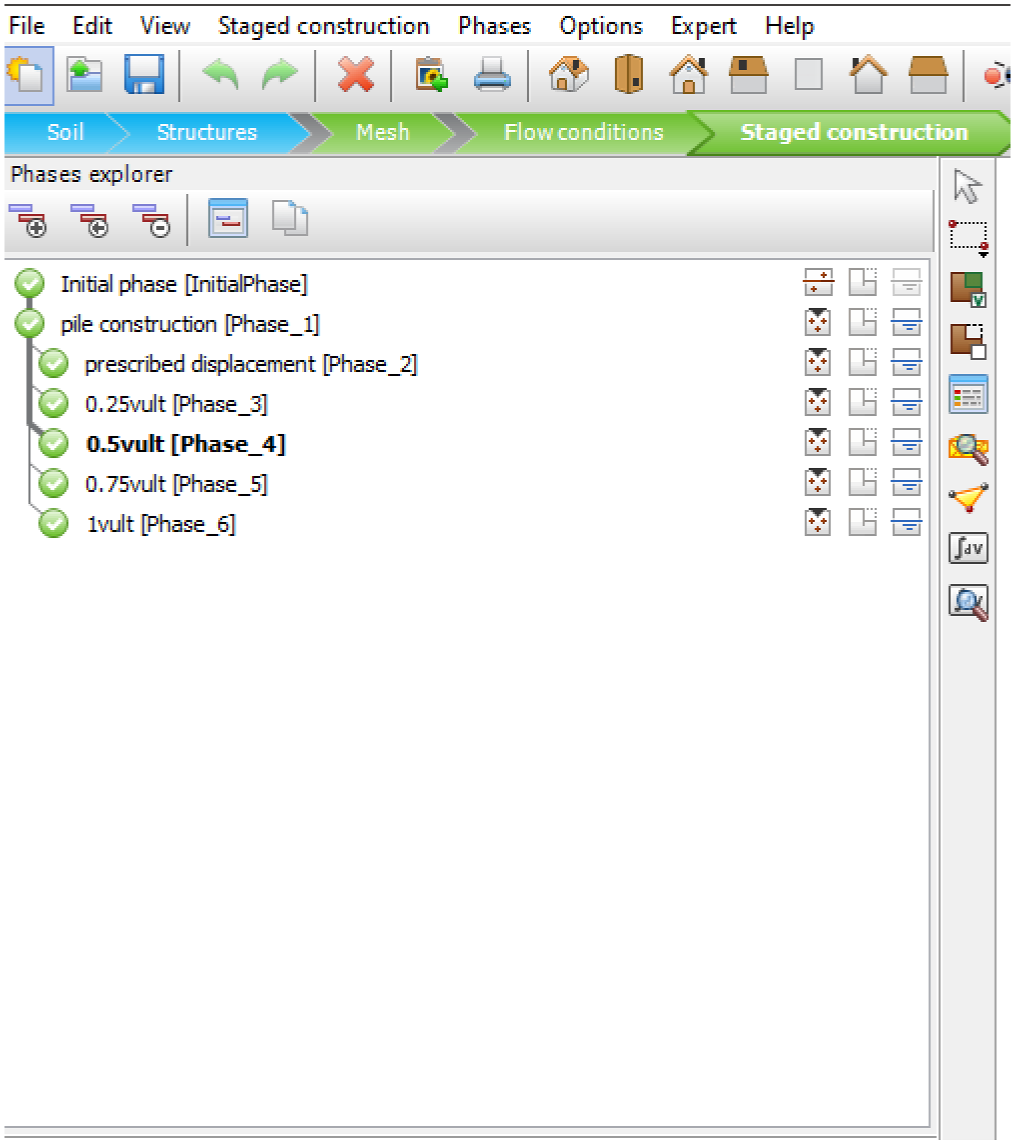

Figure 8.6: Application of load on Pile in different stages

4.4. Validation of Numerical Model

The finite element approach was used in this study to investigate the lateral response of pile when subjected to lateral loads. This section assesses the accuracy of the finite element approach in analyzing laterally loaded piles, and to verify certain details of the finite element such as pile displacement. According to literature, there are number of published cases of full-scale lateral pile response subjected to lateral loads. Thus, it deals with a full-scale laterally loaded pile (F.Ismael, 1998) to make a comparison with present study of laterally loaded piles. For the case of laterally loaded piles embedded in layered medium, some assumptions are made due to the inaccuracy of soil data obtained from the site and laboratory.

This section used to assess the accuracy of the finite element approach in analyzing laterally loaded piles and to verify certain details of the finite element such as pile displacement. Verification example was worked out to compare the result obtained by finite element analysis to those obtained from experimental study. The comparative case includes full-scale lateral load tests reported by (F.Ismael, 1998). The results of laboratory and field tests are used to identify the soil profiles and soil properties that are well instrumented.

Table 8.3: Geotechnical properties of the soil layer

Parameters	Name	Medium dense cemented silty sand layer	Medium dense to very dense silty sand	Pile	Unit
Unsaturated Soil Weight	γ_{unsat}	18	19	25	kNm^{-3}
Saturated soil weight	γ_{sat}	18	19	-	kNm^{-3}
Young's Modulus	E	13000	13000	2.00E+09	kPa
Poisson's Ratio	ν	0.3	0.3	0.15	-
Cohesion	c	20	1	-	kPa
Friction Angle	ϕ	35	45	-	°

The case study deals with lateral load in which the deflection response of bored piles in cemented sand was examined by field test on a single pile under lateral load (F.Ismael, 1998). All piles were 0.3m in diameter and had a length of 3 or 5m. The site of this load test was in Kuwait. The surface soil to a depth of 3.5m was characterized by having both component of shear strength, both effective parameters. The soil profile consists of a medium dense cemented silty sand layer to a depth of 3m. This is underlain by a medium dense to very dense silty sand with cemented lumps to the bottom of the borehole. The same load sequence as pile tests was applied to the pile after completing the whole geotechnical model for lateral pile tests. The properties of soil in the both cases are listed in Table 4.3.

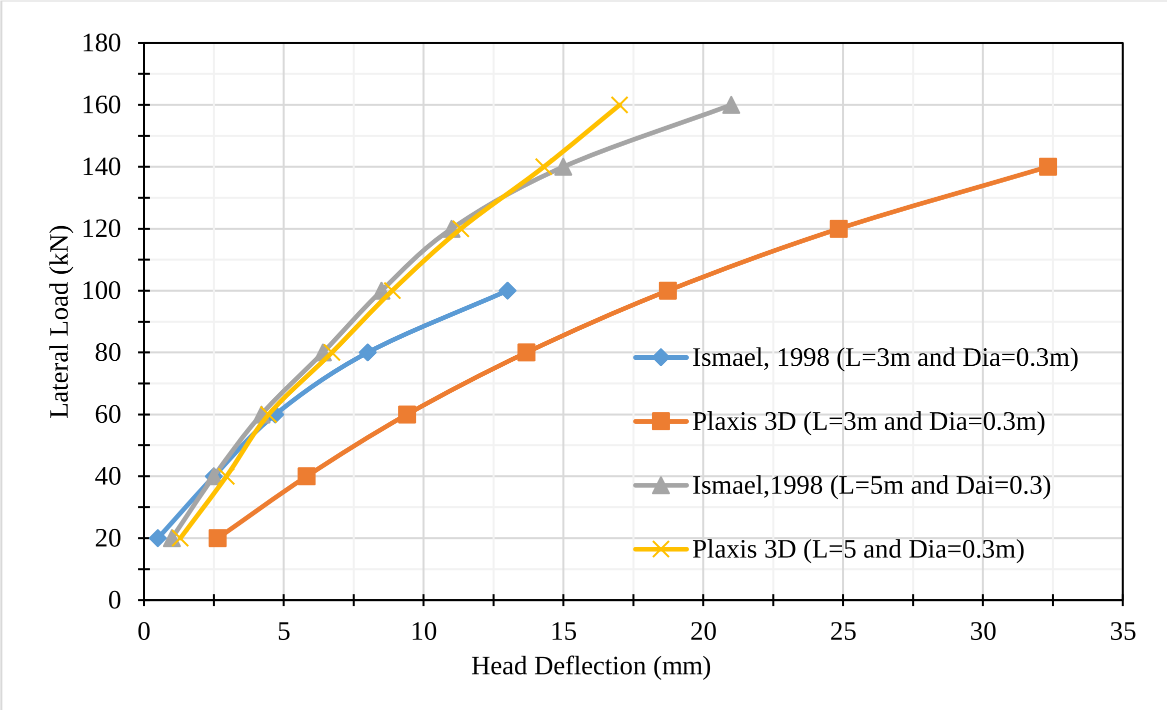

Figure 8.7: Comparison of finite element result with field test data from (F.Ismael, 1998).

The comparison between the finite element result and layered sand field test data is shown in Figure 4.7. The pile with a length of 5m is highly resistance to the lateral load from the second pile length value. Comparable data were obtained between the experimental results of the three piles and the present simulation model. The results obtained from the numerical simulation for a pile of 5m is relatively closed with the result obtained from the field test.

5. Results and Discussions

5.1. Introduction

In this chapter, a parametric study was conducted on the effects of vertical load on response of pile embedded in layered soil conditions using Plaxis 3D. One of the purposes for this study was to investigate lateral response of pile by varying, length of the piles, pile diameter, and vertical loading.

5.2. Effect of axial load on lateral response

5.2.1. Vertical capacity analysis

The load deformation analysis on a single pile of varying length (10, 15, 20m) and varying diameter (0.5, 0.75, 1, 1.25m) in the soil profile using PLAXIS 3D software was studied. The vertical ultimate capacity, Vult is is determined as the vertical load which causes a vertical displacement equating to 0.1D, obtained through analysis of a single pile subjected to a pure vertical load. Figures 5.1 to 5.3 indicates that the ultimate bearing capacity of the pile.

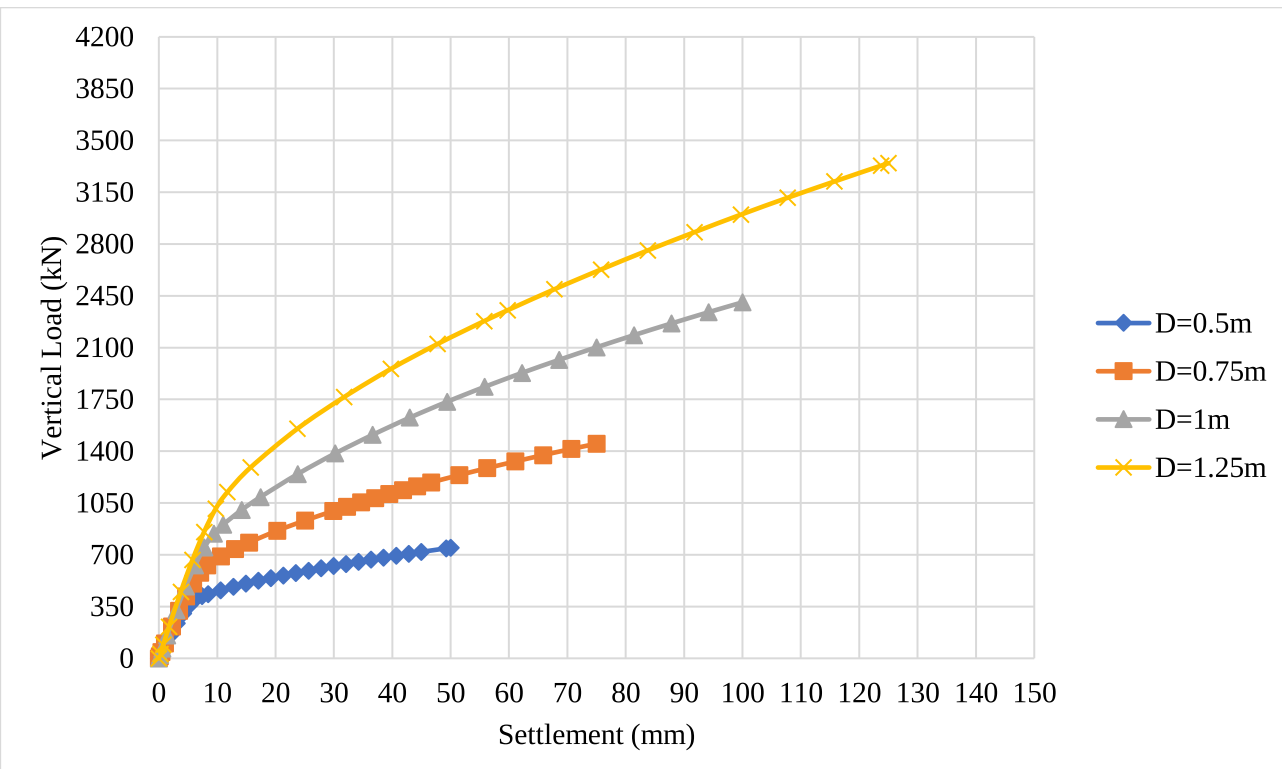

Figure 5.1: Vertical load with settlement of pile with length 10m.

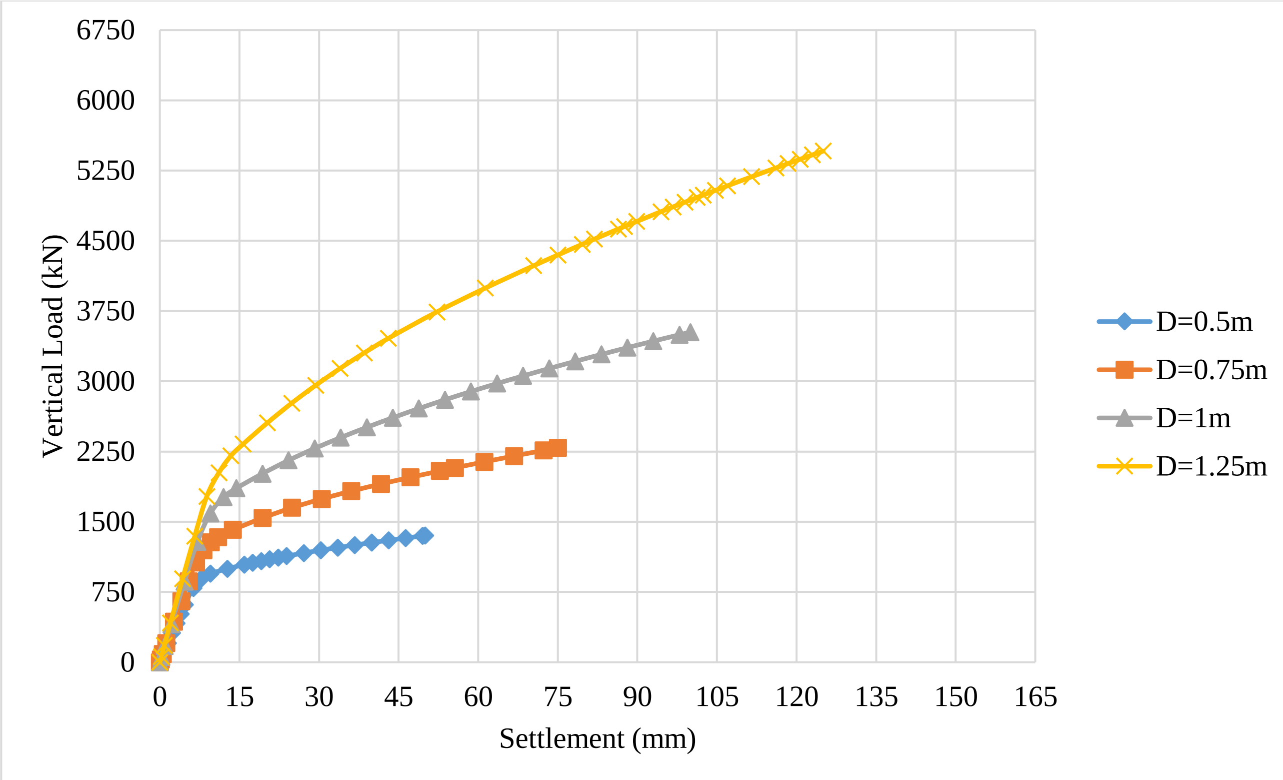

Figure 5.2: Vertical load with settlement of pile with length 15m.

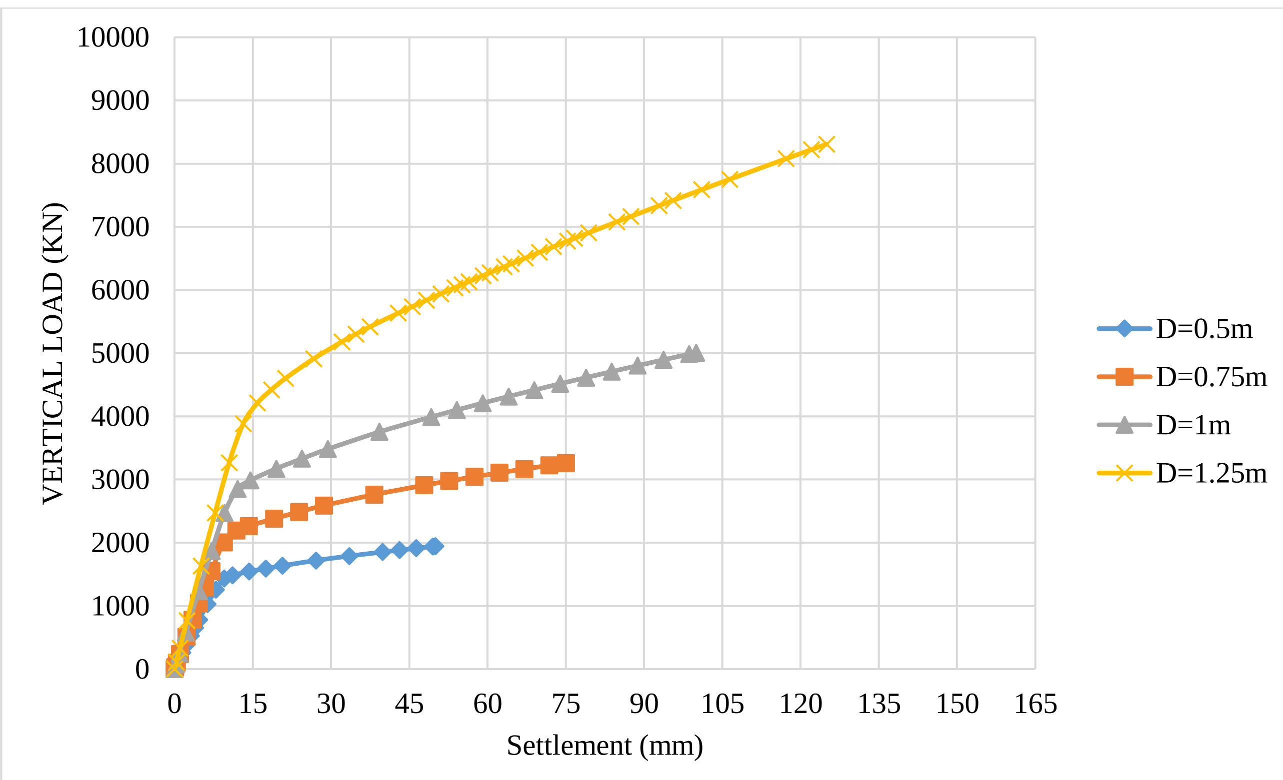

Figure 5.3: Vertical load with settlement of pile with length 20m.

5.3. Influence of vertical load on the lateral response of piles

After a vertical capacity analysis, vertical loads equal to 25%, 50%, 75%, and 100% of the vertical capacity were applied at the pile head. The lateral force-displacement for models with vertical loads are compared to a case of pure lateral loading. The results are presented in Figures 5.4 to 5.6 for pile length 10, 15 and 20 m, and diameter of 75 cm. The vertical load applied is given as a part of the vertical capacity (Vult).

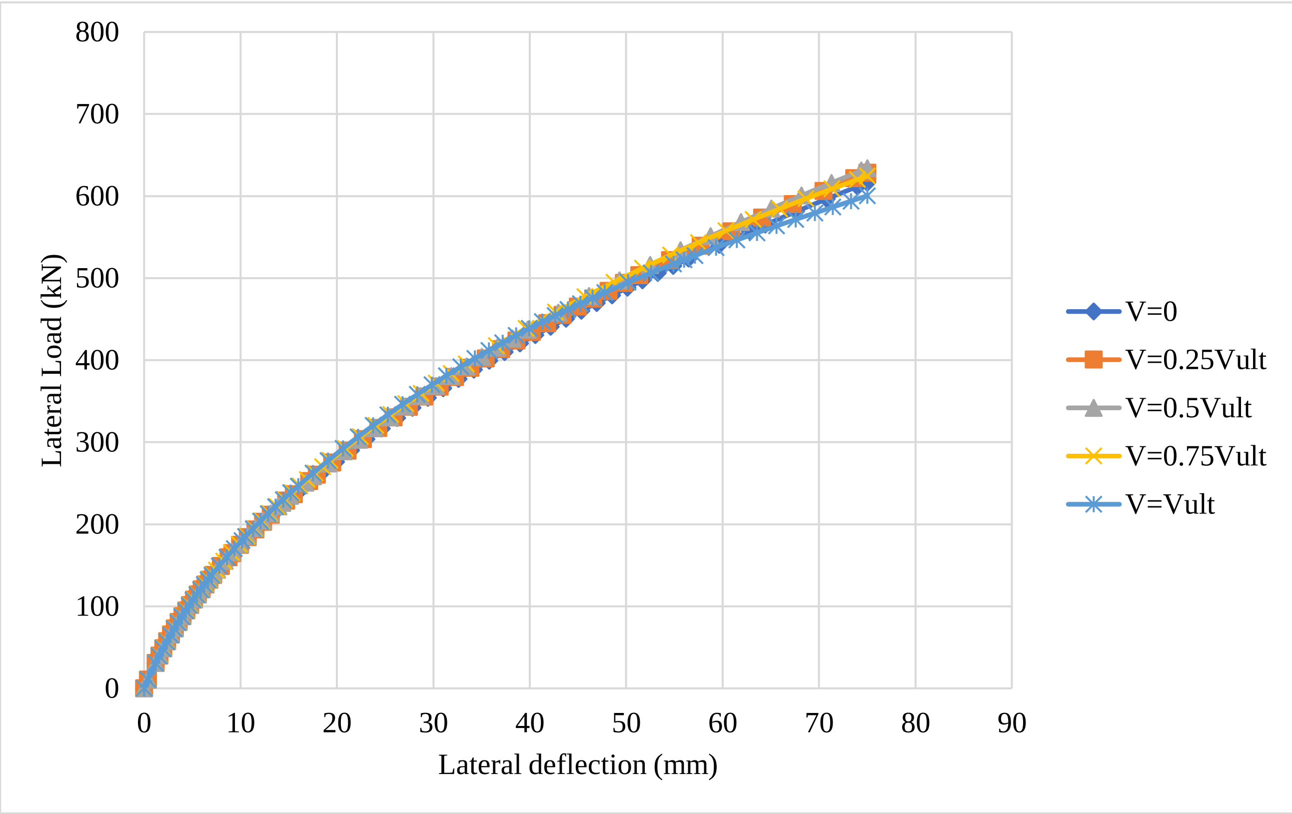

Figure 5.4: Effect of vertical load on lateral load response of pile with length 10m for pile displacement of 0.1D

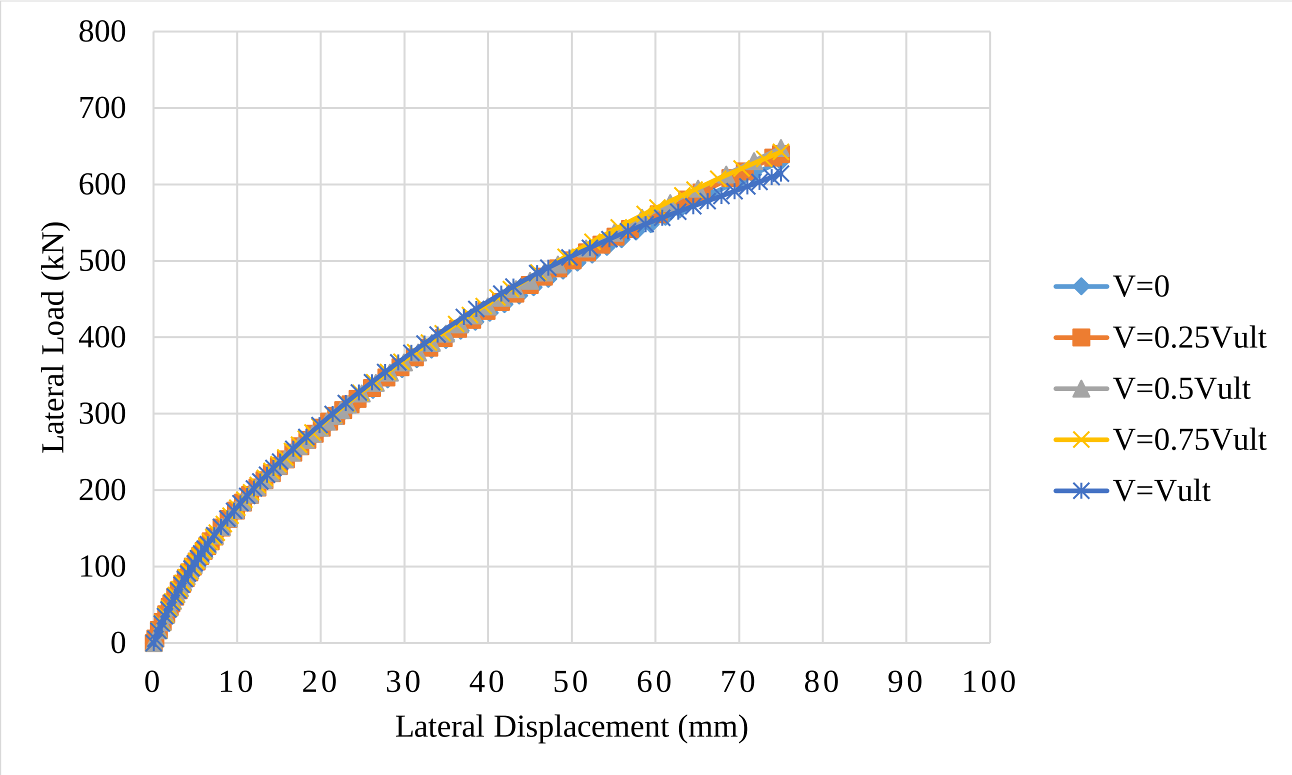

Figure 5.5: Effect of vertical load on lateral load response of pile with length 15m for pile displacement of 0.1D.

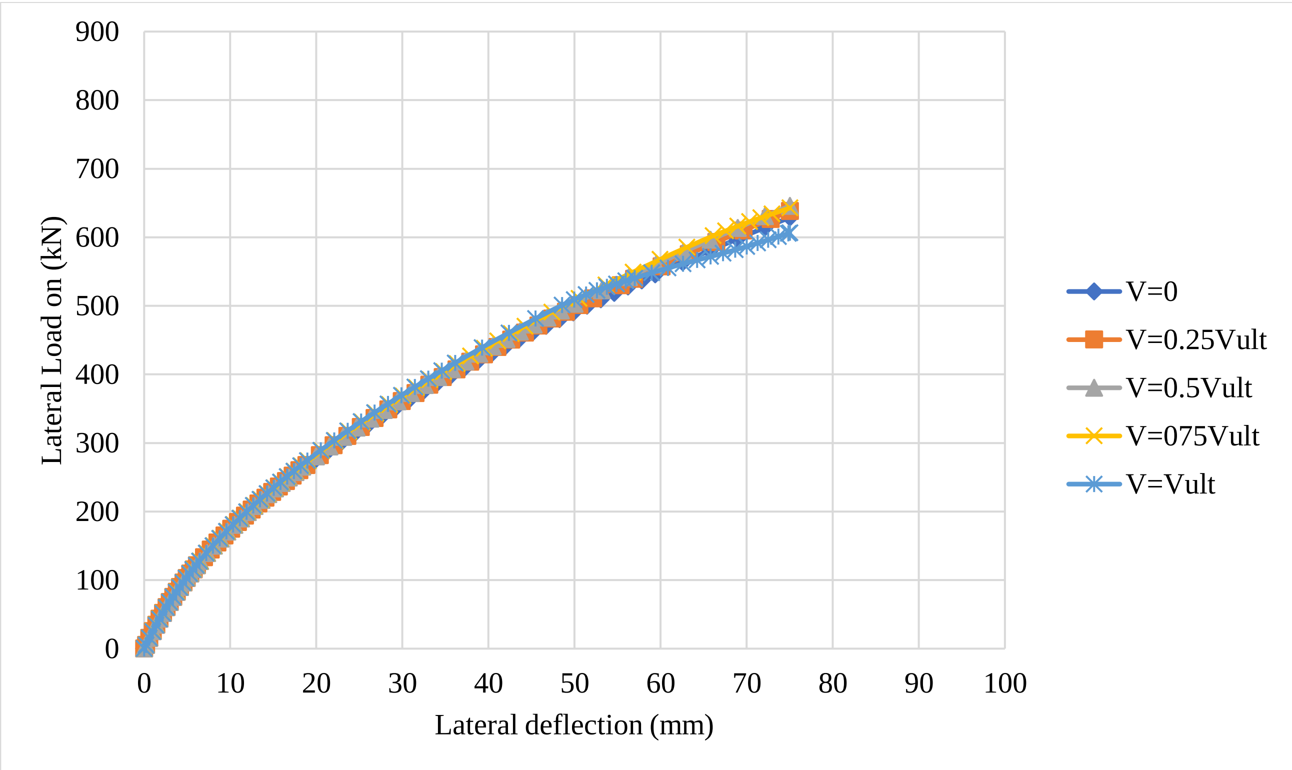

Figure 5.6: Effect of vertical load on lateral load response of pile with length 20m for pile displacement of 0.1D.

As can be seen from the Figures, the presence of vertical load causing the lateral capacity of the pile slightly increased up to 0.75Vult and reduction in lateral capacity when the ultimate vertical load reached at Vult.

For a vertical load of 0.25Vult to 0.75Vult (1 to 2%), the increase in lateral capacity is marginal. when the vertical load is reached Vult, the lateral capacity is reduced by around 4%. Lateral capacity reaches a peak value when the vertical load is between 0.5Vult and 0.75Vult. For higher vertical loads the lateral capacity is reduced. This is due to the increased mean effective stress caused by the application of vertical loading. Thus, the presence of the ultimate vertical load after yielding of lateral capacity decreases the lateral resistance of soil and subsequently leads to the development of lower resistance to the lateral pile deformation. It was observed that the presence of higher vertical load (after 75%Vult) causes a reduction in the lateral capacity in the clayey soils which agrees with the result carried out by (Hazzar et al., 2017) and (Karthigeyan et al., 2006, 2007).

Since the lateral capacity of the modelled pile decreases with increasing axial load after 75%, this means that the presence of higher axial load is not good to the lateral capacity of cohesive soil. Therefore, it is usually necessary to consider the effect of higher axial loads in the design of laterally loaded pile in cohesive soils.

5.4. Influence of vertical loading on pile bending moment

The variation of bending moment with depth for free headed piles of length 10, 15 and 20m with constant diameter of 0.75m embedded in layered soil is shown in Figures 5.7 to 5.9.

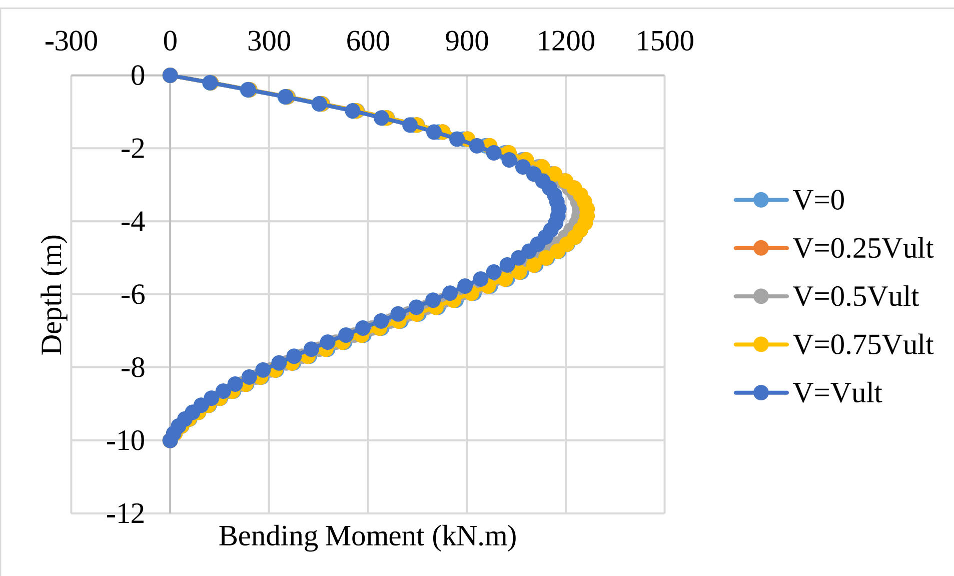

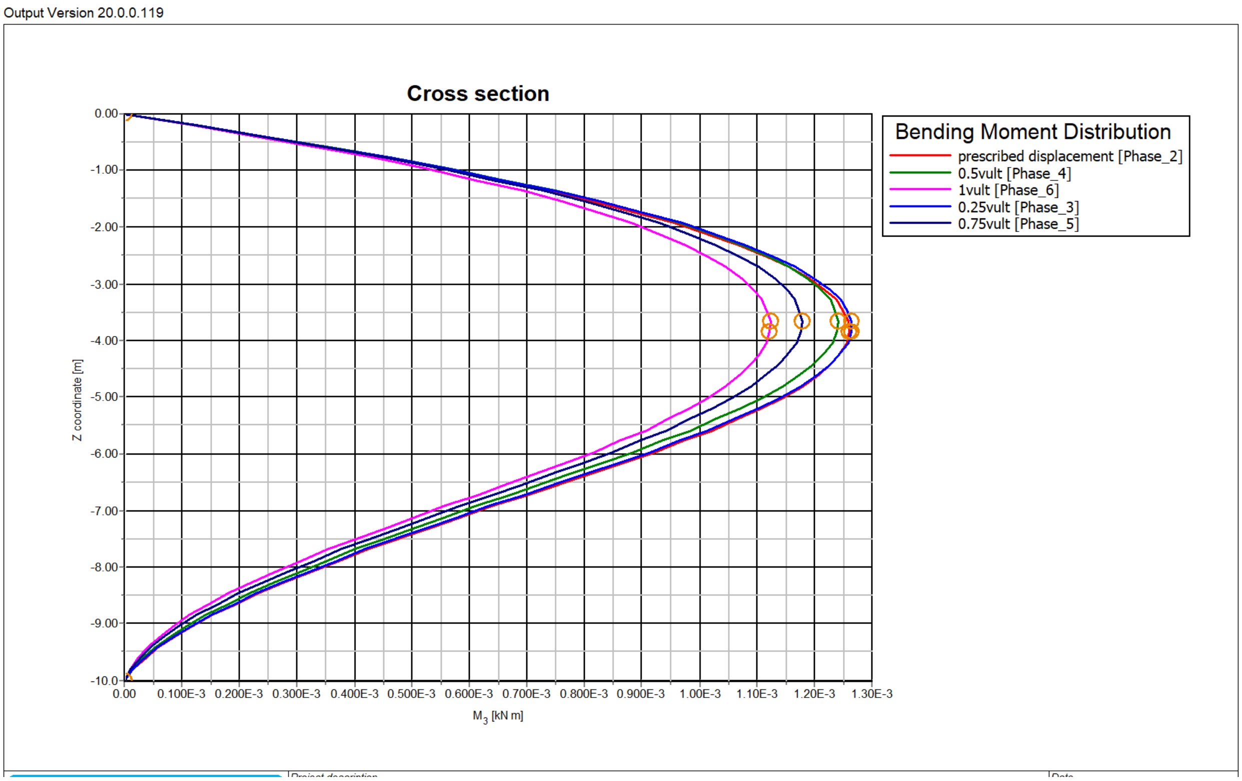

Figure 5.7: Variation of pile bending moment (kNm) with pile depth (m) for pile length 10 with diameter of 0.75m.

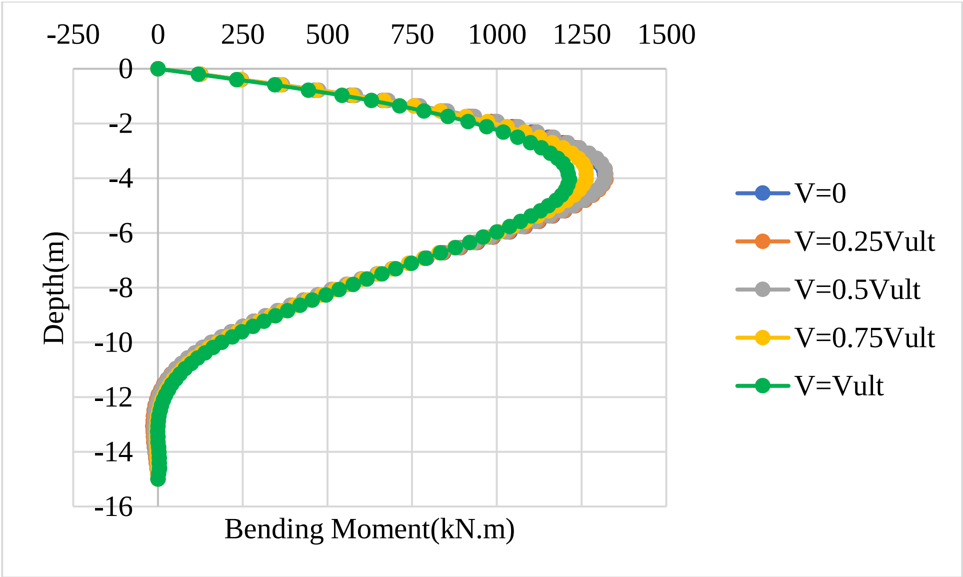

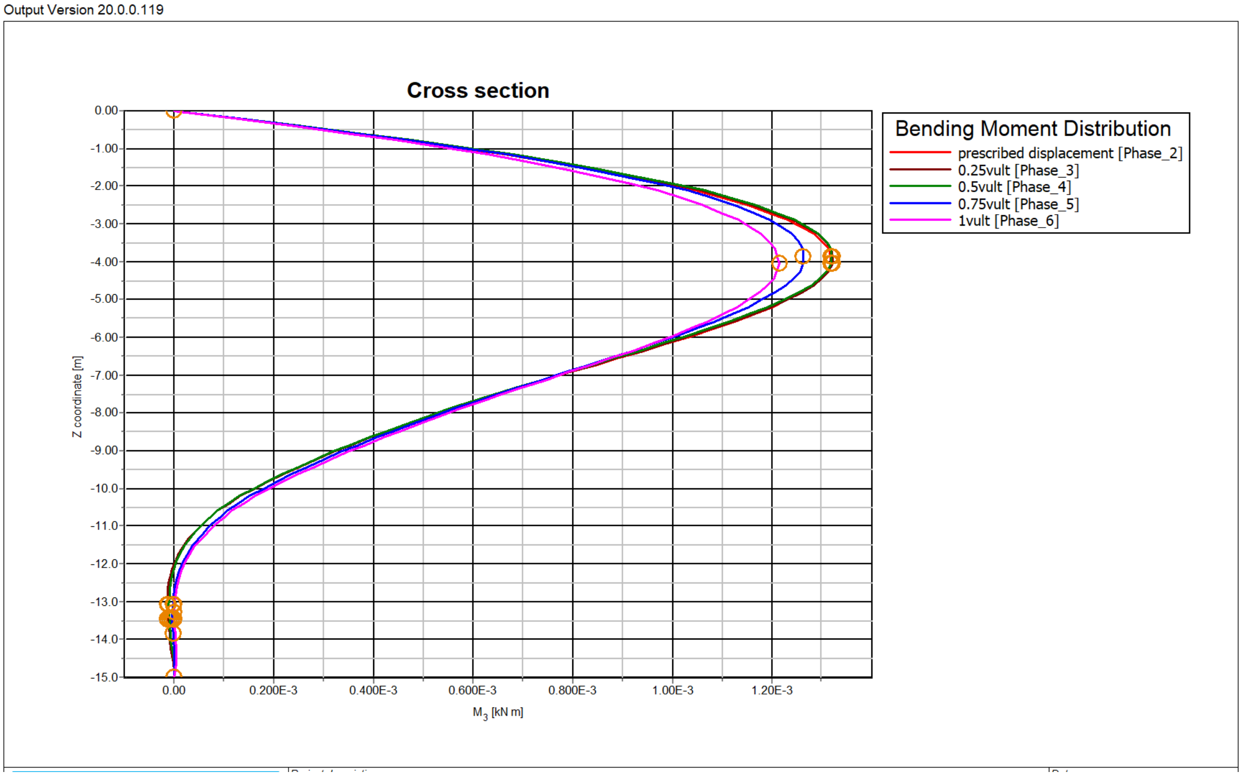

Figure 5.8: Variation of pile bending moment (kNm) with pile depth (m) for pile length 15 with diameter of 0.75m.

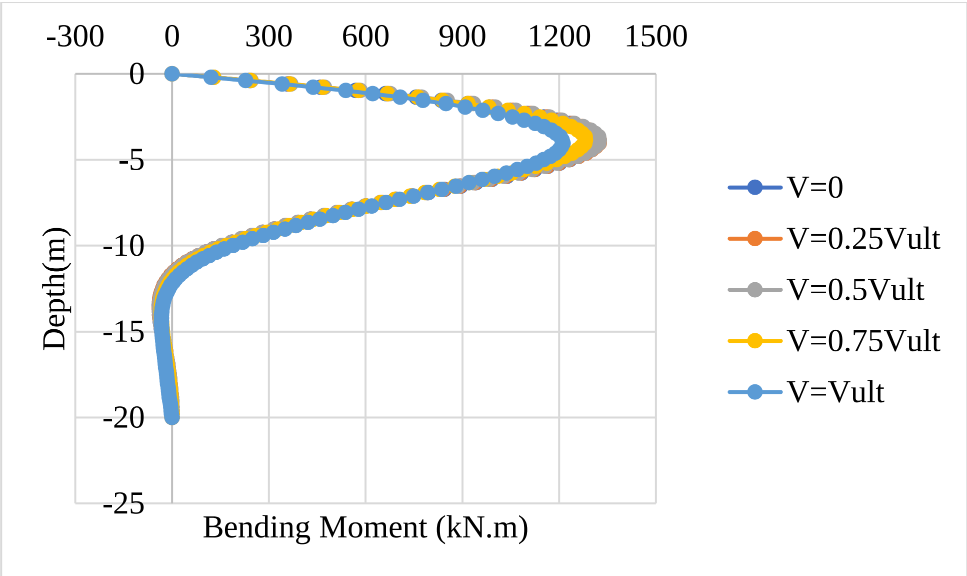

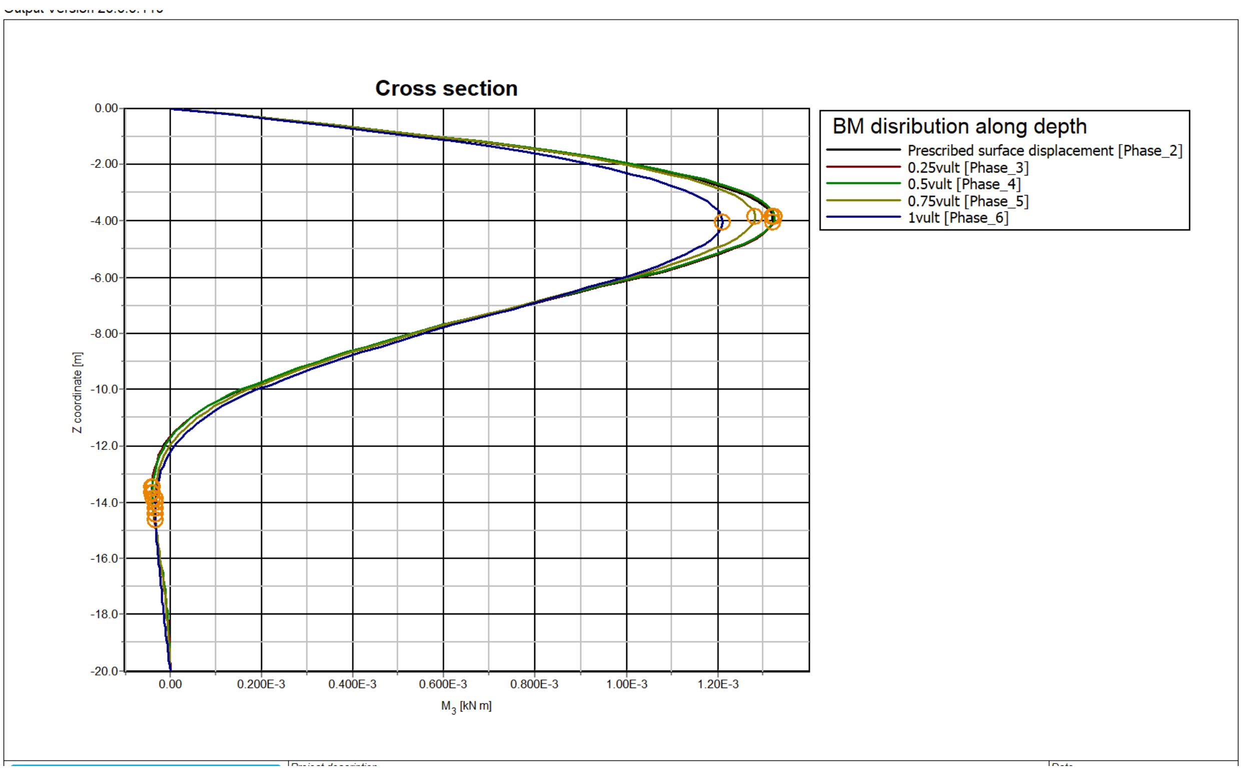

Figure 5.9: Variation of pile bending moment (kNm) with pile depth (m) for pile length 20 with diameter of 0.75m.

The calculated bending moment under different vertical forces are shown in Figures 5.6 to 5.9. The results of the cross-section are directly used from plaxis curve output of inserted beam in volume pile to consider the force components have multiplied by 10^^{6} as specified in section 4. The bending moment tends to increase first and then decrease along the depth. The bending moment *(M)* developed in each pile section was calculated by the summation of the product of the vertical stress *(σzzi)* at each element, the plan area of that element *(A)* and the *x*- distance from the center of the pile to the centroid of the element *(xc)*.

The maximum bending moment decreases with the increase of the pre-applied vertical force and its position moves upwards. When the pre-applied vertical force increases from 0 to 0.25Vult and 0.5Vult, there is no significance change on bending moment. When it increases by 0.75Vult and Vult the maximum bending moment decreases by 7% and 11% (for pile length 10m), 4% and 8% (pile length 15 & 20m) respectively, and its corresponding depth decreases by 5%. The decrease in bending moment is due to large vertical force which increases lateral displacement and decrease in the lateral capacity of the pile.

The mechanism of the decrease in both lateral capacity and bending moment of a pile under the action of vertical loads has been also examined by plotting the stress state (Mohr circle) of a soil element adjacent to the pile and at a depth of maximum stresses. The ultimate shear stress τ, corresponding to the failure, is calculated. The stress distribution of pile with length 15m and 0.75m is used to show these distributions.

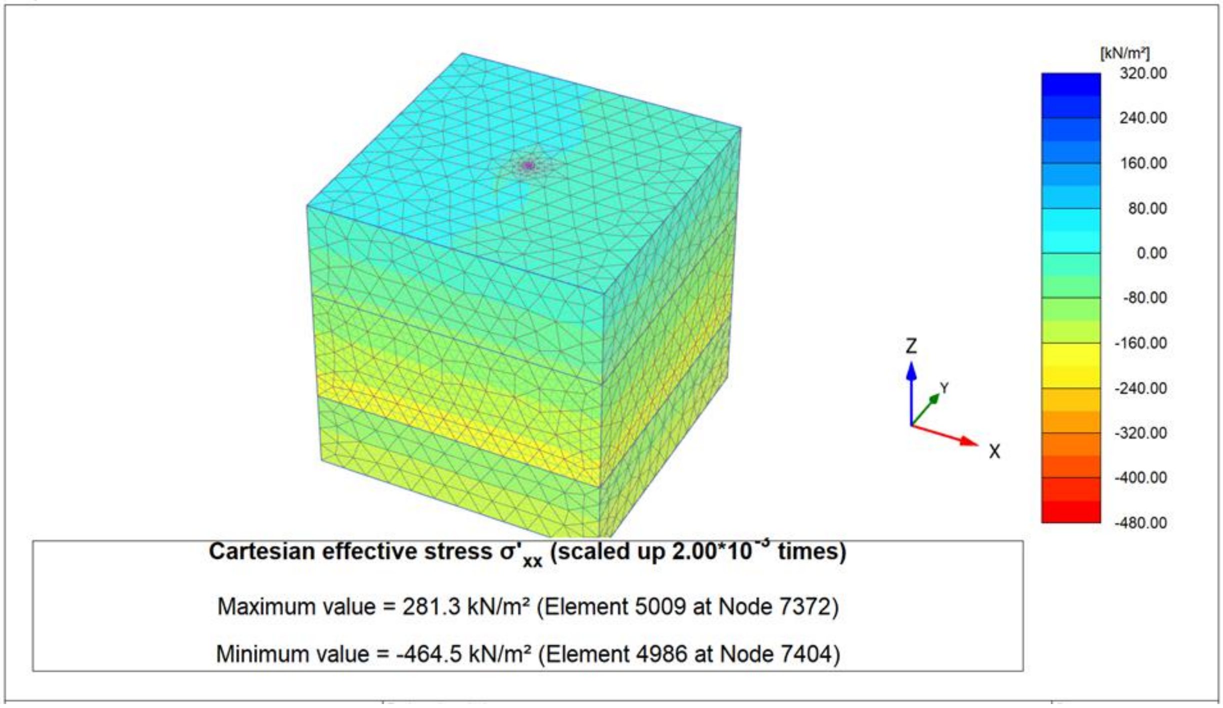

Figure 5.10: Effective stress σ'_{xx}distrubtion for V=0.

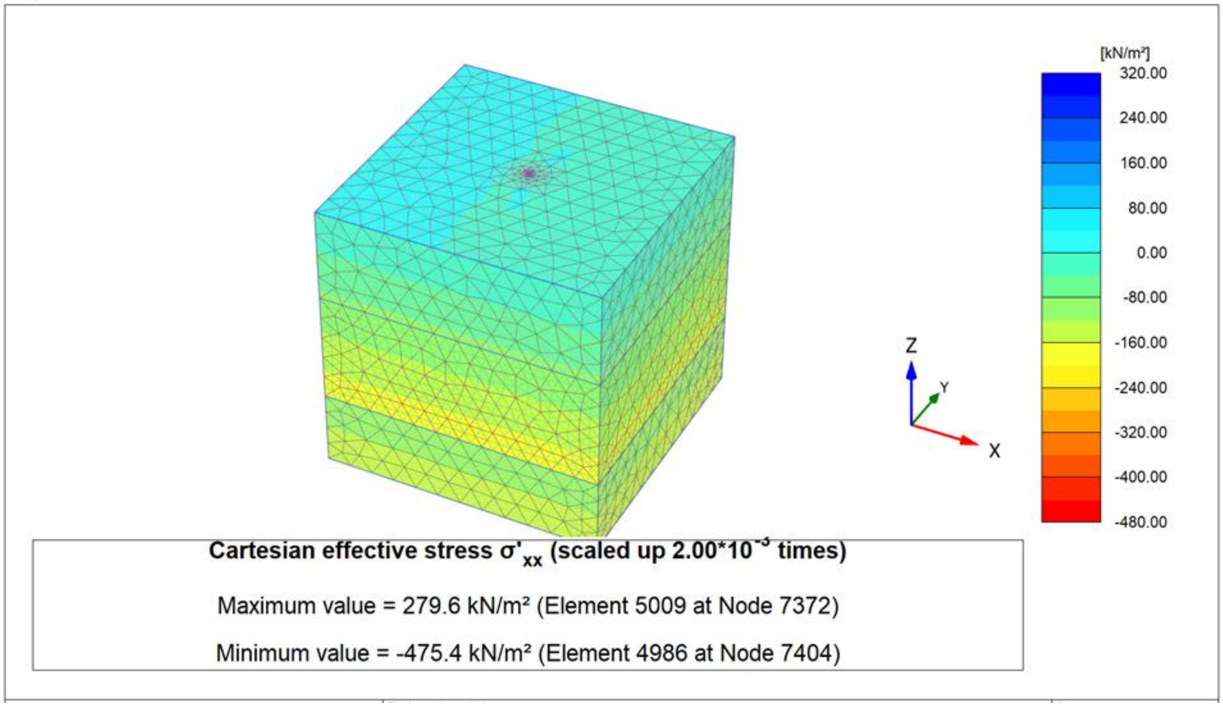

Figure 5.11: Effective stress σ'_{xx}distrubtion for V=0.25Vult.

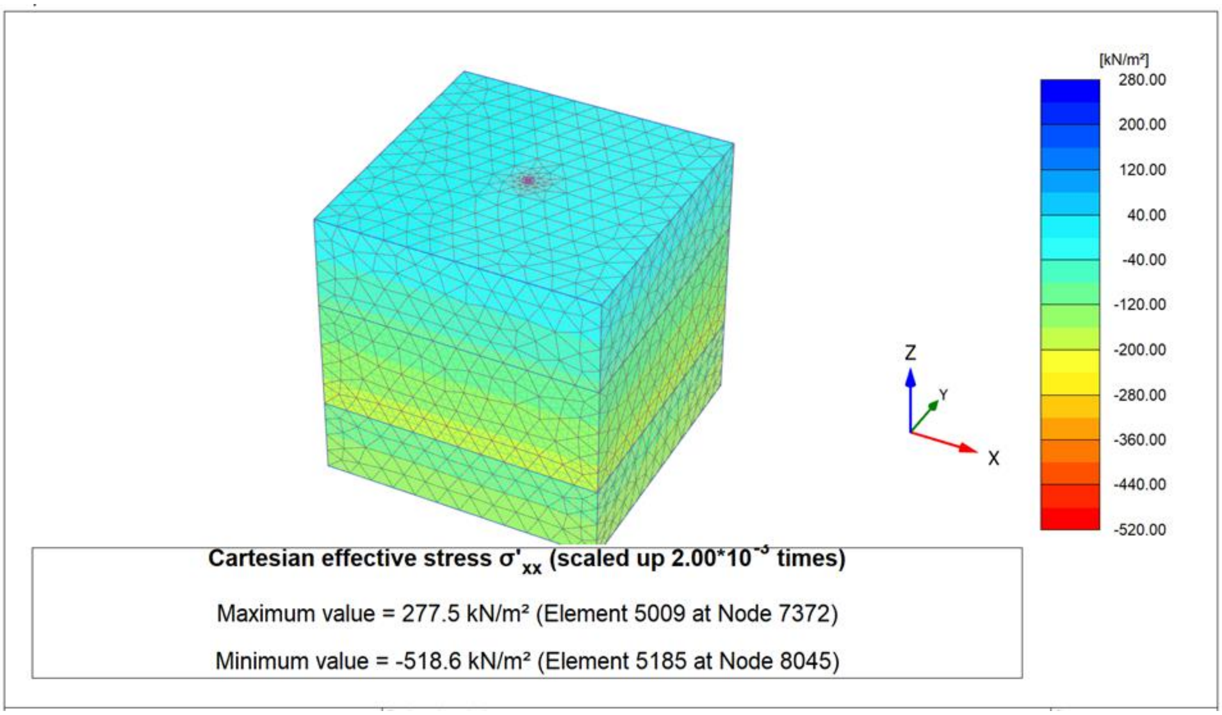

Figure 5.12: Effective stress σ'_{xx}distrubtion for V=0.5Vult.

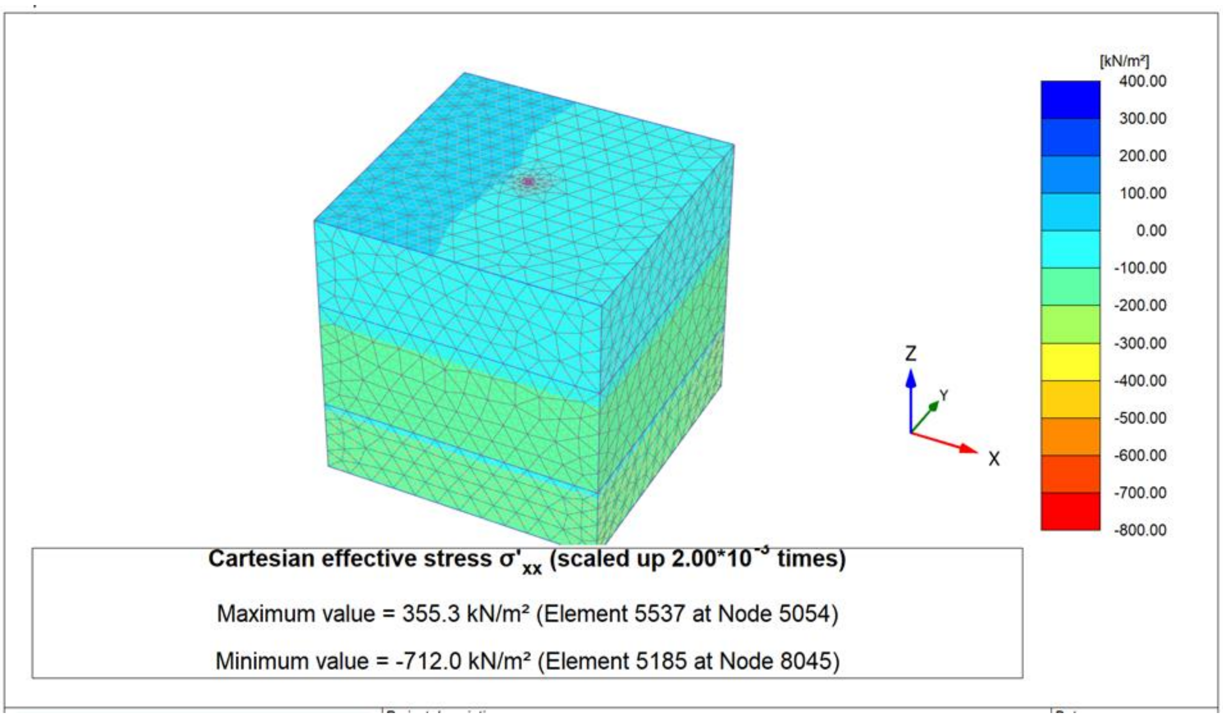

Figure 5.13: Effective stress σ'_{xx}distrubtion for V=0.75Vult.

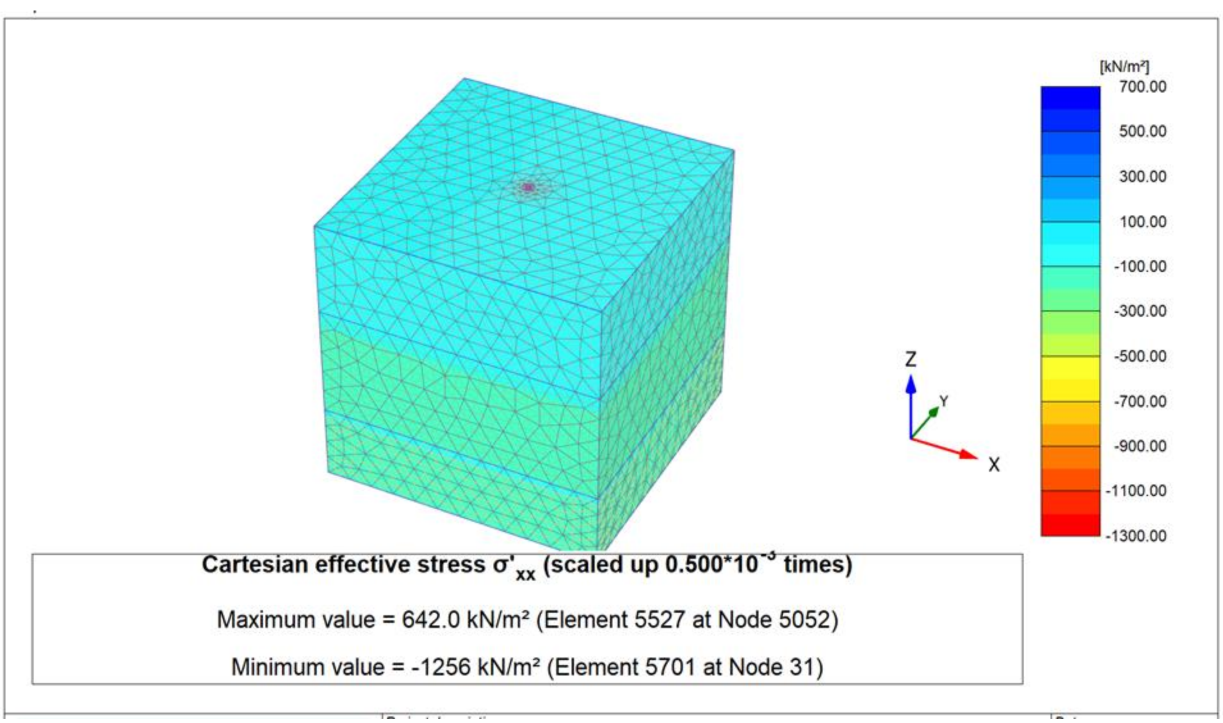

Figure 5.14: Effective stress σ'_{xx}distrubtion for V=Vult.

Figures 5.11 and 5.12 demonstrate that the introduction of vertical loading results in a reduction of soil stresses in comparison to the stresses observed under conditions of solely lateral loading, which subsequently leads to a minor decrease in lateral deflections. Furthermore, Figures 5.13 and 5.14

substantiate that the soil shear strength is attained when V equals 0.75Vult and V equals Vult, whereas a greater lateral pile deflection is requisite in the alternate scenario (V = 0) for the soil to achieve its shear strength.

5.5. Influence of pile slenderness ratio (L/D) on the lateral response of piles

The slenderness ratio means ratio of length to diameter of pile. To show the influence of slenderness ratio (L/D) on lateral response of pile under combined vertical and lateral loads, piles were analyzed with different lengths and widths on soil. The influence of the pile slenderness ratio L/ D under combined loading was studied by performing 3D finite-element analysis by keeping the pile length constant at 15 m and varying the pile widths to 500, 750, 1000, and 1,250 mm.

The lateral and vertical boundaries are changed in accordance with the model presented in section 4, with 40D in the lateral directions and L+20D in the vertical direction. As the cross-section change, the vertical capacity change. Based on the calculated vertical capacities, the effect of vertical loading on the lateral displacement is evaluated.

Based on numerical results obtained, the lateral capacity with respect to different levels of vertical loads is calculated for various L/D ratios with respect to various pile diameter (D) considered in the analysis.

Table 5.1: The lateral capacities for lateral deflection of 0.1D with combined vertical and lateral loading for different L/D – ratios.

L/D Ratio	**Ultimate lateral laod (kN)**				
	V=0	V=0.25Vult	V=0.5Vult	V=0.75Vult	V=Vult
30	253.12	256.31	258.70	260.14	256.68
20	630.15	639.75	647.53	642.38	614.17
15	1210.11	1229.01	1244.16	1233.07	1191.78
12	1978.27	2016.44	2018.45	1912.75	1835.07

As can be observed from Table 5.1, the effect of vertical loading on the lateral capacities decreases with higher L/D ratio after 0.75Vult. For a slenderness ratio of L/D = 12, an initial increase of 2% for 0.25Vult and 0.5Vult and a reduction of 3.3% and 7.2% is observed for vertical loading of 0.75Vult and Vul respectively.

For slenderness ratios L/D =15 and L/D = 20, the lateral capacity given for vertical loading of 0.25Vult, 0.5Vult, and 0.75vult showed a higher capacity then for pure lateral loading and a reduction of 1.5% and 2.5% for Vult respectively. For L/D =30 for vertical loads of 0.25Vult, 0.5Vult, 0.75Vult and Vult the lateral load is increased by 1.3, 2.2, 2.8 and 1.4% respectively. This comes from the effect of the initial stiffness is slightly higher for vertical loading, and for higher slenderness ratios the lateral force displacement curves are observed to be further from a converged value for lateral deflection of 0.1D.

6. CONCLUSIONS AND RECOMMENDATIONS

6.1. Conclusions

The main objective of this study was to investigate the effect of vertical load on the lateral capacity of a single pile by analyzing soil-pile interaction in layered soils. The effect of vertical loads on the performance of laterally loaded piles was explored through the application of numerical modeling techniques. The numerical simulations were executed utilizing the advanced computational software PLAXIS 3D, and parametric analysis, incorporating a range of pile diameters and lengths. These parameters were utilized to assess the lateral capacities and bending moments of concrete piles subjected to both lateral and vertical loading conditions. The outcomes pertaining to the lateral capacities and bending moments of the piles were ascertained and contrasted for piles experiencing solely lateral loads versus those subjected to a combination of vertical and lateral loads across multiple vertical load scenarios corresponding to 25%, 50%, 75%, and 100% of the ultimate vertical load capacity of the pile. From this comparative analysis, the following conclusions can be drawn:

- ❖ The lateral load carrying capacity of the piles is marginally increased up to 50% of vertical ultimate capacity, beyond this increase the lateral load carrying capacity of the piles becomes decreasing This could be attributed to less mobilization of soil stresses behind the piles at higher vertical loads.
- ❖ For a vertical load of up to 75% Vult, the increase in lateral capacity is marginal (1 to 2%) and after this load the lateral capacity is reduced by around 4%. This indicates that the lateral capacity reaches a peak value when the vertical load is between 0.5Vult and 0.75Vult.
- ❖ When the vertical increases by 0.75Vult and Vult the maximum bending moment decreases by 7% and 11% (for pile length 10m), 4% and 8% (pile length 15 & 20m) respectively, and its corresponding depth decreases by 5%.
- ❖ For a slenderness ratio of L/D = 12, an initial increase of 2% for 0.25Vult and 0.5Vult and a reduction of 3.3% and 7.2% is observed for vertical loading of 0.75Vult and Vult.
- ❖ For slenderness ratios L/D =15 and L/D = 20, the lateral capacity given for vertical loading of 0.25Vult, 0.5Vult, and 0.75vult showed a higher capacity then for pure lateral loading and a reduction of 1.5% and 2.5% for Vult respectively.
- ❖ For L/D =30 for vertical loads of 0.25Vult, 0.5Vult, 0.75Vult and Vult the lateral load is increased by 1.3, 2.2, 2.8 and 1.4% respectively.

- The results of this study indicate that the vertical and lateral behavior for slender piles is nearly at higher load uncoupled.
- For non-slender piles, however, the vertical and lateral behavior appears to be highly coupled for vertical loads above 75% of the vertical capacity, and neglecting the effect of vertical loading on the lateral behavior leads to an inaccurate representation of the pile behaviour.

6.2. Recommendations

The results this study will be helpful in developing a better insight into the behavior of single pile foundations and will go a long way in assisting the design and analysis of such a structure with caution.

In this study, the dynamic behavior of the laterally loaded pile is not taken into consideration. Therefore, in the future study is required to consider the dynamic load and its effects on the lateral capacity of laterally loaded pile.

In this study, free headed pile was considered. It is recommended to investigate the effects of vertical load on lateral response of pile with fixed head conditions.

References

A.M.Trochanis, J.Bielak and P.Christiano. (1991). Three-dimensional nonlinear study of piles. *J. Geotech. Eng, 117*(3), 429–447.

Anagnostopoulos, C., & Georgiadis, M. (1993). Interaction of Axial and Lateral Pile Response. *Journal of Geotechnical Engineering, 119*(4), 793–798.

B .McClelland and J. A. Jr.Focht. (1958a). *Soil modulus for laterally loaded piles.*

B.B.Broms. (1964a, b, 1965). Design of laterally loaded piles. *J. Soil Mechanics and Foundations Division, ASCE, 91*(SM3), 79-99.

B.Hansen, J. (1961). The ultimate resistance of rigid piles against transversal forces. *Bulletin, Danish Geotechnical Institue, Copenhagen, 11*, 5-9.

Basu, D., R. Salgado, and M. Prezzi. (2008). *Analysis of Laterally Loaded Piles in Multilayered Soil Deposits.* FHWA/IN/JTRP.

Bowles, J. E. (1996). *Foundation Analysis and Design* (5 ed.). McGraw-Hill Companies, Inc.

Briaud, J.-L. (2013). *Geotechnical Engineering: Unsaturated and Saturated Soil.* New Jersey Hoboken : John Wiley & Sons, Inc.

C.Desai and G.Appel. (1976). 3-D analysis of laterally loaded structures. *Proceedings of the 2nd International Conference on Numerical Methods in Geomechanics*, (pp. 405–418). Blacksburg.

C.Reese, L. (1986). *Behavior of Piles and Pile Groups Under Lateral Load.* Washington D.C: Federal Highway Administration.

D.A. Brown and C.F. Shie. (1990,1991). Three dimensional finite element model of laterally loaded piles. *Comput. Geotec, 10*(1), 59–79.

D.A.Brown,M. Kumar,et al. (1989). PY curves for laterally loaded piles derived from three-dimensional finite element model. Numerical models in geomechanics. *Numog III. Proceedings of the 3rd International Symposium Held in Niagara falls*.

D.Douglas and E.Davis. (1964). The movement of buried footings due to moment and horizontal load and the movement of anchor plates. *Geotechnique, 14*(2), 115–132.

Davisson MT and Robinson KE. (1965). Bending and buckling of partially embedded piles. *Sixth Int. Conf. on Soil Mech. and Foundation Engineering, 2*, pp. 243–246. Montreal .

E.A.Dickin and R.B.Nazir. (1999). Moment-carrying capacity of short pile foundations in cohesionless soil. *Geotechnical and Geoenvironmental Engineering ASCE, 125*(1), 1-10.

E.Barber. (1953). Discussion to paper by SM Gleser. *154*, pp. 96–99 .

F.Ismael, N. (1998). Lateral loading tests on bored piles in cemented sands. *Proceedings of the 3rd International Geotchnical Seminar on Deep Foundation on Bored and Auger piles. 3rd*, pp. 137-144. Belguim: Ghent.

F.Scott, R. (1981). *Foundation Anaysis.* Prentice-Hall, Engel Wood Cliffs, NJ.

Goryunov.BF. (1975). Discussion on analysis of piles subjected to the combined action of vertical and horizontal Loads. *J Soil Mech Foundation Eng, 10*(1).

H.G.Poulos. (1971a,b). Behavior of laterally loaded piles. *Journal of Soil Mechanics and Foundation, 97*(5), 711-751.

H.G.Poulos. (1973). Analysis of piles in soil undergoing lateral movement. *Journal of Soil Mechanics and Foundation Division, 99*(5), 391–406.

H.G.Poulos and E.H.Davis. (1980). *Pile Foundation Analysis and Design.* New York: Wiley and Sons.

H.G.Poulos and T.S.Hull. (1989). The role of analytical mechanics in foundation. *Foundation Engineering, Current Principals and Practices.*

H.Matlock and L.C.Reese. (1960). Generalized solutions for laterally loaded piles. *Journal of Soil Mechanics and Foundations Division, 86*(5), 63–94.

Hazzar, L., Hussien, M. N., & Karray, M. (2017). Influence of vertical loads on lateral response of pile foundations n sands and clays. *Journal of Rock Mechanics and Geotechnical Engineering, 9*, 291–304.

Hencher, S. (2012). *Practical engineering geology.* New York: CRC Press.

J.R.Peng, M.Rouainia,and B.Clarke. (2010). Finite element analysis of laterally loaded fin piles. *Comput. Struct, 88*(21), 1239–1247.

K.Yang and R.Liang. (2006). A 3D FEM model for laterally loaded drilled shafts in rock. *Int. GeoCongress 2006@ sGeotechnical Engineering in the Information Technology Age*, 1–6.

Karthigeyan, S., Ramakrishna, V. V. G. S. T., & Rajagopal, K. (2007). Numerical Investigation of the Effect of Vertical Load on the Lateral Response of Piles. *Journal of Geotechnical and Geoenvironmental Engineering, 133*(5), 512–521.

Ken Fleming Ken, Austin Weltman,Mark Randolph and Keith Elson. (2009). *Piling Engineering* (3rd ed.). London and New York: Taylor & Francis.

Lymon C. Reese and Hudson Matlock. (1956). Nondimensional solutions for laterally loaded piles with soil modulus assumed proportional to depth. *Proceedings of the VIII Texas Conference on Soil Mechanics and Foundation Engineering.* Austin: University of Texas.

Lymon C.Reese and William F.Van Impe. (2011). *Single Piles and Pile Groups under Lateral Loading.* CRC Press Taylor & Francis Group Boca Rotan.

M.A.Biot. (1937). Bending of an infinite beam on an elastic foundation. *Journal of Applied Mechanics, 2(3)*, 165–184.

M.Ahmadi and S.Ahmari. (2009). Finite-element modelling of laterally loaded piles in clay. *162*(3), 151–163.

M.Budhu and T.G.Davies. (1987,1988). Nonlinear analysis of laterality loaded piles in cohesionless soils. *Canadian Geotechnical Journal, 24*(2), 289–296.

M.F.Randolph. (1981). The response of flexible piles to lateral loading. *Geotechnique, 31*(2), 247–259.

M.Faruque and C.Desai. (1982). 3-D material and geometric nonlinear analysis of piles. *Proceedings of the Second International Conference on Numerical Methods in Offshore Pilling*, 553–575.

M.Hetenyi. (1946). *Beams on Elastic Foundation.* The University of Michigan Press.

M.Jamiolkowski and A.Garassino. (1977). Soil modulus for laterally loaded piles. *In Proceedings of the Specialty Session 10, Ninth International Conference on Soil Mechanics and Foundation Engineering,* (pp. 43-58). Tokyo.

M.Mardfekri, P.Gardoni and J.M. Rosset. (2013). Modeling laterally loaded single piles accounting for nonlinear soil-pile interactions. *J. Eng, 3*, 1-7.

M.Wood, D. (1990). *Soil Behaviour and Critical State Soil Mechanics*. New York: Cambridge University Press.

N. Sivakugan, B. M. Das, J. Lovisa and C. R. Patra. (2014). Determination of c and w of rocks from indirect tensile strength and uniaxial compression tests. *International Journal of Geotechnical Engineering, 8*.

P.K.Banerjee and T.G Davis. (1978). The behaviour of axially and laterally loaded single piles embedded in non-homogeneous soils. *Geotechnique, 28*, 309–326.

P.Kavitha, K.Beena and K.Narayanan. (2016). A review on soil–structure interaction analysis of laterally loaded piles. *Innov. Infrastruct. Solut, 1*, 1-15.

P.W.Rowe. (1956). The single pile subject to horizontal force. *Géotechnique, 6*(2), 70-85.

Peck RB, Hanson WE and Thornburn TH. (1974). *Foundation engineering* (2nd edn ed.). New York: Wiley & Sons Inc.

R.B.J. Brinkgreve and W. Broere. (2006). *Plaxis 3D Foundation Reference Manual Version 1.5.* DELFT, Netherlands.

R.D.Mindlin. (1936). Force at a point in the interior of a semi-infinite solid. *Journal of Applied Physics, 7*(5), 195–202.

R.Tuladhar, H. Mutsuyoshi and T.Maki. (2013). Numerical modelling and full-scale testing of concrete piles under lateral loading. *Aust. J. Struct. Eng, 14*(3), 229–242 .

S. Karthigeyan, V. V. G. S. T. Ramakrishna and K. Rajagopal. (2007). Numerical investigation of the effect of vertical load on the. *Journal of Geotechnical and Geoenvironmental Engineering, Vol. 133, No. 5,* .

Sawwaf, M. E. (2006). Lateral Resistance of Single Pile Located Near Geosynthetic Reinforced Slope. *Geotechnical and Geoenvironmental Engineering*.

Shamsher Prakash and Hari D. Sharma. (1990). *Pile foundations in engineering practice.* John Wiley & Sons, Inc.

Stroud, M. A. (1974). The Standard Penetration Test in Insensitive Clays and Soft Rocks. *Proceedings of the European Symposium on Penetration Testing, 2*, pp. 367-375. Stockholm.

T.Davies and M.Budhu. (1986). Non-linear analysis of laterally loaded piles in heavily overconsolidated clays. *Geotechnique, 36*(4), 527–538.

Terzaghi, K. (1955). Evaluation of coefficient of subgrade reaction. *Geotechniques, 5(4),* 297-326.

W.R.Spillers and R.D.Stoll. (1964). Lateral response of piles. *Journal of Soil Mechanics and Foundation Division, 90*(6), 1–10.

Z.Yang and B.Jeremi. (2005). Study of soil layering effects on lateral loading behavior of piles. . *Geotech. Geoenviron. Eng, 131*(6), 762–770 .

APPENDICES

The appendices include the following

- Appendix A: Soil profile from Geotechnical Investigation
- Appendix B: Vertical capacity analyses
- Appendix C: Lateral response to axial loading

Appendix A: Soil profile from Geotechnical Investigation

Table A-1: Description of strata and corrected SPT blow count for BH1

BH No.	Depth of test	N	Description of stratum based on visual inspection and lab index property test results	N'55 (corrected)
1	1.50 – 1.95	26	Medium stiff, black, highly plastic silty CLAY(CH)mixed with some gravel.	28.5
	2.00 – 7.00	-	Ignimbrite	-
	7.50 – 7.95	17	Very stiff to hard, reddish brown, highly plastic clayey SILT (MH) with traces of sand	11.1
	9.00 – 9.45	20		11.9
	10.50 – 10.95	33		19.2
	12.00 – 12.45	21	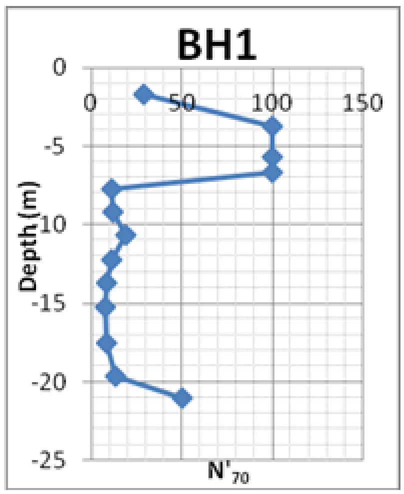	11.5
	13.50 – 13.95	16	Stiff, variegated color, highly plastic SILT(MH) with weak core stones (weathering product of vesicular/scoracious BASALT).	8.2
	15.00-15.45	16		7.8
	17.25 – 17.70	18		8.2
	19.40 – 19.85	30		12.9
	21.00	R		50
	22.40 -59.85	-	BASALTIC layer with a wide range of degree of fracturing and intensity of weathering (gravely soil of varying thickness is intercalated with this rock layer at varying depths)	

Table A-2: Description of strata and corrected SPT blow count for BH2

BH No.	Depth of test	N	Description of stratum based on visual inspection and lab index property test results	N'55 (corrected)
2	1.50 – 1.95	22/R	Contact between medium stiff soil and decomposed IGNIMBRITE	76.7
	3.00 – 3.45	21	Stiff to v. stiff red to yellowish, highly plastic SILT(MH) with traces of sand	16.3
	5.00 – 5.45	21		14.5
	6.50 – 6.95	22	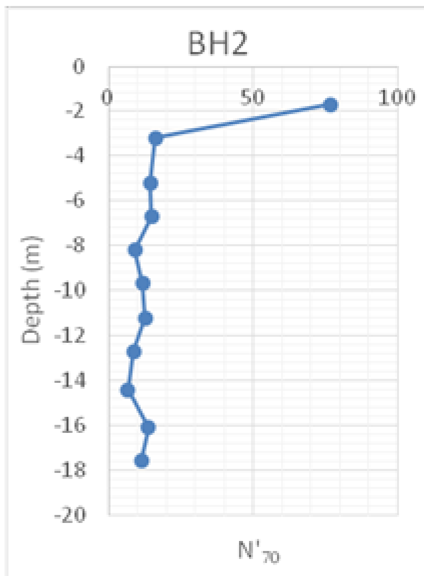	15.0
	8.00 – 8.45	15		9.2
	9.50 – 9.95	21		11.9
	11.00 – 11.45	23		12.7
	12.50 – 12.95	17		8.8
	14.2 – 14.65	14	Stiff to hard, variegated color, highly plastic SILT(MH) with weak core stones (weathering product of vesicular scorious basalt)	6.8
	15.90 - 16.35	30		13.8
	17.40 – 17.85	26		11.5
	22.40 – 65.00	-	BASALTIC layer with a wide range of degree of fracturing and intensity of weathering (gravely soil of varying thickness is intercalated with this rock layer at varying depths)	-

Table A-3: Description of strata and corrected SPT blow count for BH3

BH No.	Depth of test	N	Description of stratum based on visual inspection and lab index property test results	N'55 (corrected)
3	4.50 – 4.95	30	Very stiff to hard, red, highly plastic SILT(MH)	21.8
	6.50 – 6.95	21	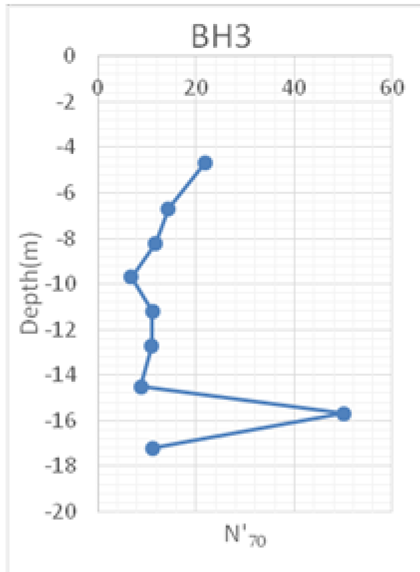	14.3
	8.00 – 8.45	19		11.7
	9.50 – 9.95	12		6.8
	11.00 – 11.45	20		11.1
	12.50 – 12.95	21		10.9
	14.00 -14.95	18		8.8
	15.50 – 15.95	R		50
	17.00 – 17.45	25		11.2
	20.00 – 80.00	-	BASALTIC layer with a wide range of degree of fracturing and intensity of weathering (gravely soil of varying thickness is intercalated with this rock layer at varying depths)	

Table A-4: Description of strata and corrected SPT blow count for BH4

BH No.	Depth of test	N	Description of stratum based on visual inspection and lab index property test results	N'55 (corrected)
4	1.50 – 1.95	7	Medium stiff, dark to light gray, highly plastic CLAY to SILT (CH-MH)	7.5
	3.00 -3.45	19	Very stiff, reddish brown, highly plastic silty Clay (MH)	14.8
	4.50 – 4.95	18		13.1
	6.00 – 6.45	19		13.4
	7.65 – 8.10	10	Stiff to hard, variegated color (predominantly brown), highly plastic SILT with clay (MH)	6.3
	9.15 – 9.60	10	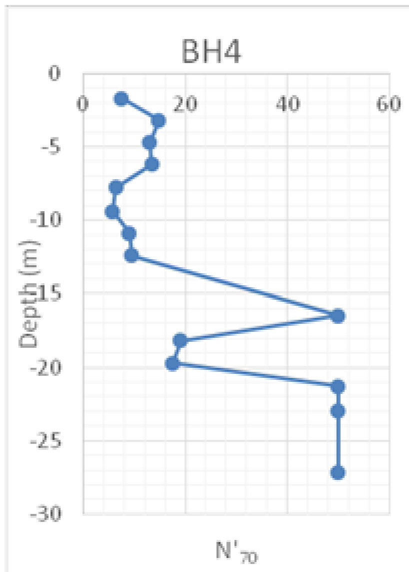	5.7
	10.65 – 11.10	16		9.0
	12.15 – 12.60	18		9.5
	16.50	R		50
	18.00 – 18.45	44		19.1
	19.50 – 19.95	42		17.5
	21.30	R		50
	23.00	R		50
	27.15	R	V. dense, reddish brown silty Sand (SM) with gravel and weak core stones	50
	23.15 – 70.00		BASALTIC layer with a wide range of degree of fracturing and intensity of weathering (gravely soil of varying thickness is intercalated with this rock layer at varying depths)	

Table A-5: Description of strata and corrected SPT blow count for BH5

BH No.	Depth of test	N	Description of stratum based on visual inspection and lab index property test results	N’55 (corrected)
5	2.00 – 2.45	9	Stiff, dark brown, highly plastic SILT (MH)	8.4
	4.00 – 4.45	18	Stiff to v. stiff, reddish brown, highly plastic SILT(MH) (weathering product of ignimbrite)	13.8
	5.70 – 6.15	22		14.3
	7.50 – 7.95	18		11.4
	11.00 – 11.45	25	V. stiff, variegated color (dark brown), highly plastic SILT (MH) with intermittent weak core stone	13.1
	12.50 – 12.95	R	Hard, variegated color, non to low plastic sandy SILT (MS) with weak core stones (weathering product of vesicular/scoracious BASALT); Below 19.25m: rockier 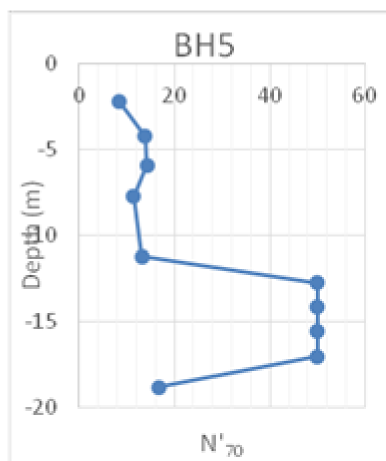	50
	14.05	R		50
	15.50	R		50
	17.00	R		50
	18.80	39		16.7
	20.00 – 85.00		BASALTIC layer with a wide range of degree of fracturing and intensity of weathering (gravely soil of varying thickness is intercalated with this rock layer at varying depths)	

Appendix B: Vertical capacity analyses

The vertical capacities are calculated by applying a prescribed surface displacement at the top of the pile in Plaxis 3D. The purpose of using a surface displacement is to distribute the stresses at the top of the pile evenly.

Table B. 1: Vertical capacities of pile with length 10m

L=10m, Dia=0.5m		L=10m, Dia=0.75m		L=10m, Dia=1m		L=10m, Dia=1.25m	
Vertical Load (kN)	Vertical Displacement (mm)	Vertical Load (kN)	Vertical Displacement (mm)	Vertical Load (kN)	Vertical Displacement (mm)	Vertical Load (kN)	Vertical Displacement (mm)
0.00	0.00	0.00	0.00	0.00	0.00	0.00	0.00
10.86	0.13	14.51	0.15	22.10	0.20	30.58	0.25
32.59	0.40	43.53	0.45	66.29	0.60	91.74	0.75
76.03	0.94	101.57	1.05	154.67	1.40	213.96	1.75
160.31	2.01	215.65	2.25	326.67	3.00	448.89	3.75
236.71	3.09	322.20	3.45	485.54	4.60	664.36	5.75
303.86	4.16	418.77	4.65	627.88	6.20	853.92	7.75
360.52	5.23	505.21	5.85	748.97	7.80	1011.61	9.75
403.06	6.31	578.80	7.05	843.47	9.40	1123.50	11.75
420.49	7.38	629.63	8.25	903.49	11.00	1291.30	15.75
434.01	8.45	689.07	10.65	1003.58	14.20	1552.09	23.75
460.22	10.60	739.25	13.05	1089.72	17.40	1766.00	31.75
483.79	12.74	783.13	15.45	1245.83	23.80	1955.84	39.75
504.91	14.89	862.41	20.25	1384.67	30.20	2124.32	47.75
524.30	17.04	931.61	25.05	1510.01	36.60	2279.18	55.75
542.73	19.18	995.17	29.85	1626.75	43.00	2352.35	59.75
560.13	21.33	1025.25	32.25	1734.26	49.40	2493.87	67.75
576.87	23.48	1054.86	34.65	1834.38	55.80	2627.77	75.75
592.82	25.62	1083.39	37.05	1928.73	62.20	2756.57	83.75
608.33	27.77	1111.04	39.45	2017.46	68.60	2879.66	91.75
623.44	29.92	1137.71	41.85	2102.41	75.00	2998.93	99.75
638.20	32.06	1163.68	44.25	2184.21	81.40	3113.07	107.75
652.52	34.21	1189.04	46.65	2263.05	87.80	3222.67	115.75
666.44	36.36	1238.47	51.45	2339.31	94.20	3329.76	123.75
680.04	38.50	1285.55	56.25	2406.10	100.00	3346.14	125.00
693.34	40.65	1330.40	61.05				
706.36	42.80	1373.51	65.85				
719.07	44.94	1414.81	70.65				
743.58	49.24	1450.76	75.00				
747.82	50.00						

Table B. 2: Vertical capacities of pile with length 15m

L=15m, Dia=0.5m		L=15m, Dia=0.75m		L=15m, Dia=1m		L=15m, Dia=1.25m	
Vertical Load (kN)	Vertical Displacement (mm)	Vertical Load (kN)	Vertical Displacement (mm)	Vertical Load (kN)	Vertical Displacement (mm)	Vertical Load (kN)	Vertical Displacement (mm)
0.00	0.00	0.00	0.00	0.00	0.00	0.00	0.00
13.69	0.10	28.87	0.17	58.05	0.31	59.78	0.29
41.06	0.30	86.60	0.52	174.14	0.92	179.34	0.86
95.82	0.70	202.07	1.22	406.30	2.15	418.45	2.00
205.25	1.50	431.47	2.61	859.11	4.60	890.44	4.28
312.50	2.30	652.94	4.01	1285.88	7.06	1344.18	6.56
416.26	3.10	865.17	5.40	1589.98	9.52	1770.98	8.84
516.41	3.90	1066.81	6.79	1761.53	11.97	2023.66	11.12
613.06	4.70	1197.00	8.19	1857.72	14.43	2204.73	13.41
792.97	6.30	1282.45	9.58	2013.53	19.34	2329.17	15.69
896.84	7.90	1335.06	10.98	2155.52	24.25	2555.41	20.25
944.15	9.50	1413.15	13.76	2282.60	29.16	2764.92	24.82
998.28	12.70	1539.99	19.34	2398.76	34.08	2957.46	29.38
1040.80	15.90	1649.71	24.91	2507.73	38.99	3136.26	33.95
1060.57	17.50	1743.43	30.49	2610.61	43.90	3302.80	38.51
1079.98	19.10	1827.07	36.06	2708.78	48.81	3458.47	43.07
1098.51	20.70	1902.88	41.64	2802.00	53.72	3740.34	52.20
1116.29	22.30	1974.30	47.21	2890.60	58.63	3994.80	61.33
1133.14	23.90	2042.23	52.79	2975.71	63.55	4234.03	70.46
1165.57	27.10	2075.08	55.58	3057.32	68.46	4348.85	75.02
1195.91	30.30	2139.66	61.15	3136.13	73.37	4462.13	79.59
1224.22	33.50	2201.62	66.73	3212.65	78.28	4517.60	81.87
1251.20	36.70	2261.81	72.30	3286.58	83.19	4626.13	86.43
1277.05	39.90	2290.15	75.00	3358.68	88.11	4652.77	87.57
1301.85	43.10			3428.57	93.02	4705.85	89.86
1325.75	46.30			3496.71	97.93	4810.43	94.42
1348.89	49.50			3524.46	100.00	4861.64	96.70
1352.43	50.00					4912.83	98.98
						4963.35	101.27
						4988.21	102.41
						5037.85	104.69
						5087.05	106.97
						5183.81	111.53
						5278.02	116.10
						5324.51	118.38

						5370.77	120.66
						5416.64	122.94
						5457.68	125.00

Table B. 3: Vertical capacities of pile with length 20m

L=20m, Dia=0.5m		L=20m, Dia=0.75m		L=20m, Dia=1m		L=20m, Dia=1.25m	
Vertical Load (Kn)	Vertical Displacement (mm)	Vertical Load (Kn)	Vertical Displacement (mm)	Vertical Load (Kn)	Vertical Displacement (mm)	Vertical Load (Kn)	Vertical Displacement (mm)
0.00	0.00	0.00	0.00	0.00	0.00	0.00	0.00
17.16	0.10	34.11	0.15	82.96	0.31	109.39	0.34
51.48	0.30	102.33	0.45	248.88	0.93	328.16	1.01
120.13	0.70	238.77	1.05	580.71	2.16	765.70	2.36
257.40	1.50	511.41	2.25	1235.65	4.64	1632.13	5.07
392.84	2.30	779.94	3.45	1867.58	7.11	2468.70	7.77
525.23	3.10	1042.21	4.65	2471.37	9.59	3265.53	10.47
654.76	3.90	1298.52	5.85	2848.40	12.06	3885.36	13.17
781.38	4.70	1548.53	7.05	2986.51	14.53	4210.00	15.88
1027.02	6.30	2005.67	9.45	3171.56	19.48	4421.31	18.58
1255.42	7.90	2195.07	11.85	3330.49	24.43	4602.05	21.28
1434.95	9.50	2265.07	14.25	3482.01	29.38	4912.81	26.69
1484.37	11.10	2378.74	19.05	3754.09	39.27	5180.64	32.09
1543.57	14.30	2488.50	23.85	3989.61	49.17	5302.78	34.79
1591.12	17.50	2588.97	28.65	4100.37	54.12	5418.69	37.49
1636.38	20.70	2760.27	38.25	4209.48	59.07	5634.82	42.90
1719.42	27.10	2909.40	47.85	4314.13	64.02	5736.70	45.60
1789.48	33.50	2977.50	52.65	4415.79	68.96	5838.53	48.30
1852.99	39.90	3043.60	57.45	4515.59	73.91	5937.93	51.01
1882.71	43.10	3106.35	62.25	4612.91	78.86	6036.05	53.71
1911.95	46.30	3166.54	67.05	4708.41	83.81	6083.83	55.06
1939.83	49.50	3224.54	71.85	4801.97	88.76	6131.79	56.41
1944.08	50.00	3261.58	75.00	4894.10	93.70	6226.33	59.11
				4984.48	98.65	6273.07	60.46
				5008.86	100.00	6366.31	63.17
						6412.19	64.52
						6504.08	67.22
						6594.66	69.92
						6684.65	72.62
						6773.70	75.33

						6817.60	76.68
						6905.10	79.38
						7078.19	84.78
						7163.67	87.49
						7333.94	92.89
						7418.24	95.59
						7585.85	101.00
						7750.95	106.40
						8076.63	117.21
						8221.44	122.08
						8307.72	125.00

Appendix C: Lateral response to axial loading

C.1: Lateral Load Capacity

The lateral capacities for lateral deflection of 0.1D with combined vertical and lateral loading for different pile length and diameters are presented below.

Table C. 1: The lateral capacities for lateral deflection of 0.1D with combined vertical and lateral load of pile 10m length with different diameters.

Pile Diameter (m)	**Pile Length (m)**	**Lateral capacity(kN)**				
		V=0	V=0.25Vult	V=0.5Vult	V=0.75Vult	V=Vult
0.5	10	253.12	256.31	258.70	260.14	256.68
0.75	10	616.38	628.43	633.84	624.35	600.32
1	10	1014.55	1043.24	1043.24	1028.43	984.58
1.25	10	1405.03	1455.74	1467.00	1439.88	1377.42

Figure B.1, B.2, B.3, and B.4 presents the lateral force - displacement for pile diameters of D=0.5m, D=0.75m, D=1.00m, D=1.25m for lateral deflection of 0.1D.

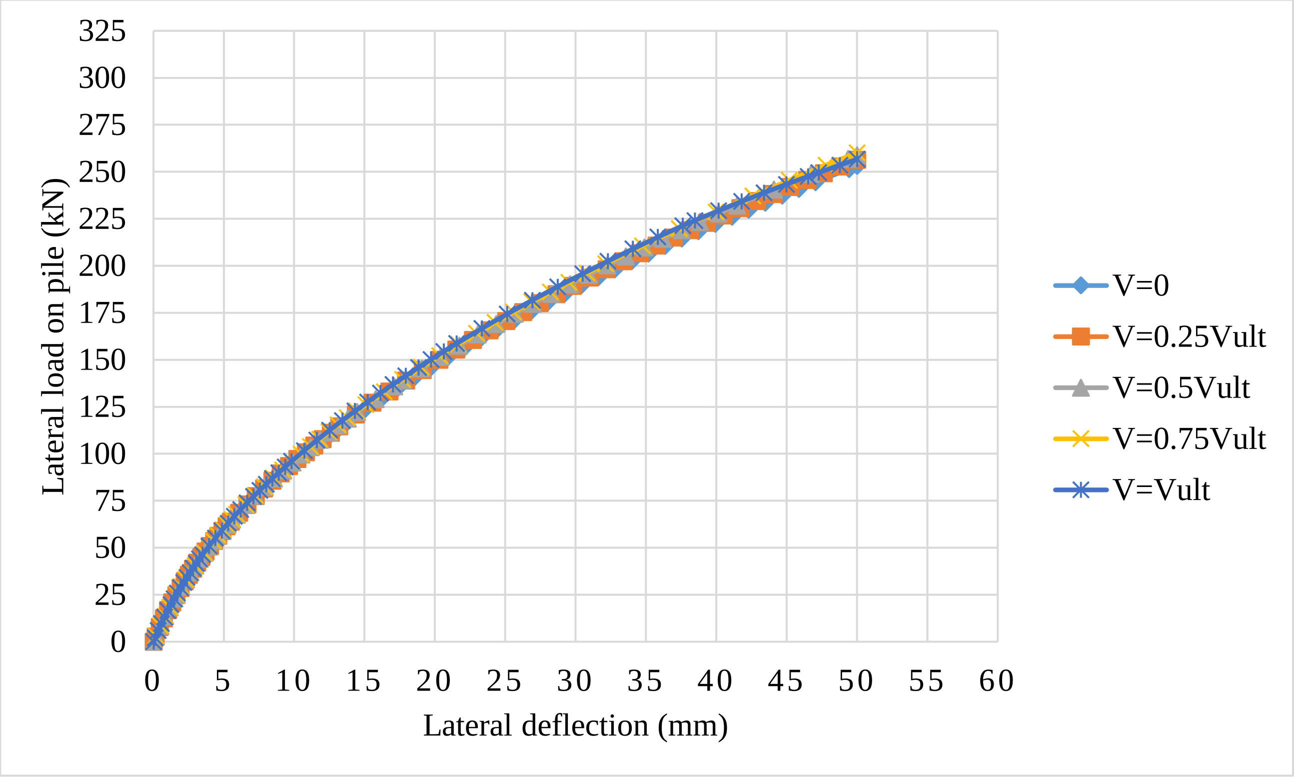

Figure C. 1: Lateral force-displacement for D=0.5m.

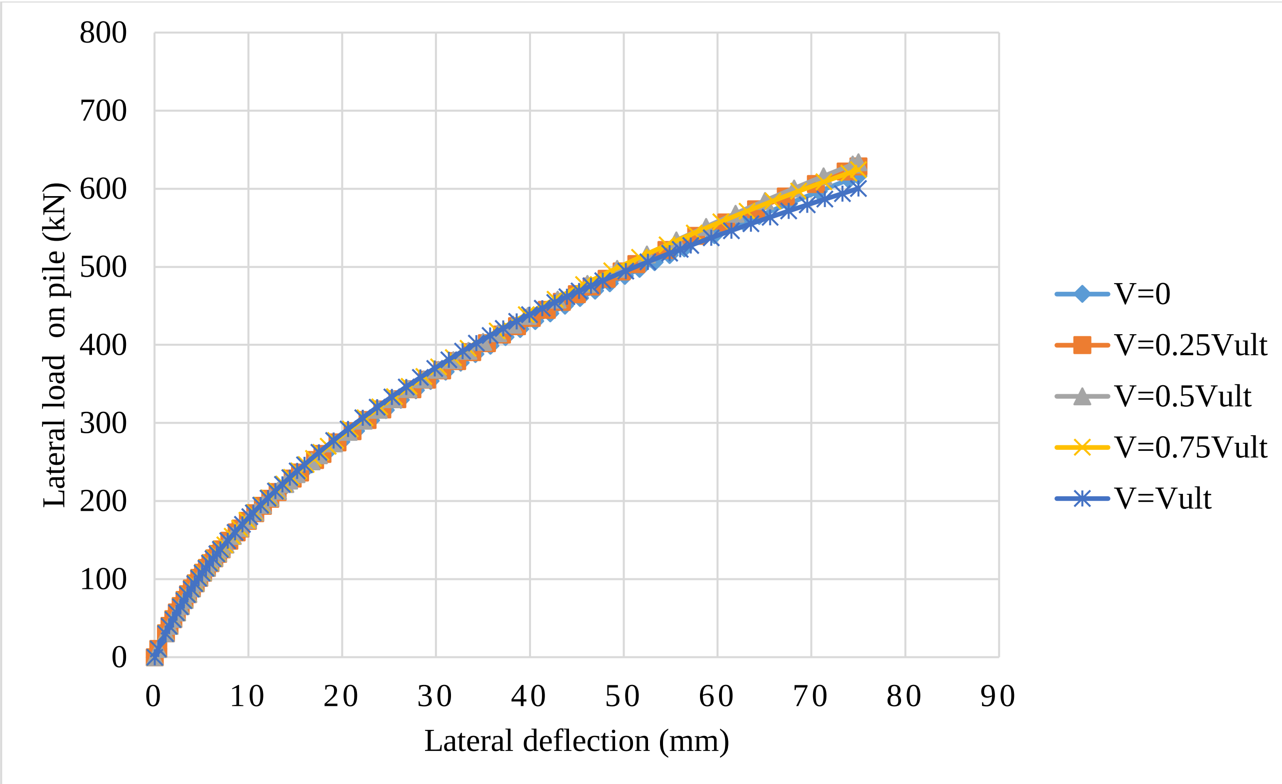

Figure C. 2: Lateral force-displacement for D=0.75m.

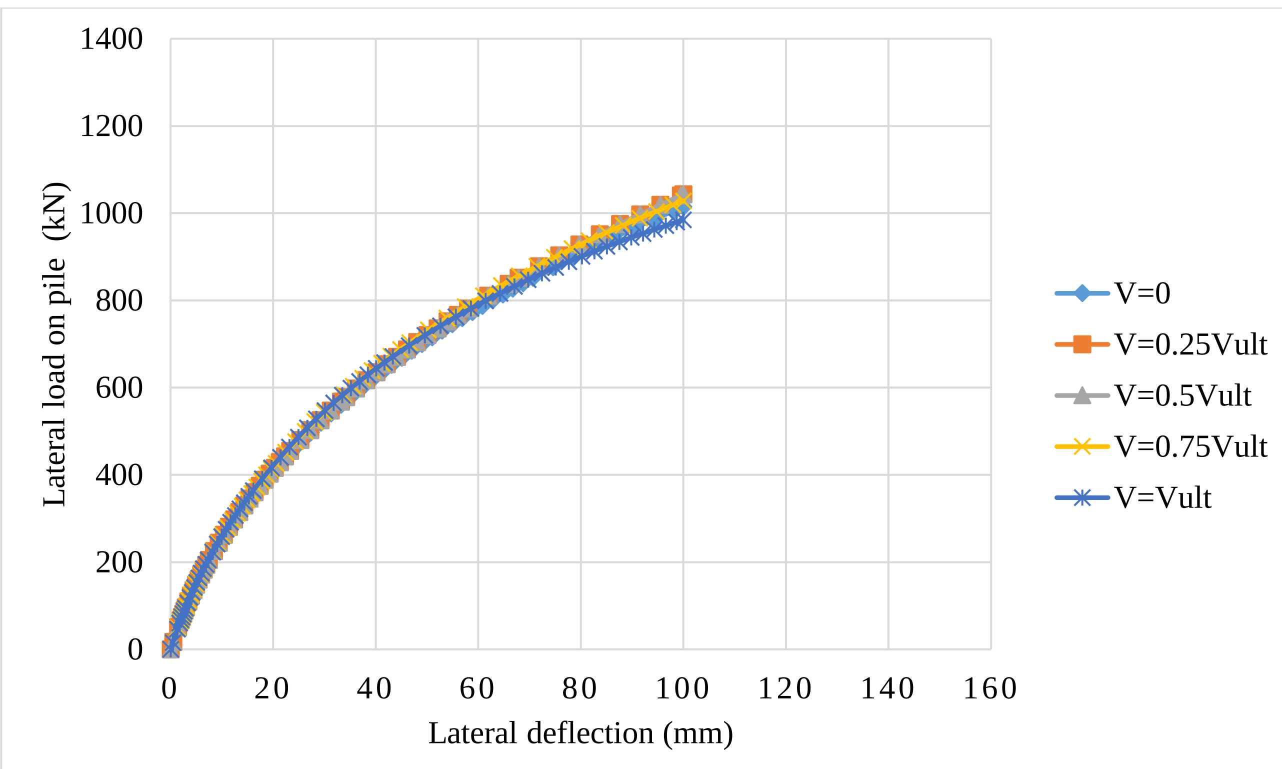

Figure C. 3: Lateral force-displacement for D=1.00m.

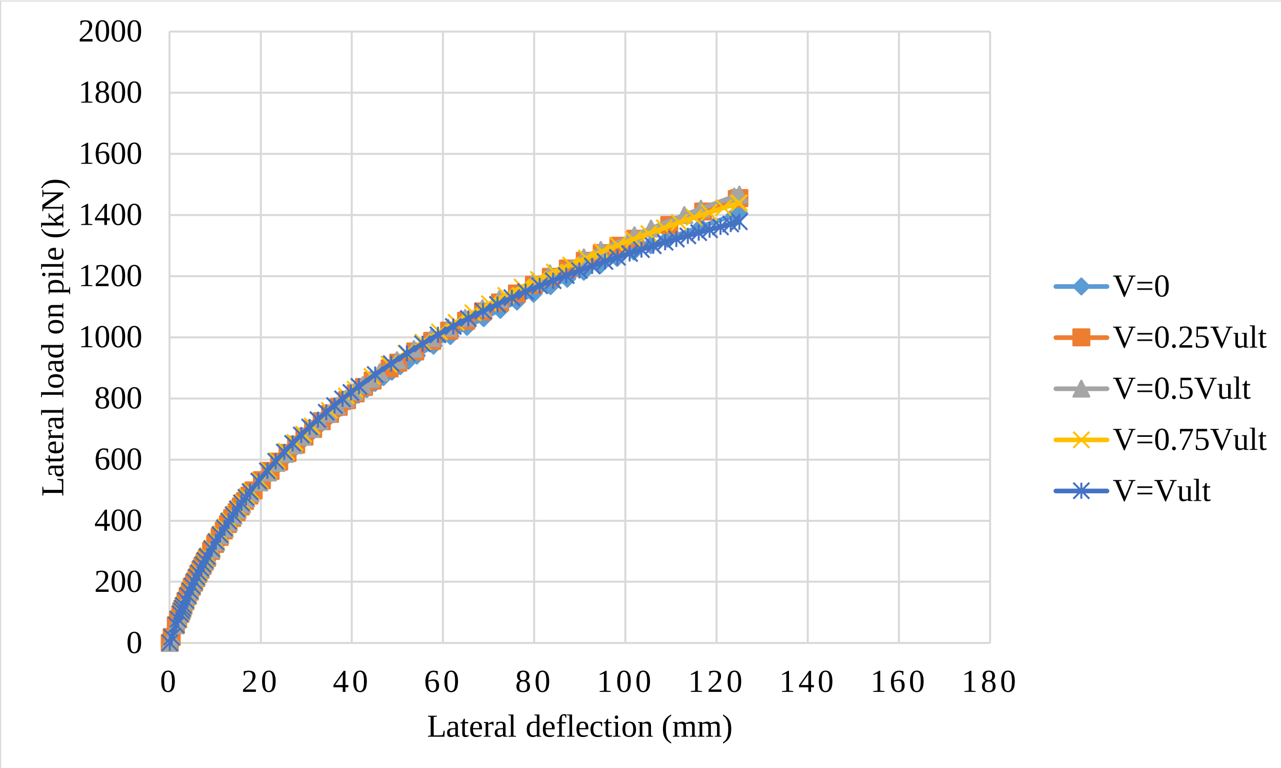

Figure C. 4: Lateral force-displacement for D=1.25m.

Table C. 2: The lateral capacities for lateral deflection of 0.1D with combined vertical and lateral load of pile 15m length with different diameters.

Pile Diameter (m)	Pile Lenght (m)	lateral capacity(kN)				
		V=0	V=0.25Vult	V=0.5Vult	V=0.75Vult	V=Vult
0.5	15	253.12	256.31	258.70	260.14	256.68
0.75	15	630.15	639.75	647.53	642.38	614.17
1	15	1210.11	1229.01	1244.16	1233.07	1191.78
1.25	15	1978.27	2016.44	2018.45	1912.75	1835.07

Figure C.5, C.6, C.7, and C.8 presents the lateral force - displacement for pile diameters of D=0.5m, D=0.75m, D=1.00m, D=1.25m for lateral deflection of 0.1D.

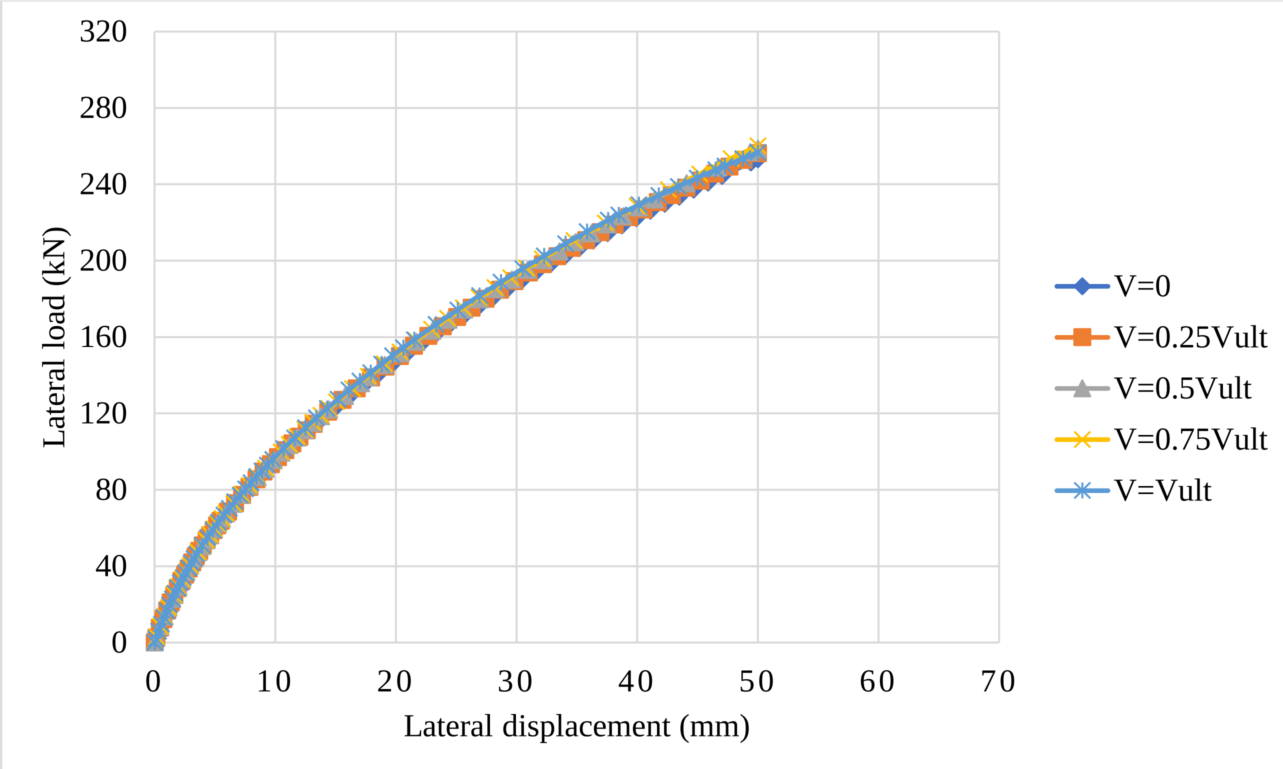

Figure C. 5: Lateral force-displacement for D=0.5m.

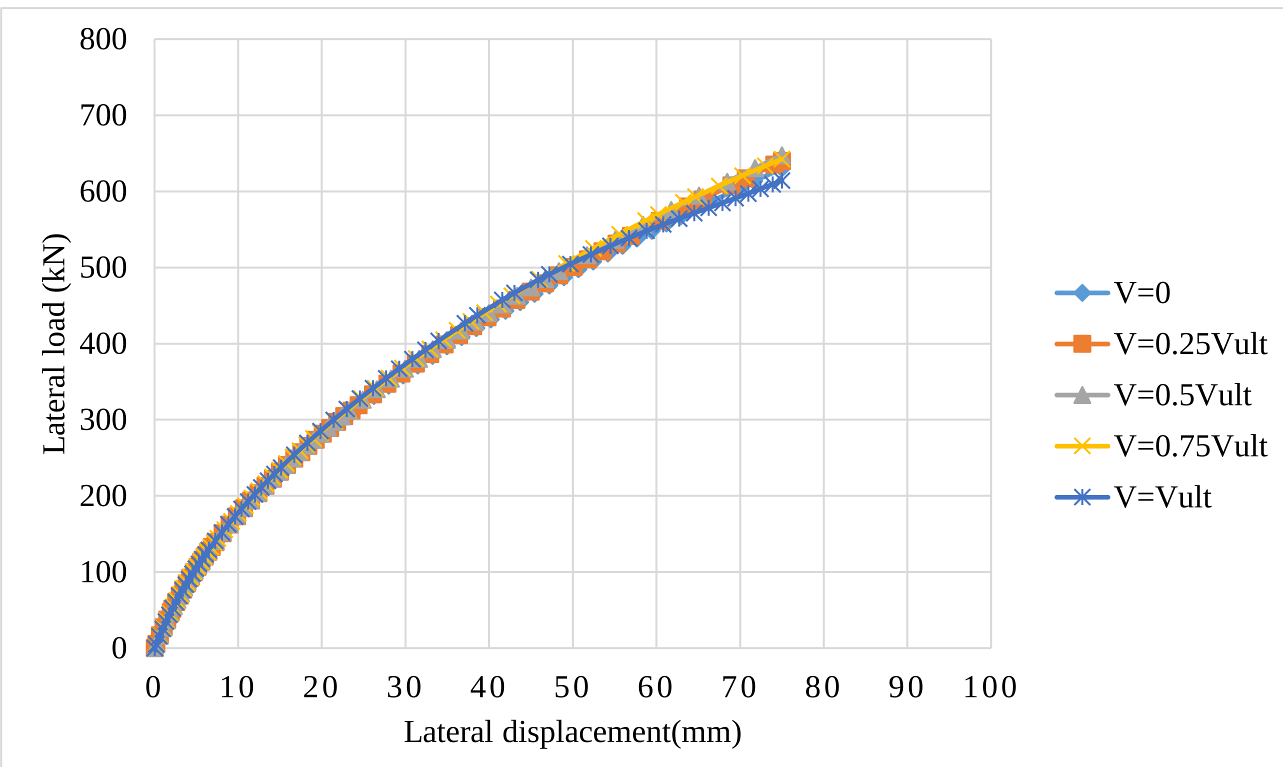

Figure C. 6: Lateral force-displacement for D=0.75m.

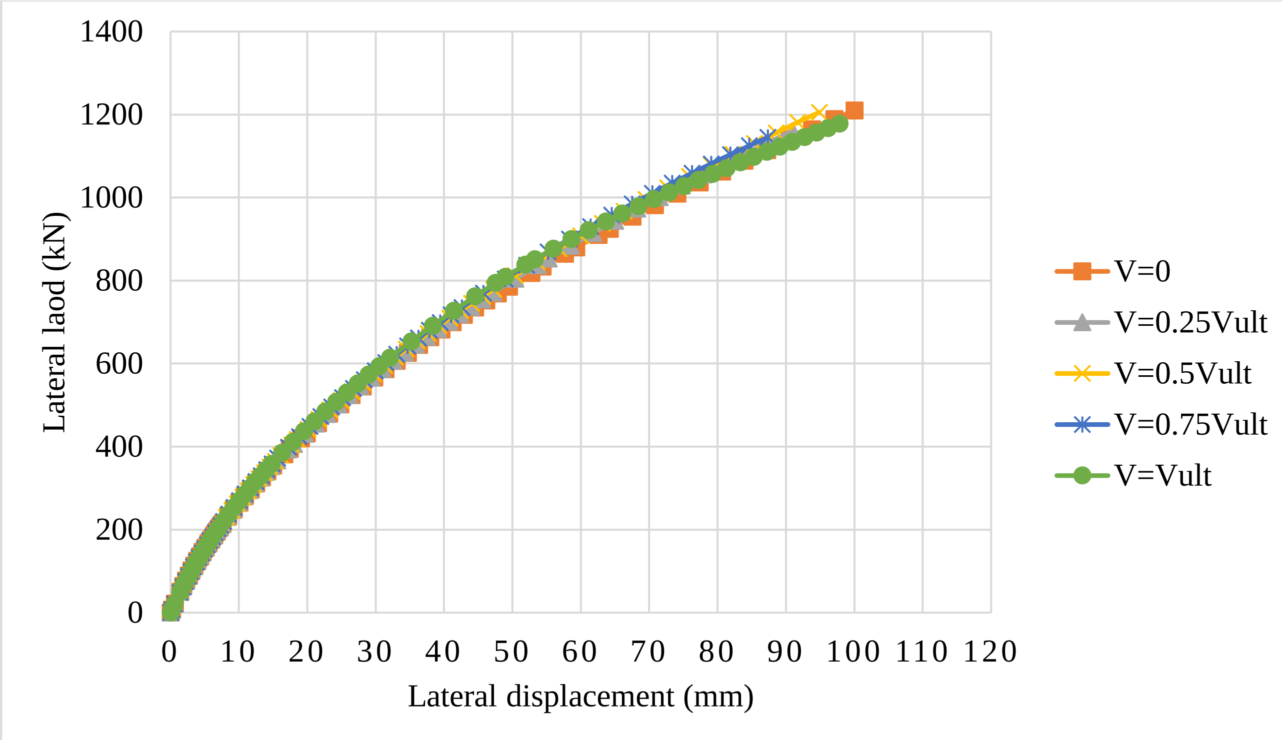

Figure C. 7: Lateral force-displacement for D=1.00m.

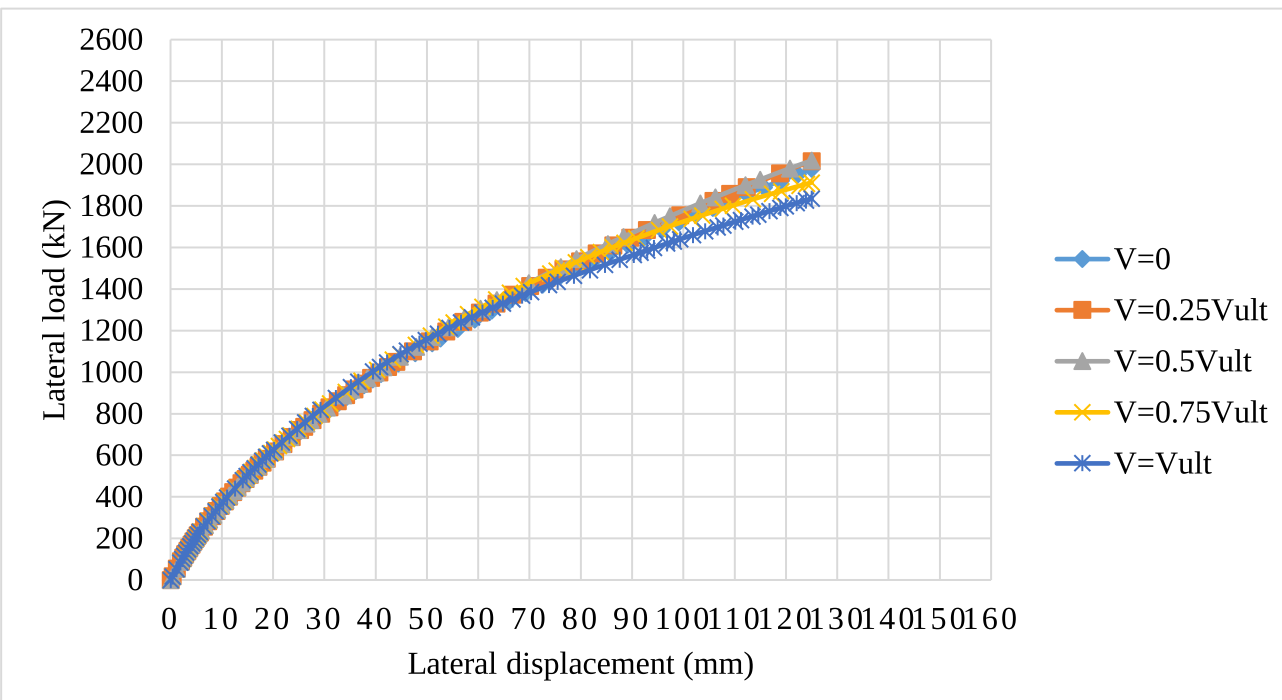

Figure C. 8: Lateral force-displacement for D=1.25m.

Table C. 3: The lateral capacities for lateral deflection of 0.1D with combined vertical and lateral load of pile 20m length with different diameters.

Pile Diameter (m)	Pile Lenght (m)	Ultimate lateral laod (kN)				
		V=0	V=0.25Vult	V=0.5Vult	V=0.75Vult	V=Vult
0.5	20	250.93	251.80	252.64	253.44	254.22
0.75	20	628.81	638.03	645.68	642.73	606.37
1	20	1221.77	1239.72	1255.24	1246.54	1194.82
1.25	20	2021.54	2055.10	2083.12	2056.54	1989.51

Figure C.9, C.10, C.11, and C.12 presents the lateral force - displacement for pile diameters of D=0.5m, D=0.75m, D=1.00m, D=1.25m for lateral deflection of 0.1D

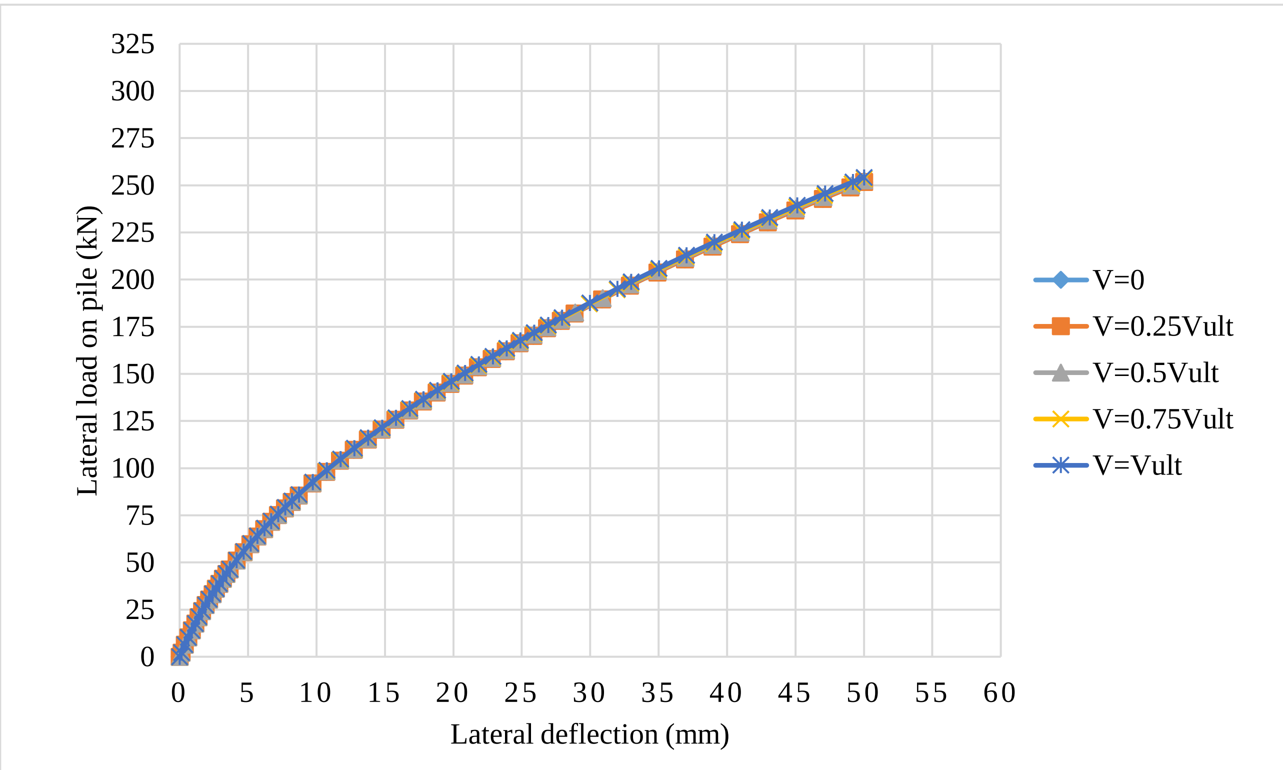

Figure C. 9: Lateral force-displacement for D=0.5m.

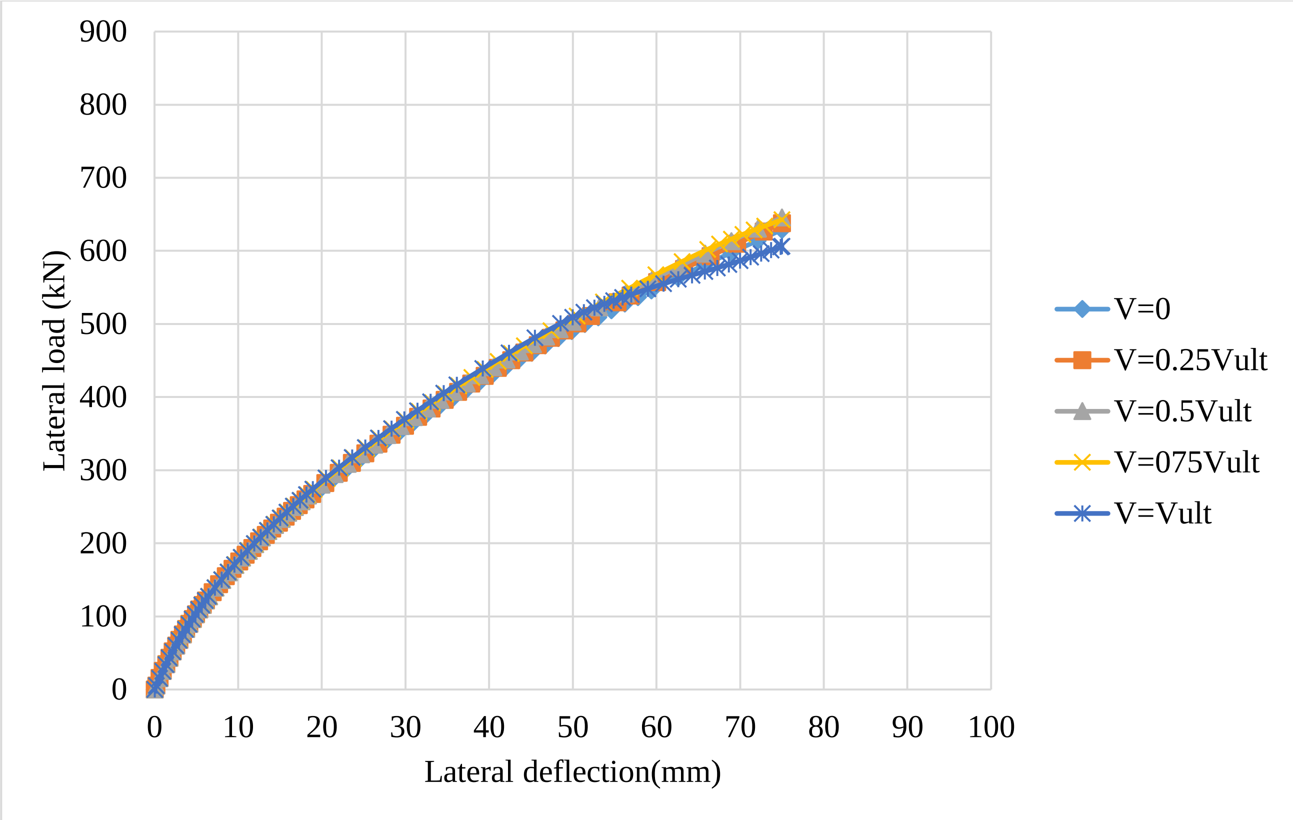

Figure C. 10: Lateral force-displacement for D=0.75m.

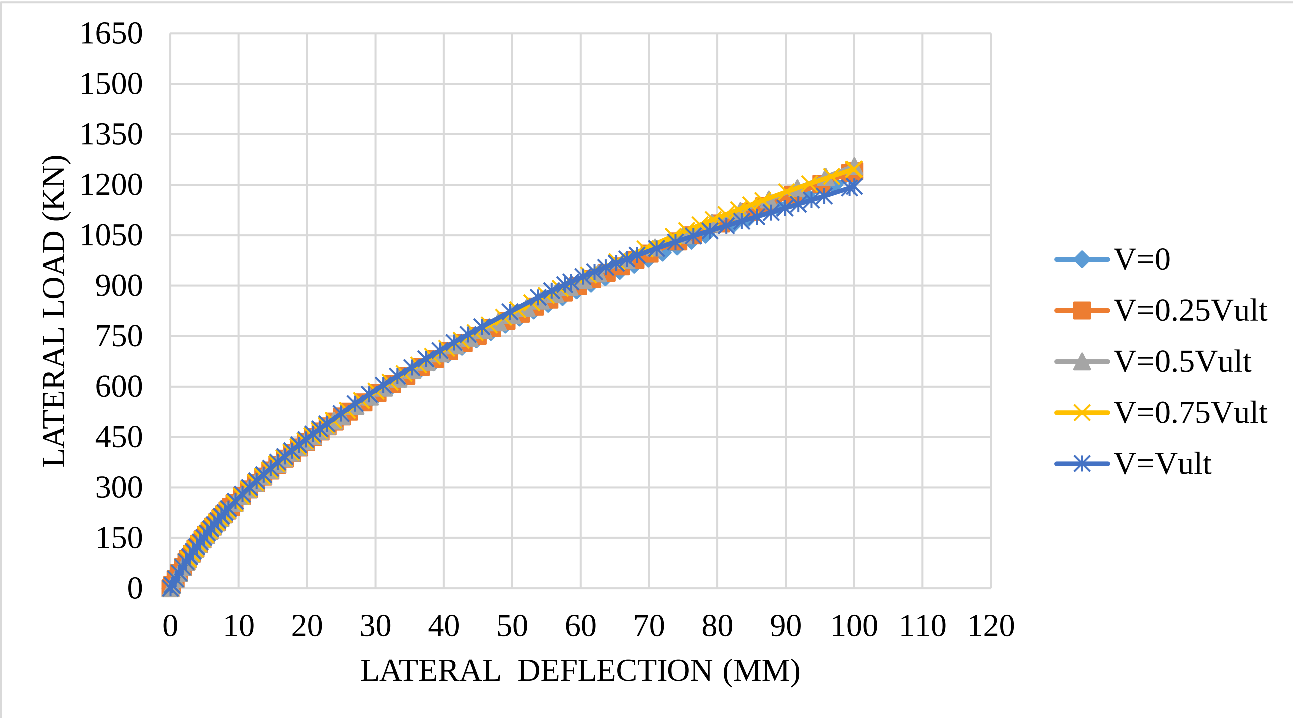

Figure C. 11: Lateral force-displacement for D=1.00m.

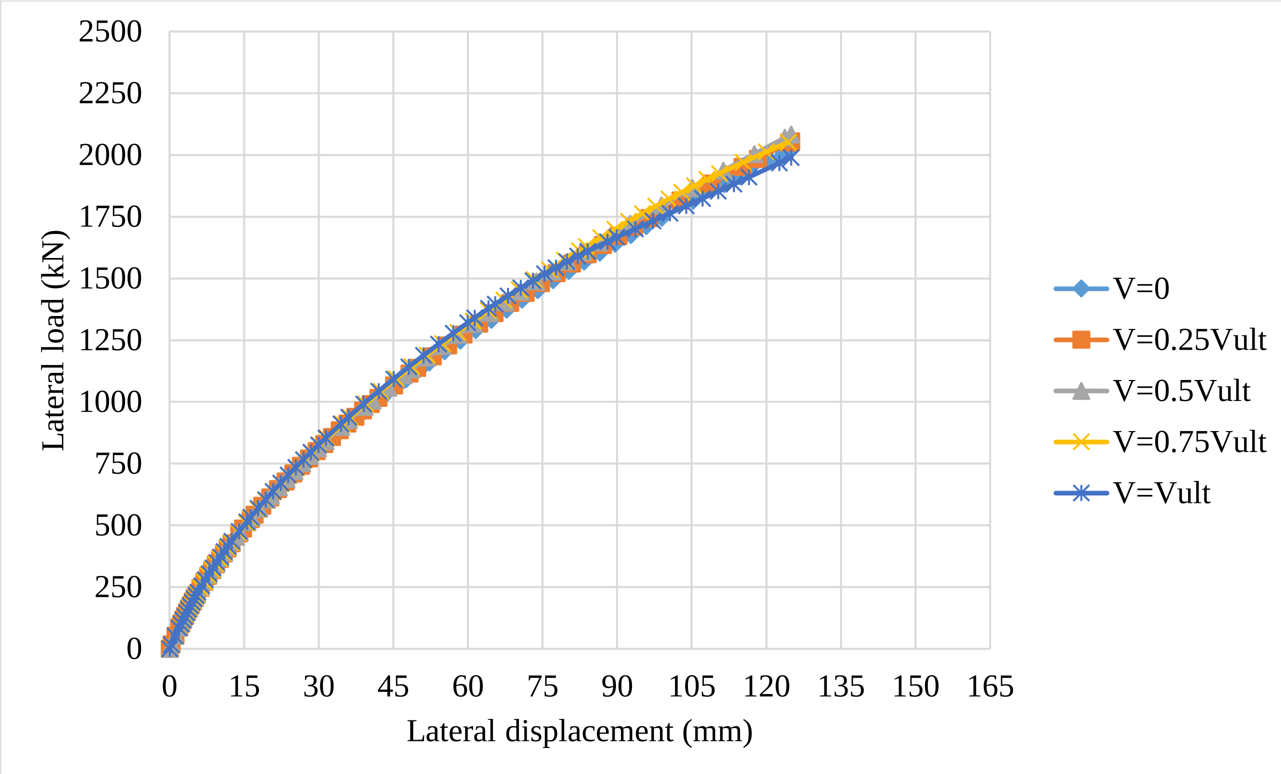

Figure C. 12: Lateral force-displacement for D=1.25m.

C.2: Effect of L/D-ratio

The lateral capacities for lateral deflection of 0.1D with combined vertical and lateral loading for different slenderness ratios are presented in Table C.4 to C.6.

Table C. 4: The lateral capacities for lateral deflection of 0.1D with combined vertical and lateral load of constant pile length 10m.

L/D ratio	**Pile Diameter (m)**	**Pile length (m)**	**latera capacity (kN)**				
			V=0	V=0.25Vult	V=0.5Vult	V=0.75Vult	V=Vult
20	0.5	10	253.12	256.31	258.70	260.14	256.68
13.33	0.75	10	616.38	628.43	633.84	624.35	600.32
10	1	10	1014.55	1043.24	1043.24	1028.43	984.58
8	1.25	10	1405.03	1455.74	1467.00	1439.88	1377.42

Table C. 5: The lateral capacities for lateral deflection of 0.1D with combined vertical and lateral load of constant pile length 15m.

L/D Ratio	Pile Diameter (m)	Pile length (m)	latera capacity (kN))				
			V=0	V=0.25Vult	V=0.5Vult	V=0.75Vult	V=Vult
30	0.5	15	253.12	256.31	258.70	260.14	256.68
20	0.75	15	630.15	639.75	647.53	642.38	614.17
15	1	15	1210.11	1229.01	1244.16	1233.07	1191.78
12	1.25	15	1978.27	2016.44	2018.45	1912.75	1835.07

Table C. 6: The lateral capacities for lateral deflection of 0.1D with combined vertical and lateral load of constant pile length 20m

L/D Ratio	Pile Diameter (m)	Pile length (m)	latera capacity (kN)				
			V=0	V=0.25Vult	V=0.5Vult	V=0.75Vult	V=Vult
40.00	0.5	20	250.93	251.80	252.64	253.44	254.22
26.67	0.75	20	628.81	638.03	645.68	642.73	606.37
20.00	1	20	1221.77	1239.72	1255.24	1246.54	1194.82
16.00	1.25	20	2021.54	2055.10	2083.12	2056.54	1989.51

C.3: Bending Moment Capacity

Table C. 7: The bending moment capacity for lateral deflection of 0.1D with combined vertical and lateral load of constant pile length 10m

A. For D=0.5m

Depth [m]	Prescribed displacement [Phase_2] [kN m]	0.25vult [Phase_3] [kN m]	0.5vult [Phase_4] [kN m]	0.75vult [Phase_5] [kN m]	1vult [Phase_6] [kN m]
0.00	0.00	0.00	0.00	0.00	0.00
-0.13	32.98	33.39	33.71	33.90	33.38
-0.26	64.37	65.16	65.74	66.08	64.99
-0.39	95.99	97.17	98.04	98.53	96.80
-0.52	123.89	125.39	126.48	127.05	124.58
-0.65	152.91	154.72	156.02	156.62	153.24

-0.78	178.32	180.37	181.81	182.38	178.01
-0.90	203.56	205.83	207.37	207.87	202.38
-1.03	225.65	228.07	229.66	230.05	223.45
-1.16	246.81	249.33	250.95	251.18	243.45
-1.29	265.35	267.92	269.49	269.54	260.71
-1.42	282.59	285.18	286.67	286.49	276.58
-1.54	297.27	299.83	301.20	300.77	289.89
-1.67	311.83	314.33	315.54	314.83	302.96
-1.80	323.50	325.91	326.96	325.97	313.30
-1.93	334.01	336.30	337.16	335.86	322.47
-2.06	342.30	344.45	345.11	343.51	329.53
-2.18	349.84	351.84	352.28	350.37	335.87
-2.31	354.78	356.61	356.80	354.58	339.75
-2.44	359.26	360.87	360.81	358.27	343.24
-2.57	361.24	362.66	362.36	359.55	344.56
-2.70	362.52	363.70	363.13	360.04	345.24
-2.82	361.77	362.74	361.93	358.61	344.20
-2.95	359.97	360.70	359.64	356.09	342.26
-3.08	356.55	357.06	355.78	352.08	338.96
-3.21	351.96	352.23	350.72	346.89	334.67
-3.34	346.39	346.45	344.75	340.86	329.62
-3.46	339.02	338.87	337.01	333.13	322.99
-3.59	330.40	330.07	328.07	324.28	315.30
-3.72	321.06	320.56	318.44	314.81	307.05
-3.85	311.14	310.50	308.32	304.91	298.31
-3.98	299.98	299.23	297.02	293.87	288.48
-4.10	287.56	286.73	284.55	281.70	277.49
-4.23	275.54	274.66	272.54	269.97	266.86
-4.36	262.35	261.45	259.48	257.17	255.06
-4.49	248.86	247.97	246.21	244.14	242.96
-4.62	236.00	235.13	233.60	231.76	231.31
-4.74	222.02	221.19	219.93	218.35	218.61
-4.87	209.18	208.39	207.39	206.05	206.86
-5.00	195.42	194.69	193.95	192.88	194.22
-5.13	183.01	182.32	181.81	180.98	182.75
-5.26	170.23	169.60	169.31	168.73	170.87
-5.38	157.91	157.33	157.23	156.90	159.34
-5.51	146.13	145.59	145.68	145.58	148.28
-5.64	134.78	134.29	134.54	134.65	137.53
-5.77	123.96	123.51	123.90	124.22	127.24

-5.90	113.55	113.14	113.65	114.14	117.26
-6.02	103.73	103.35	103.96	104.61	107.80
-6.15	94.32	93.97	94.66	95.46	98.67
-6.28	85.80	85.47	86.21	87.13	90.34
-6.41	77.15	76.86	77.64	78.66	81.83
-6.54	69.55	69.28	70.08	71.20	74.31
-6.66	62.35	62.10	62.91	64.10	67.11
-6.79	55.60	55.37	56.16	57.42	60.32
-6.92	49.38	49.17	49.94	51.23	54.00
-7.05	43.58	43.38	44.11	45.44	48.06
-7.18	38.28	38.11	38.79	40.13	42.58
-7.30	33.38	33.22	33.85	35.19	37.46
-7.43	28.97	28.82	29.39	30.72	32.79
-7.56	24.90	24.77	25.29	26.60	28.47
-7.69	21.31	21.19	21.65	22.92	24.58
-7.82	17.96	17.84	18.25	19.46	20.92
-7.94	15.17	15.06	15.43	16.57	17.82
-8.07	12.45	12.35	12.67	13.73	14.77
-8.20	10.25	10.16	10.43	11.41	12.26
-8.33	8.21	8.12	8.35	9.24	9.89
-8.46	6.46	6.38	6.57	7.37	7.82
-8.58	5.03	4.96	5.11	5.82	6.10
-8.71	3.74	3.67	3.80	4.41	4.52
-8.84	2.72	2.65	2.75	3.27	3.25
-8.97	1.89	1.82	1.89	2.32	2.18
-9.10	1.21	1.14	1.19	1.53	1.29
-9.22	0.69	0.63	0.64	0.91	0.61
-9.35	0.31	0.25	0.25	0.45	0.12
-9.48	0.04	-0.02	-0.03	0.10	-0.21
-9.61	-0.11	-0.16	-0.19	-0.09	-0.33
-9.74	-0.17	-0.20	-0.21	-0.15	-0.21
-9.87	-0.15	-0.20	-0.25	-0.26	-0.32
-10.00	0.00	0.00	0.00	0.00	0.00

B. For D=0.75m

Depth [m]	prescribed displacement [Phase_2] [kN m]	0.5vult [Phase_4] [kN m]	1vult [Phase_6] [kN m]	0.25vult [Phase_3] [kN m]	0.75vult [Phase_5] [kN m]
0.00	0.00	0.00	0.00	0.00	0.00
-0.20	120.27	123.61	116.53	122.61	121.49
-0.39	235.15	241.30	226.95	239.55	236.85
-0.59	348.06	356.97	335.21	354.54	349.97
-0.78	451.39	462.30	432.64	459.59	452.29
-0.97	554.38	566.91	528.30	564.16	553.26
-1.16	645.31	658.65	610.86	656.26	640.98
-1.35	735.46	749.10	691.42	747.37	726.91
-1.55	814.03	827.13	760.25	826.48	800.39
-1.74	889.08	901.03	825.02	901.79	869.54
-1.93	956.05	966.20	881.80	968.70	930.02
-2.12	1014.43	1022.47	930.62	1026.82	981.86
-2.31	1068.11	1073.55	974.87	1080.00	1028.49
-2.51	1116.56	1119.24	1014.39	1127.85	1069.96
-2.70	1155.95	1155.59	1045.85	1166.43	1102.61
-2.89	1189.62	1186.12	1072.40	1199.19	1129.90
-3.08	1216.75	1209.70	1093.13	1225.19	1150.67
-3.27	1237.40	1226.95	1108.50	1244.72	1165.74
-3.47	1250.04	1235.98	1116.90	1256.05	1173.28
-3.66	1259.77	1242.12	1123.10	1264.44	1178.47
-3.85	1260.81	1239.64	1122.07	1264.06	1175.97
-4.04	1256.66	1232.28	1116.79	1258.56	1169.15
-4.23	1243.44	1215.83	1103.72	1243.87	1154.10
-4.42	1228.35	1197.86	1089.38	1227.43	1137.85
-4.62	1205.45	1172.53	1068.60	1203.25	1114.93
-4.81	1178.71	1143.75	1044.68	1175.31	1088.86
-5.00	1144.32	1107.94	1014.24	1139.86	1056.17
-5.19	1108.47	1071.08	982.60	1103.06	1022.40
-5.38	1065.03	1027.23	944.27	1058.82	981.87
-5.58	1022.32	984.38	906.47	1015.44	942.11
-5.77	971.23	933.64	860.94	963.85	894.57
-5.96	921.86	884.77	816.59	914.15	848.50
-6.15	867.36	831.23	767.17	859.60	797.50
-6.34	813.07	778.10	717.50	805.40	746.50
-6.54	754.80	721.33	663.66	747.37	691.55
-6.73	700.31	668.36	612.99	693.15	640.02
-6.92	641.49	611.33	558.04	634.68	584.27

-7.11	586.98	558.56	507.00	580.53	532.53
-7.30	529.46	502.97	453.09	523.43	477.88
-7.49	477.35	452.67	404.29	471.74	428.36
-7.69	422.22	399.55	352.85	417.09	376.03
-7.88	373.46	352.60	307.59	368.78	329.82
-8.07	322.43	303.55	260.75	318.26	281.67
-8.26	277.69	260.59	220.22	273.99	239.70
-8.45	232.00	216.81	179.76	228.79	197.27
-8.65	192.24	178.78	145.34	189.47	160.71
-8.84	152.58	140.97	112.21	150.26	124.89
-9.03	118.20	108.30	84.44	116.26	94.41
-9.22	86.59	78.47	60.12	85.00	67.33
-9.41	58.50	52.18	39.37	57.25	44.02
-9.61	34.29	29.82	22.33	33.33	24.83
-9.80	14.61	12.15	9.29	14.04	10.02
-10.00	0.00	0.00	0.00	0.00	0.00

C. For D=1.00m

Depth [m]	prescribed displacement [Phase_2] [kN m]	0.25vult [Phase_3] [kN m]	0.5vult [Phase_4] [kN m]	0.75vult [Phase_5] [kN m]	1vult [Phase_6] [kN m]
0.00	0.00	0.00	0.00	0.00	0.00
-0.26	260.64	267.84	268.92	262.94	250.89
-0.51	493.06	506.45	508.00	495.95	472.51
-0.76	743.05	762.78	764.27	744.80	708.43
-1.01	954.88	979.59	980.11	952.83	904.47
-1.26	1173.54	1202.96	1201.55	1164.61	1102.66
-1.51	1357.05	1389.79	1385.44	1338.41	1263.84
-1.76	1544.47	1580.06	1571.61	1513.02	1424.94
-2.01	1694.30	1731.43	1718.47	1649.41	1550.37
-2.26	1844.23	1882.29	1863.69	1783.02	1672.73
-2.51	1964.33	2002.47	1977.97	1886.44	1767.37
-2.75	2072.76	2110.33	2079.17	1976.54	1849.64
-3.00	2161.78	2198.15	2159.92	2047.02	1913.95
-3.25	2238.95	2273.77	2228.25	2105.74	1967.44
-3.50	2295.72	2328.53	2275.67	2144.90	2003.04
-3.75	2341.12	2371.62	2311.31	2173.10	2028.50
-4.00	2361.68	2389.63	2322.40	2178.79	2033.06
-4.25	2377.21	2402.44	2328.18	2179.83	2033.22
-4.50	2367.20	2389.34	2308.76	2158.06	2012.09

-4.75	2347.04	2366.03	2279.52	2127.73	1982.82
-5.00	2302.29	2318.13	2226.83	2076.33	1933.75
-5.25	2250.15	2263.02	2167.75	2019.39	1879.36
-5.50	2175.42	2185.43	2087.62	1943.09	1806.53
-5.75	2093.39	2100.89	2001.77	1861.52	1728.54
-5.99	1990.56	1995.94	1897.31	1762.52	1633.87
-6.24	1882.30	1886.00	1788.87	1659.63	1535.30
-6.49	1753.11	1755.71	1661.84	1539.12	1419.97
-6.74	1621.50	1623.59	1533.36	1416.91	1302.83
-6.99	1479.57	1482.18	1396.39	1286.50	1178.22
-7.24	1328.78	1332.75	1251.83	1148.60	1046.77
-7.49	1176.71	1183.02	1107.56	1011.07	916.95
-7.74	1018.89	1028.12	959.01	869.70	784.75
-7.99	869.14	880.97	819.10	737.41	662.64
-8.24	721.58	735.54	681.69	608.36	544.61
-8.49	578.33	593.38	548.31	484.59	432.63
-8.74	451.97	467.25	430.49	376.52	335.60
-8.98	329.41	343.55	315.41	273.01	243.35
-9.23	226.44	238.69	218.30	187.17	167.32
-9.48	131.89	140.87	128.50	110.04	99.54
-9.74	53.36	58.09	51.91	43.73	39.49
-10.00	0.00	0.00	0.00	0.00	0.00

D. For D=1.25m

Depth [m]	precribed displacemet [Phase_2] [kN m]	0.25vult [Phase_3] [kN m]	0.5vult [Phase_4] [kN m]	0.75vult [Phase_5] [kN m]	1vult [Phase_6] [kN m]
0.00	0.00	0.00	0.00	0.00	0.00
-0.32	446.76	462.44	465.21	455.07	433.35
-0.64	842.61	871.78	876.08	855.48	813.26
-0.95	1264.65	1307.77	1312.69	1279.03	1213.26
-1.26	1614.82	1668.76	1672.18	1624.18	1536.37
-1.57	1972.65	2036.87	2036.67	1970.64	1857.76
-1.88	2263.61	2335.01	2329.24	2244.97	2108.87
-2.19	2555.47	2633.03	2619.46	2514.03	2352.89
-2.50	2785.42	2866.62	2844.03	2718.31	2536.53
-2.82	2988.59	3072.05	3038.96	2892.34	2691.54
-3.13	3145.99	3229.65	3184.58	3017.91	2802.13
-3.44	3280.08	3362.97	3304.86	3118.70	2890.13

-3.75	3362.10	3442.63	3371.13	3168.58	2932.33
-4.06	3424.26	3501.85	3416.57	3199.13	2957.21
-4.37	3437.24	3510.91	3412.45	3184.25	2940.57
-4.68	3427.53	3496.95	3385.95	3149.76	2905.79
-5.00	3372.29	3436.75	3314.88	3075.65	2834.26
-5.31	3289.43	3348.79	3217.52	2978.20	2740.78
-5.62	3163.60	3217.94	3080.65	2845.33	2614.18
-5.93	3015.91	3065.53	2924.23	2694.51	2470.41
-6.24	2833.35	2879.29	2738.46	2517.25	2302.23
-6.55	2620.92	2663.94	2526.04	2315.03	2110.54
-6.86	2384.17	2426.18	2294.20	2095.15	1903.01
-7.18	2120.82	2163.46	2039.24	1853.69	1676.00
-7.49	1846.96	1892.57	1778.01	1607.25	1446.36
-7.80	1566.33	1615.64	1512.32	1357.60	1216.00
-8.11	1275.56	1327.73	1239.12	1103.25	985.02
-8.42	1009.21	1062.30	989.19	872.76	777.97
-8.73	750.08	799.93	743.90	650.48	580.20
-9.04	520.38	564.14	524.43	454.94	407.20
-9.36	311.19	344.12	320.22	277.52	250.38
-9.68	128.61	147.59	136.06	117.52	106.47
-10.00	0.00	0.00	0.00	0.00	0.00

Table B. 8: The bending moment capacity for lateral deflection of 0.1D with combined vertical and lateral load of constant pile length 15m

E. For D=0.5m

Depth [m]	prescribed displacement [Phase_2] [kN m]	0.25vult [Phase_3] [kN m]	0.5vult [Phase_4] [kN m]	0.75vult [Phase_5] [kN m]	1vult [Phase_6] [kN m]
0.00	0.00	0.00	0.00	0.00	0.00
-0.13	33.25	33.78	34.17	34.04	31.77
-0.27	64.90	65.87	66.55	66.19	61.67
-0.39	96.87	98.35	99.40	98.83	91.92
-0.52	124.66	126.56	127.87	127.00	117.88
-0.65	154.00	156.29	157.85	156.57	144.92
-0.78	179.11	181.71	183.43	181.67	167.73
-0.91	204.73	207.62	209.47	207.11	190.71
-1.03	226.50	229.57	231.49	228.52	209.99

-1.16	247.94	251.15	253.08	249.43	228.84
-1.29	266.37	269.64	271.52	267.17	244.91
-1.42	283.72	286.99	288.76	283.69	259.93
-1.55	298.71	301.94	303.55	297.76	272.89
-1.68	312.71	315.86	317.28	310.78	285.00
-1.80	324.18	327.21	328.41	321.26	294.96
-1.93	335.17	338.03	338.98	331.16	304.55
-2.06	343.14	345.82	346.51	338.15	311.61
-2.19	350.77	353.23	353.62	344.70	318.45
-2.32	355.75	357.99	358.09	348.76	323.07
-2.44	359.84	361.81	361.59	351.87	327.01
-2.57	361.96	363.68	363.16	353.18	329.32
-2.70	362.94	364.36	363.53	353.35	330.76
-2.83	362.01	363.16	362.04	351.83	330.60
-2.96	360.02	360.87	359.46	349.30	329.67
-3.08	356.37	356.95	355.28	345.34	327.31
-3.21	351.91	352.21	350.29	340.67	324.37
-3.34	345.56	345.61	343.47	334.35	319.81
-3.47	338.45	338.24	335.91	327.40	314.72
-3.60	330.30	329.88	327.41	319.59	308.64
-3.72	320.84	320.22	317.63	310.63	301.57
-3.85	310.61	309.84	307.21	301.04	293.71
-3.98	299.39	298.49	295.85	290.59	285.05
-4.11	287.53	286.53	283.95	279.55	275.69
-4.24	275.31	274.24	271.76	268.18	265.88
-4.36	261.40	260.31	258.01	255.21	254.42
-4.49	248.73	247.65	245.56	243.43	243.92
-4.62	235.23	234.17	232.37	230.83	232.42
-4.75	222.05	221.04	219.54	218.55	221.09
-4.88	208.64	207.69	206.50	206.00	209.35
-5.00	195.12	194.23	193.35	193.36	197.43
-5.13	182.89	182.06	181.45	181.88	186.50
-5.26	169.63	168.87	168.54	169.41	174.56
-5.39	157.89	157.20	157.11	158.34	163.88
-5.52	145.83	145.20	145.34	146.93	152.81
-5.64	134.28	133.71	134.05	135.95	142.08
-5.77	123.48	122.96	123.48	125.68	132.01
-5.90	113.13	112.66	113.32	115.77	122.22
-6.03	102.85	102.42	103.22	105.91	112.45
-6.16	93.87	93.48	94.37	97.25	103.82

-6.28	84.74	84.38	85.36	88.40	94.97
-6.41	76.34	76.02	77.04	80.21	86.73
-6.54	68.14	67.84	68.90	72.19	78.63
-6.67	61.16	60.88	61.95	65.32	71.66
-6.80	53.76	53.52	54.58	58.02	64.23
-6.92	47.57	47.36	48.40	51.89	57.95
-7.05	41.35	41.16	42.17	45.69	51.58
-7.18	35.70	35.53	36.49	40.02	45.72
-7.31	30.72	30.58	31.49	35.00	40.52
-7.44	25.81	25.69	26.52	30.00	35.29
-7.56	21.40	21.30	22.08	25.51	30.59
-7.69	17.56	17.48	18.19	21.55	26.40
-7.82	13.85	13.78	14.43	17.68	22.30
-7.95	10.48	10.42	11.01	14.15	18.54
-8.08	7.55	7.51	8.05	11.06	15.22
-8.20	4.72	4.69	5.18	8.05	11.96
-8.33	2.38	2.36	2.81	5.54	9.22
-8.46	0.10	0.10	0.49	3.06	6.49
-8.59	-1.77	-1.76	-1.40	1.01	4.22
-8.72	-3.53	-3.51	-3.19	-0.97	1.99
-8.84	-5.10	-5.08	-4.81	-2.76	-0.04
-8.97	-6.38	-6.35	-6.12	-4.24	-1.75
-9.10	-7.62	-7.60	-7.40	-5.71	-3.46
-9.23	-8.63	-8.60	-8.44	-6.94	-4.91
-9.36	-9.50	-9.47	-9.34	-8.01	-6.21
-9.48	-10.25	-10.22	-10.12	-8.97	-7.39
-9.61	-10.89	-10.85	-10.77	-9.79	-8.41
-9.74	-11.40	-11.36	-11.31	-10.49	-9.33
-9.87	-11.82	-11.78	-11.75	-11.07	-10.12
-10.00	-12.13	-12.09	-12.08	-11.54	-10.80
-10.13	-12.32	-12.27	-12.29	-11.84	-11.31
-10.25	-12.30	-12.26	-12.28	-11.92	-11.56
-10.38	-12.19	-12.15	-12.19	-11.91	-11.72
-10.50	-11.96	-11.92	-11.97	-11.78	-11.74
-10.63	-11.64	-11.60	-11.66	-11.55	-11.66
-10.75	-11.23	-11.20	-11.27	-11.25	-11.51
-10.88	-10.80	-10.77	-10.84	-10.91	-11.32
-11.00	-10.31	-10.28	-10.36	-10.52	-11.06
-11.13	-9.80	-9.78	-9.87	-10.11	-10.79
-11.25	-9.24	-9.22	-9.32	-9.66	-10.46

-11.37	-8.71	-8.70	-8.80	-9.23	-10.15
-11.50	-8.13	-8.13	-8.24	-8.75	-9.78
-11.62	-7.60	-7.61	-7.72	-8.30	-9.45
-11.75	-7.02	-7.04	-7.15	-7.80	-9.08
-11.87	-6.51	-6.53	-6.64	-7.36	-8.76
-12.00	-5.96	-5.98	-6.10	-6.88	-8.41
-12.12	-5.48	-5.51	-5.64	-6.47	-8.12
-12.25	-4.96	-5.01	-5.14	-6.04	-7.83
-12.37	-4.53	-4.59	-4.72	-5.68	-7.59
-12.49	-4.07	-4.14	-4.28	-5.29	-7.32
-12.62	-3.67	-3.75	-3.90	-4.96	-7.09
-12.74	-3.26	-3.35	-3.50	-4.61	-6.88
-12.87	-2.91	-3.01	-3.17	-4.32	-6.71
-12.99	-2.56	-2.67	-2.83	-4.04	-6.55
-13.12	-2.26	-2.38	-2.55	-3.80	-6.41
-13.24	-1.96	-2.08	-2.26	-3.55	-6.28
-13.37	-1.71	-1.84	-2.02	-3.36	-6.17
-13.49	-1.46	-1.60	-1.79	-3.16	-6.04
-13.62	-1.25	-1.40	-1.59	-2.99	-5.92
-13.74	-1.05	-1.20	-1.40	-2.81	-5.78
-13.86	-0.88	-1.04	-1.24	-2.65	-5.64
-13.99	-0.72	-0.89	-1.09	-2.49	-5.41
-14.11	-0.58	-0.75	-0.96	-2.34	-5.12
-14.24	-0.46	-0.63	-0.83	-2.16	-4.68
-14.36	-0.35	-0.52	-0.72	-1.97	-4.20
-14.49	-0.26	-0.42	-0.61	-1.72	-3.63
-14.61	-0.18	-0.32	-0.49	-1.43	-2.88
-14.74	-0.11	-0.21	-0.34	-1.01	-1.79
-14.87	-0.04	-0.09	-0.16	-0.54	-0.77
-15.00	0.00	0.00	0.00	0.00	0.00

F. For D=0.75m

Depth [m]	prescribed displacement [Phase_2] [kN m]	0.25vult [Phase_3] [kN m]	0.5vult [Phase_4] [kN m]	0.75vult [Phase_5] [kN m]	1vult [Phase_6] [kN m]
0.00	0.00	0.00	0.00	0.00	0.00
-0.20	122.69	124.55	126.05	124.77	118.85
-0.40	240.25	243.76	246.55	243.68	231.88
-0.59	357.55	362.83	367.02	362.37	344.43

-0.78	462.18	468.90	474.14	467.21	443.31
-0.97	568.69	576.73	582.89	573.02	542.55
-1.16	663.19	672.24	679.04	665.87	629.24
-1.36	754.89	764.79	772.07	755.18	712.33
-1.55	835.51	845.97	853.43	832.68	784.52
-1.74	915.39	926.21	933.67	908.67	855.42
-1.93	983.03	993.93	1001.12	972.03	914.86
-2.12	1045.38	1056.19	1062.93	1029.71	969.22
-2.32	1102.42	1112.94	1119.04	1081.61	1018.84
-2.51	1151.54	1161.68	1167.08	1125.83	1061.63
-2.70	1194.12	1203.69	1208.22	1163.30	1098.78
-2.89	1231.17	1240.13	1243.78	1195.66	1131.35
-3.08	1260.52	1268.69	1271.33	1220.41	1157.38
-3.28	1285.02	1292.37	1293.99	1240.75	1179.43
-3.47	1301.85	1308.26	1308.78	1253.82	1195.07
-3.66	1313.72	1319.17	1318.61	1262.47	1206.54
-3.85	1316.82	1321.27	1319.65	1263.25	1210.64
-4.04	1318.48	1321.86	1319.16	1263.02	1214.04
-4.23	1310.70	1313.10	1309.47	1254.56	1209.34
-4.43	1299.82	1301.15	1296.56	1243.57	1202.66
-4.62	1282.52	1282.93	1277.58	1227.20	1190.44
-4.81	1260.16	1259.68	1253.63	1206.55	1174.20
-5.00	1231.06	1229.80	1223.21	1180.06	1152.13
-5.19	1199.76	1197.78	1190.71	1151.92	1128.48
-5.39	1164.97	1162.44	1155.08	1120.66	1101.33
-5.58	1124.71	1121.68	1114.07	1084.63	1069.74
-5.77	1084.22	1080.87	1073.22	1048.31	1037.32
-5.96	1038.19	1034.64	1027.13	1006.81	999.71
-6.15	989.90	986.34	979.22	962.99	959.37
-6.35	942.76	939.26	932.75	920.19	919.62
-6.54	893.22	889.86	884.11	874.90	876.90
-6.73	843.53	840.32	835.39	829.35	833.61
-6.92	793.50	790.45	786.31	783.24	789.41
-7.11	746.30	743.41	739.98	739.60	747.39
-7.31	695.49	692.79	690.07	692.42	701.67
-7.50	650.47	647.94	645.78	650.43	660.79
-7.69	602.07	599.72	598.05	604.97	616.27
-7.88	558.43	556.24	554.95	563.86	575.93
-8.07	513.92	511.89	510.90	521.63	534.29
-8.27	472.69	470.82	470.03	482.40	495.49

-8.46	430.55	428.85	428.15	442.01	455.38
-8.65	392.68	391.14	390.46	405.59	419.14
-8.84	354.21	352.83	352.07	368.30	381.86
-9.03	318.25	317.02	316.12	333.33	346.82
-9.23	283.70	282.60	281.49	299.45	312.74
-9.42	251.38	250.41	249.07	267.65	280.68
-9.61	218.08	217.25	215.63	234.69	247.35
-9.81	189.34	188.62	186.82	206.28	218.55
-10.00	159.16	158.56	156.78	176.53	188.24
-10.19	132.62	132.12	130.72	150.69	161.81
-10.39	109.43	109.01	108.25	128.06	138.48
-10.58	87.77	87.43	87.45	106.87	116.55
-10.77	69.59	69.32	70.06	88.83	97.80
-10.96	52.91	52.70	54.14	72.14	80.37
-11.15	39.03	38.88	40.89	57.99	65.49
-11.35	26.99	26.88	29.40	45.54	52.34
-11.54	16.57	16.50	19.43	34.48	40.59
-11.73	8.22	8.18	11.44	25.50	31.03
-11.92	1.21	1.21	4.70	17.67	22.66
-12.11	-4.24	-4.23	-0.55	11.41	15.97
-12.30	-8.49	-8.45	-4.67	6.22	10.41
-12.50	-11.55	-11.49	-7.63	2.30	6.24
-12.69	-13.54	-13.45	-9.58	-0.65	3.12
-12.88	-14.71	-14.60	-10.77	-2.75	0.94
-13.07	-15.01	-14.90	-11.18	-4.03	-0.25
-13.26	-14.75	-14.64	-11.07	-4.71	-0.71
-13.46	-13.82	-13.71	-10.36	-4.76	-0.45
-13.65	-12.58	-12.47	-9.38	-4.44	0.19
-13.84	-10.86	-10.76	-8.00	-3.68	1.36
-14.03	-9.07	-8.98	-6.57	-2.81	2.51
-14.22	-6.99	-6.92	-4.94	-1.78	3.46
-14.41	-5.06	-4.98	-3.42	-0.82	4.07
-14.61	-3.02	-2.89	-1.79	0.34	4.87
-14.80	-1.29	-1.37	-0.99	-0.42	1.74
-15.00	0.00	0.00	0.00	0.00	0.00

G. For D=1.00m

Depth [m]	prescribed displacement [Phase_2] [kN m]	0.25vult [Phase_3] [kN m]	0.5vult [Phase_4] [kN m]	0.75vult [Phase_5] [kN m]	1vult [Phase_6] [kN m]
0.00	0.00	0.00	0.00	0.00	0.00
-0.25	308.65	313.29	316.87	313.11	301.68
-0.51	591.09	599.97	606.69	598.87	576.67
-0.76	887.71	900.79	910.45	897.40	863.17
-1.01	1146.75	1163.21	1174.86	1155.33	1109.69
-1.26	1416.44	1436.21	1449.54	1421.63	1363.26
-1.51	1652.42	1674.67	1688.72	1651.44	1580.99
-1.76	1879.28	1903.54	1917.70	1869.89	1787.19
-2.01	2083.75	2109.25	2122.67	2063.59	1970.08
-2.26	2285.72	2311.99	2324.02	2252.66	2148.61
-2.51	2451.23	2477.61	2487.75	2405.05	2293.08
-2.75	2620.71	2646.72	2654.28	2559.02	2439.72
-3.00	2759.24	2784.46	2789.24	2683.03	2558.99
-3.25	2886.83	2910.86	2912.44	2795.34	2667.87
-3.50	2991.74	3014.19	3012.30	2885.43	2756.73
-3.75	3088.37	3109.04	3103.57	2967.78	2839.03
-4.00	3160.81	3179.34	3170.10	3027.00	2900.10
-4.25	3224.21	3240.44	3227.37	3078.12	2953.77
-4.50	3262.72	3276.47	3259.67	3106.74	2986.26
-4.75	3295.54	3306.70	3286.16	3130.90	3014.71
-5.00	3308.22	3316.77	3292.73	3137.57	3026.54
-5.25	3303.89	3309.88	3282.67	3129.42	3023.85
-5.50	3282.13	3285.39	3255.09	3106.23	3007.08
-5.75	3252.45	3253.34	3220.48	3077.04	2983.89
-6.00	3200.63	3199.13	3163.96	3028.54	2942.29
-6.25	3146.32	3142.74	3105.59	2978.68	2898.86
-6.50	3070.64	3065.27	3026.55	2909.86	2836.78
-6.75	2991.33	2984.43	2944.40	2838.15	2771.43
-7.00	2894.84	2886.67	2845.64	2750.64	2690.27
-7.25	2798.54	2789.34	2747.45	2663.23	2608.70
-7.50	2684.90	2675.11	2632.78	2559.31	2510.33
-7.75	2572.75	2562.68	2520.15	2456.42	2412.27
-8.00	2447.27	2437.24	2395.07	2340.30	2300.28
-8.25	2329.20	2319.32	2277.72	2230.54	2193.71
-8.50	2196.23	2186.62	2145.99	2105.93	2071.60

-8.75	2074.12	2064.76	2025.06	1990.91	1958.27
-9.00	1938.11	1929.03	1890.33	1861.75	1830.22
-9.24	1816.32	1807.47	1769.44	1745.49	1714.49
-9.49	1681.53	1672.94	1635.47	1615.94	1585.04
-9.75	1557.21	1548.84	1511.82	1495.92	1464.60
-10.00	1425.74	1417.68	1381.69	1368.69	1336.49
-10.25	1299.71	1292.01	1257.71	1246.41	1212.64
-10.50	1178.85	1171.78	1139.72	1128.67	1092.81
-10.75	1058.93	1052.57	1022.86	1011.17	972.72
-11.00	947.88	942.29	914.55	901.42	860.23
-11.25	840.63	835.84	809.80	794.71	750.66
-11.50	740.25	736.18	711.49	694.12	647.55
-11.75	647.31	643.87	620.33	600.64	552.01
-12.00	555.87	552.98	530.42	508.25	458.12
-12.25	477.00	474.53	452.76	428.41	377.52
-12.49	399.87	397.74	376.75	350.47	300.09
-12.74	333.05	331.15	310.93	283.31	234.64
-12.99	269.26	267.51	248.22	220.17	175.45
-13.24	214.51	212.84	194.57	167.07	127.53
-13.49	164.13	162.51	145.68	120.61	88.20
-13.74	121.33	119.76	104.67	83.46	58.15
-13.99	83.70	82.19	69.53	54.41	36.60
-14.24	52.95	51.59	41.77	33.43	23.24
-14.49	27.73	26.82	20.99	20.25	18.77
-14.74	9.01	8.09	5.25	6.92	8.48
-15.00	0.00	0.00	0.00	0.01	0.01

H. For D=1.25m

Depth [m]	prescribed displacement [Phase_2][kN m]	0.25vult [Phase_3] [kN m]	0.5vult [Phase_4] [kN m]	0.75vult [Phase_5] [kN m]	1vult [Phase_6] [kN m]
0.00	0.00	0.00	0.00	0.00	0.00
-0.32	621.44	632.71	631.61	595.53	570.00
-0.64	1217.41	1239.40	1236.66	1165.23	1115.32
-0.95	1810.01	1841.07	1833.65	1723.00	1647.47
-1.26	2348.73	2387.53	2373.37	2223.53	2125.00
-1.57	2885.50	2931.06	2907.21	2713.89	2591.72
-1.89	3358.36	3408.15	3371.49	3136.29	2994.43
-2.20	3829.69	3882.03	3829.10	3550.20	3389.46
-2.51	4241.96	4294.15	4222.19	3903.27	3727.21

-2.82	4619.05	4669.28	4576.31	4219.74	4029.88
-3.13	4960.29	5006.44	4889.86	4499.20	4297.15
-3.45	5284.18	5324.91	5183.06	4760.78	4546.79
-3.76	5546.01	5580.18	5414.39	4968.53	4744.57
-4.07	5797.22	5823.25	5631.76	5164.99	4930.90
-4.38	5984.32	6001.79	5787.50	5307.54	5065.24
-4.69	6162.95	6170.47	5932.02	5441.42	5190.54
-5.01	6293.22	6290.64	6030.83	5534.90	5276.45
-5.32	6384.75	6371.63	6092.40	5595.32	5329.94
-5.63	6431.32	6407.07	6110.82	5617.78	5346.17
-5.94	6467.17	6431.82	6120.18	5632.46	5354.34
-6.25	6446.16	6400.21	6077.85	5599.83	5316.63
-6.57	6406.66	6349.49	6017.79	5550.95	5262.02
-6.88	6333.65	6266.63	5930.14	5475.60	5181.72
-7.19	6223.30	6146.61	5808.36	5368.22	5069.70
-7.50	6077.78	5992.26	5655.78	5231.14	4928.49
-7.81	5914.62	5820.24	5487.06	5077.99	4770.37
-8.13	5729.83	5627.85	5300.08	4905.87	4593.99
-8.44	5518.81	5409.44	5088.35	4709.11	4392.84
-8.75	5270.46	5154.26	4841.26	4477.09	4156.88
-9.06	5029.30	4906.82	4601.04	4249.68	3925.30
-9.37	4744.91	4617.13	4319.34	3981.20	3654.06
-9.69	4482.59	4350.18	4058.63	3731.17	3402.19
-10.00	4169.03	4032.41	3747.74	3431.73	3104.36
-10.32	3846.54	3705.90	3426.86	3121.33	2799.45
-10.63	3525.53	3384.44	3110.49	2815.52	2505.91
-10.94	3176.52	3037.35	2768.05	2485.25	2194.55
-11.25	2851.36	2716.89	2453.20	2185.74	1920.05
-11.56	2494.12	2366.70	2110.38	1864.17	1632.37
-11.87	2181.39	2062.18	1815.32	1593.63	1396.75
-12.19	1852.44	1743.65	1509.83	1318.87	1160.30
-12.50	1554.08	1456.54	1238.48	1080.15	954.91
-12.81	1259.98	1174.73	975.76	853.49	760.99
-13.12	999.73	926.78	750.52	664.44	601.74
-13.43	758.74	698.41	548.32	497.12	462.94
-13.74	539.82	492.69	373.36	349.87	337.84
-14.05	357.10	322.66	234.46	230.88	233.81
-14.36	199.32	178.20	123.35	127.80	135.43
-14.68	79.22	69.77	44.17	47.80	54.40
-15.00	0.00	0.00	0.00	0.00	0.00

Table B. 9: The bending moment capacity for lateral deflection of 0.1D with combined vertical and lateral load of constant pile length 20m.

I. For D=0.5m

Depth [m]	Prescribed displacement [Phase_2] [kN m]	0.25vult [Phase_3] [kN m]	0.5vult [Phase_4] [kN m]	0.75vult [Phase_5] [kN m]	1vult [Phase_6] [kN m]
0.00	0.00	0.00	0.00	0.00	0.00
-0.13	33.88	34.00	34.11	34.22	34.33
-0.27	64.42	64.64	64.85	65.05	65.24
-0.40	96.44	96.76	97.06	97.36	97.64
-0.53	123.95	124.35	124.74	125.11	125.47
-0.65	152.88	153.36	153.83	154.28	154.70
-0.78	177.33	177.88	178.41	178.91	179.39
-0.91	202.79	203.40	203.99	204.55	205.08
-1.04	224.07	224.72	225.35	225.94	226.50
-1.17	245.90	246.59	247.25	247.88	248.47
-1.29	263.82	264.53	265.21	265.85	266.46
-1.42	281.83	282.55	283.24	283.88	284.49
-1.55	296.52	297.24	297.92	298.55	299.15
-1.68	310.93	311.64	312.30	312.93	313.51
-1.81	322.36	323.05	323.70	324.30	324.85
-1.93	333.13	333.79	334.41	334.98	335.50
-2.06	341.24	341.88	342.46	343.00	343.48
-2.19	348.59	349.19	349.74	350.23	350.66
-2.32	353.42	353.98	354.48	354.93	355.31
-2.45	357.92	358.42	358.88	359.27	359.60
-2.57	360.08	360.54	360.94	361.28	361.56
-2.70	361.34	361.74	362.08	362.37	362.59
-2.83	360.99	361.33	361.62	361.85	362.02
-2.96	359.00	359.29	359.52	359.69	359.80
-3.09	355.24	355.47	355.64	355.75	355.80
-3.21	351.01	351.18	351.30	351.35	351.35
-3.34	344.75	344.86	344.91	344.91	344.86
-3.47	338.10	338.16	338.16	338.11	338.02
-3.60	329.54	329.54	329.50	329.41	329.28
-3.73	320.27	320.22	320.13	320.01	319.84
-3.85	310.39	310.31	310.19	310.03	309.84

-3.98	298.91	298.78	298.63	298.45	298.24
-4.11	287.72	287.57	287.39	287.20	286.97
-4.24	275.27	275.10	274.91	274.71	274.47
-4.37	261.58	261.39	261.19	260.99	260.76
-4.49	248.56	248.36	248.16	247.95	247.73
-4.62	236.00	235.79	235.59	235.39	235.18
-4.75	221.97	221.77	221.58	221.39	221.19
-4.88	209.35	209.15	208.96	208.78	208.59
-5.01	195.59	195.40	195.22	195.04	194.87
-5.13	183.36	183.17	182.99	182.83	182.67
-5.26	170.20	170.02	169.85	169.70	169.56
-5.39	158.55	158.37	158.22	158.07	157.95
-5.52	146.17	146.01	145.86	145.73	145.61
-5.64	135.33	135.18	135.04	134.92	134.81
-5.77	124.14	123.99	123.86	123.75	123.66
-5.90	113.60	113.46	113.34	113.24	113.16
-6.03	103.76	103.62	103.51	103.41	103.34
-6.16	94.40	94.28	94.17	94.08	94.02
-6.28	85.14	85.02	84.92	84.84	84.79
-6.41	77.07	76.96	76.87	76.80	76.74
-6.54	69.03	68.92	68.84	68.77	68.73
-6.67	61.46	61.37	61.29	61.23	61.19
-6.80	54.64	54.56	54.49	54.43	54.40
-6.92	47.85	47.77	47.71	47.66	47.63
-7.05	42.05	41.98	41.93	41.89	41.87
-7.18	36.22	36.16	36.11	36.07	36.06
-7.31	31.14	31.08	31.04	31.01	31.00
-7.44	26.35	26.29	26.26	26.23	26.22
-7.56	21.98	21.93	21.90	21.88	21.87
-7.69	17.87	17.82	17.79	17.77	17.77
-7.82	14.27	14.23	14.21	14.19	14.19
-7.95	10.80	10.77	10.75	10.73	10.74
-8.08	7.89	7.86	7.84	7.83	7.84
-8.20	5.04	5.02	5.01	5.00	5.01
-8.33	2.60	2.58	2.57	2.57	2.57
-8.46	0.38	0.36	0.35	0.35	0.36
-8.59	-1.60	-1.61	-1.62	-1.62	-1.61
-8.72	-3.39	-3.40	-3.40	-3.40	-3.39
-8.84	-4.92	-4.93	-4.93	-4.93	-4.92
-8.97	-6.33	-6.34	-6.34	-6.33	-6.32

-9.10	-7.50	-7.50	-7.50	-7.49	-7.48
-9.23	-8.59	-8.59	-8.58	-8.58	-8.56
-9.36	-9.45	-9.45	-9.44	-9.43	-9.42
-9.48	-10.25	-10.24	-10.23	-10.22	-10.21
-9.61	-10.87	-10.87	-10.86	-10.85	-10.83
-9.74	-11.42	-11.42	-11.41	-11.40	-11.38
-9.87	-11.86	-11.85	-11.84	-11.83	-11.82
-10.00	-12.19	-12.18	-12.17	-12.16	-12.14
-10.13	-12.40	-12.39	-12.38	-12.37	-12.35
-10.26	-12.39	-12.37	-12.36	-12.35	-12.33
-10.39	-12.27	-12.26	-12.25	-12.24	-12.22
-10.52	-12.05	-12.04	-12.02	-12.01	-12.00
-10.64	-11.72	-11.70	-11.69	-11.68	-11.67
-10.77	-11.30	-11.29	-11.28	-11.27	-11.26
-10.90	-10.86	-10.85	-10.84	-10.83	-10.82
-11.03	-10.34	-10.33	-10.32	-10.31	-10.30
-11.15	-9.82	-9.81	-9.80	-9.80	-9.79
-11.28	-9.23	-9.23	-9.22	-9.21	-9.20
-11.41	-8.69	-8.69	-8.68	-8.67	-8.67
-11.54	-8.10	-8.09	-8.08	-8.07	-8.07
-11.67	-7.54	-7.54	-7.53	-7.52	-7.52
-11.79	-6.95	-6.94	-6.93	-6.93	-6.92
-11.92	-6.43	-6.42	-6.41	-6.41	-6.40
-12.05	-5.86	-5.86	-5.85	-5.84	-5.84
-12.18	-5.37	-5.36	-5.36	-5.35	-5.35
-12.31	-4.85	-4.84	-4.83	-4.83	-4.82
-12.43	-4.40	-4.39	-4.39	-4.38	-4.38
-12.56	-3.93	-3.93	-3.92	-3.92	-3.91
-12.69	-3.52	-3.51	-3.50	-3.50	-3.50
-12.82	-3.12	-3.12	-3.11	-3.11	-3.11
-12.95	-2.75	-2.75	-2.74	-2.74	-2.74
-13.07	-2.41	-2.41	-2.40	-2.40	-2.40
-13.20	-2.09	-2.09	-2.08	-2.08	-2.08
-13.33	-1.80	-1.80	-1.80	-1.80	-1.79
-13.46	-1.53	-1.53	-1.53	-1.53	-1.53
-13.59	-1.29	-1.29	-1.28	-1.28	-1.28
-13.71	-1.07	-1.07	-1.07	-1.07	-1.07
-13.84	-0.86	-0.86	-0.85	-0.85	-0.85
-13.97	-0.69	-0.68	-0.68	-0.68	-0.68
-14.10	-0.52	-0.52	-0.51	-0.51	-0.51

-14.23	-0.37	-0.37	-0.37	-0.37	-0.36
-14.35	-0.25	-0.24	-0.24	-0.24	-0.24
-14.48	-0.14	-0.14	-0.14	-0.13	-0.13
-14.61	-0.04	-0.04	-0.03	-0.03	-0.03
-14.74	0.05	0.05	0.05	0.05	0.05
-14.87	0.12	0.12	0.12	0.12	0.12
-14.99	0.18	0.18	0.18	0.18	0.18
-15.12	0.23	0.23	0.23	0.23	0.23
-15.25	0.27	0.27	0.27	0.27	0.27
-15.38	0.30	0.30	0.30	0.30	0.30
-15.51	0.33	0.33	0.33	0.33	0.33
-15.63	0.35	0.35	0.35	0.35	0.36
-15.76	0.36	0.37	0.37	0.37	0.37
-15.89	0.37	0.38	0.38	0.38	0.38
-16.02	0.38	0.39	0.39	0.39	0.39
-16.15	0.38	0.38	0.38	0.39	0.39
-16.27	0.38	0.38	0.39	0.39	0.39
-16.40	0.37	0.37	0.38	0.38	0.38
-16.53	0.36	0.36	0.37	0.37	0.37
-16.66	0.35	0.35	0.35	0.36	0.36
-16.78	0.34	0.34	0.34	0.34	0.35
-16.91	0.33	0.33	0.33	0.33	0.33
-17.04	0.31	0.31	0.32	0.32	0.32
-17.17	0.30	0.30	0.30	0.30	0.30
-17.30	0.28	0.28	0.29	0.29	0.29
-17.42	0.27	0.27	0.27	0.27	0.28
-17.55	0.25	0.25	0.26	0.26	0.26
-17.68	0.23	0.24	0.24	0.25	0.25
-17.81	0.22	0.22	0.23	0.23	0.24
-17.94	0.20	0.21	0.21	0.22	0.22
-18.06	0.19	0.19	0.20	0.21	0.21
-18.19	0.17	0.18	0.19	0.19	0.20
-18.32	0.16	0.17	0.18	0.18	0.19
-18.45	0.14	0.15	0.16	0.17	0.18
-18.58	0.13	0.14	0.14	0.15	0.16
-18.70	0.11	0.12	0.13	0.14	0.15
-18.83	0.09	0.11	0.12	0.13	0.14
-18.96	0.08	0.09	0.10	0.11	0.13
-19.09	0.07	0.08	0.09	0.10	0.12
-19.22	0.05	0.06	0.08	0.09	0.10

-19.34	0.04	0.05	0.07	0.08	0.09
-19.47	0.03	0.04	0.05	0.07	0.08
-19.60	0.02	0.03	0.04	0.06	0.07
-19.73	0.01	0.02	0.03	0.04	0.05
-19.86	0.01	0.01	0.02	0.03	0.03
-20.00	0.00	0.00	0.00	0.00	0.00

J. For D=0.75m

Depth [m]	Prescribed surface displacement [Phase_2] [kN m]	0.25vult [Phase_3] [kN m]	0.5vult [Phase_4] [kN m]	0.75vult [Phase_5] [kN m]	1vult [Phase_6] [kN m]
0.00	0.00	0.00	0.00	0.00	0.00
-0.20	125.59	127.42	128.94	128.17	120.47
-0.40	238.23	241.62	244.42	242.68	227.74
-0.59	358.05	363.07	367.20	364.20	341.25
-0.78	460.26	466.59	471.77	467.30	436.98
-0.97	569.42	577.03	583.21	576.70	537.91
-1.17	660.93	669.47	676.34	667.60	621.30
-1.36	756.13	765.51	772.95	761.45	706.99
-1.55	834.77	844.68	852.42	838.19	776.99
-1.74	916.12	926.42	934.28	916.87	848.76
-1.93	983.69	994.11	1001.84	981.43	907.98
-2.13	1047.24	1057.58	1064.99	1041.40	963.25
-2.32	1101.74	1111.80	1118.71	1092.04	1010.60
-2.51	1152.83	1162.50	1168.80	1139.11	1055.18
-2.70	1193.52	1202.65	1208.23	1175.83	1090.81
-2.89	1233.14	1241.64	1246.39	1211.30	1125.93
-3.08	1262.38	1270.19	1274.10	1236.86	1152.17
-3.28	1287.20	1294.19	1297.15	1257.91	1174.74
-3.47	1302.89	1308.98	1310.97	1270.25	1189.74
-3.66	1316.02	1321.18	1322.19	1280.24	1202.93
-3.85	1319.94	1324.12	1324.16	1281.59	1208.56
-4.04	1320.37	1323.57	1322.66	1279.81	1211.48
-4.24	1311.69	1313.90	1312.09	1269.67	1206.77
-4.43	1300.36	1301.58	1298.89	1257.32	1200.17
-4.62	1282.69	1283.04	1279.64	1239.55	1188.06
-4.81	1259.83	1259.29	1255.20	1217.18	1171.92
-5.00	1232.25	1230.98	1226.35	1190.88	1151.56
-5.20	1200.78	1198.85	1193.72	1161.29	1128.20
-5.39	1164.66	1162.21	1156.73	1127.59	1100.46

-5.58	1124.87	1121.96	1116.18	1090.66	1069.63
-5.77	1082.89	1079.69	1073.78	1051.72	1036.22
-5.96	1037.80	1034.42	1028.50	1009.95	999.98
-6.16	990.76	987.39	981.74	966.28	961.05
-6.35	941.96	938.67	933.50	921.03	920.24
-6.54	894.31	891.13	886.51	876.69	879.47
-6.73	843.52	840.49	836.50	829.39	835.53
-6.92	794.62	791.75	788.32	783.65	792.52
-7.12	745.23	742.51	739.64	737.37	748.75
-7.31	696.08	693.50	691.12	691.03	704.47
-7.50	650.15	647.71	645.75	647.68	662.93
-7.69	601.63	599.36	597.79	601.63	618.41
-7.88	557.89	555.78	554.54	560.14	578.25
-8.08	513.75	511.82	510.85	518.01	537.16
-8.27	472.10	470.34	469.58	478.17	498.18
-8.46	430.00	428.42	427.81	437.68	458.30
-8.65	391.51	390.08	389.56	400.51	421.54
-8.84	352.55	351.27	350.77	362.63	383.92
-9.04	317.02	315.87	315.37	327.97	349.38
-9.23	281.25	280.23	279.69	292.83	314.16
-9.42	248.64	247.72	247.14	260.71	281.88
-9.61	215.75	214.94	214.30	228.18	249.03
-9.81	185.74	185.02	184.37	198.51	218.99
-10.00	155.79	155.18	154.63	169.09	188.99
-10.19	128.20	127.68	127.41	142.28	161.50
-10.39	104.11	103.70	103.89	118.95	137.36
-10.58	81.70	81.38	82.09	97.22	114.73
-10.77	62.78	62.54	63.71	78.63	95.15
-10.97	44.88	44.73	46.34	60.90	76.40
-11.16	30.27	30.18	32.11	46.19	60.72
-11.35	16.98	16.96	19.12	32.67	46.23
-11.54	5.43	5.45	7.75	20.65	33.18
-11.73	-4.15	-4.08	-1.74	10.56	22.12
-11.93	-12.59	-12.49	-10.19	1.39	11.93
-12.12	-19.38	-19.25	-17.05	-6.13	3.50
-12.31	-25.11	-24.95	-22.91	-12.71	-4.04
-12.50	-29.64	-29.46	-27.59	-18.06	-10.28
-12.69	-33.23	-33.04	-31.37	-22.59	-15.74
-12.89	-35.92	-35.73	-34.23	-26.16	-20.16
-13.08	-37.85	-37.65	-36.34	-29.06	-23.92
-13.27	-39.10	-38.91	-37.76	-31.19	-26.80
-13.46	-39.69	-39.50	-38.51	-32.69	-29.06
-13.65	-39.90	-39.71	-38.85	-33.70	-30.78

-13.85	-39.56	-39.37	-38.63	-34.16	-31.93
-14.04	-38.94	-38.76	-38.12	-34.28	-32.72
-14.23	-37.90	-37.72	-37.20	-33.98	-33.09
-14.42	-36.73	-36.57	-36.14	-33.47	-33.20
-14.61	-35.19	-35.04	-34.70	-32.58	-32.92
-14.81	-33.69	-33.55	-33.29	-31.64	-32.51
-15.00	-31.86	-31.74	-31.56	-30.39	-31.85
-15.19	-30.14	-30.04	-29.92	-29.16	-31.14
-15.38	-28.21	-28.13	-28.06	-27.69	-30.21
-15.57	-26.40	-26.33	-26.32	-26.28	-29.29
-15.77	-24.42	-24.37	-24.40	-24.66	-28.13
-15.96	-22.55	-22.51	-22.57	-23.09	-26.98
-16.15	-20.68	-20.66	-20.75	-21.48	-25.80
-16.34	-18.92	-18.91	-19.02	-19.94	-24.65
-16.53	-17.10	-17.11	-17.25	-18.33	-23.42
-16.73	-15.48	-15.50	-15.67	-16.89	-22.32
-16.92	-13.79	-13.83	-14.02	-15.33	-21.06
-17.11	-12.29	-12.35	-12.55	-13.93	-19.89
-17.30	-10.82	-10.89	-11.09	-12.51	-18.68
-17.49	-9.48	-9.56	-9.77	-11.23	-17.54
-17.69	-8.16	-8.26	-8.47	-9.94	-16.35
-17.88	-7.01	-7.11	-7.33	-8.79	-15.21
-18.07	-5.88	-5.99	-6.20	-7.64	-13.92
-18.26	-4.91	-5.02	-5.22	-6.63	-12.72
-18.45	-3.98	-4.09	-4.29	-5.65	-11.40
-18.65	-3.19	-3.31	-3.50	-4.80	-10.17
-18.84	-2.43	-2.56	-2.74	-3.98	-8.85
-19.03	-1.83	-1.96	-2.14	-3.31	-7.55
-19.22	-1.26	-1.40	-1.57	-2.66	-5.84
-19.41	-0.83	-0.95	-1.10	-2.05	-4.15
-19.61	-0.44	-0.54	-0.66	-1.38	-3.05
-19.80	-0.17	-0.22	-0.29	-0.67	-1.97
-20.00	0.00	0.00	0.00	0.00	0.00

K. For D=1.00m

Depth[m]	Prescribed displacement [Phase_2] [kN m]	Combined 0.25vult [Phase_3] [kN m]	Combined 0.5vult [Phase_4] [kN m]	Combined 0.75vult [Phase_5] [kN m]	Combined 1vult [Phase_6] [kN m]
0.00	0.00	0.00	0.00	0.00	0.00
-0.25	313.24	317.70	321.53	318.44	304.23
-0.51	594.16	602.53	609.67	602.96	575.49

-0.76	898.77	911.19	921.74	910.00	867.47
-1.01	1160.19	1175.86	1189.06	1171.13	1114.49
-1.26	1432.72	1451.57	1467.26	1441.34	1368.93
-1.51	1665.58	1686.82	1704.24	1669.71	1582.93
-1.76	1906.43	1929.78	1948.63	1903.74	1801.64
-2.01	2111.58	2136.20	2155.63	2099.98	1985.36
-2.26	2303.38	2328.71	2348.13	2280.88	2154.87
-2.51	2475.41	2500.84	2519.66	2440.67	2305.53
-2.76	2640.84	2665.97	2683.77	2592.77	2449.79
-3.01	2774.34	2798.75	2815.21	2713.55	2565.98
-3.26	2905.81	2929.16	2943.90	2831.28	2680.68
-3.51	3004.79	3026.76	3039.55	2917.97	2767.05
-3.76	3106.14	3126.42	3136.87	3006.11	2856.21
-4.00	3178.75	3197.12	3205.18	3067.40	2920.66
-4.25	3239.40	3255.64	3261.14	3117.53	2975.36
-4.50	3277.27	3291.18	3294.05	3146.86	3011.09
-4.75	3308.47	3320.06	3320.40	3170.88	3041.84
-5.00	3317.28	3326.39	3324.16	3174.86	3054.33
-5.25	3316.16	3322.89	3318.28	3170.75	3058.92
-5.50	3296.25	3300.60	3293.78	3150.49	3048.24
-5.75	3265.96	3268.02	3259.14	3121.75	3029.40
-6.00	3215.46	3215.42	3204.77	3075.36	2993.41
-6.25	3159.47	3157.48	3145.20	3024.82	2953.35
-6.50	3082.97	3079.29	3065.61	2955.92	2895.23
-6.75	3005.80	3000.68	2985.74	2886.88	2836.48
-7.00	2909.53	2903.27	2887.30	2800.41	2760.40
-7.25	2809.52	2802.39	2785.47	2710.86	2681.09
-7.50	2707.39	2699.78	2682.27	2618.97	2598.21
-7.75	2590.16	2582.33	2564.51	2512.82	2501.09
-8.00	2463.72	2455.94	2438.26	2397.40	2393.70
-8.25	2349.24	2341.60	2324.17	2293.03	2296.30
-8.50	2218.95	2211.57	2194.51	2173.42	2183.22
-8.75	2098.02	2090.92	2074.13	2062.18	2077.58
-9.00	1966.08	1959.30	1942.71	1939.99	1960.57
-9.25	1845.07	1838.60	1822.09	1827.85	1852.98
-9.50	1713.80	1707.69	1691.26	1705.45	1734.85
-9.75	1593.53	1587.73	1571.47	1593.20	1626.28
-10.00	1466.74	1461.32	1445.86	1474.66	1510.90
-10.25	1338.87	1333.85	1320.15	1355.59	1394.57
-10.51	1226.05	1221.48	1210.22	1250.22	1290.85
-10.76	1105.82	1101.80	1093.70	1137.74	1179.69
-11.01	1001.85	998.31	993.04	1039.72	1082.32
-11.26	894.68	891.62	889.37	938.36	981.42

-11.50	801.27	798.62	798.94	849.32	892.47
-11.75	708.49	706.22	709.16	760.69	803.82
-12.00	626.70	624.73	629.85	681.78	724.57
-12.25	546.70	545.02	552.18	604.17	646.49
-12.50	475.45	474.03	482.80	534.32	576.01
-12.75	410.34	409.13	419.23	470.01	510.98
-13.00	348.77	347.76	358.87	408.49	448.62
-13.25	295.41	294.57	306.44	354.88	394.28
-13.50	246.70	246.01	258.33	305.30	343.90
-13.75	202.26	201.71	214.28	259.71	297.50
-14.00	163.19	162.76	175.35	219.08	256.10
-14.25	129.31	129.01	141.45	183.50	219.75
-14.50	97.82	97.63	109.72	149.87	185.25
-14.75	72.52	72.42	84.07	122.54	157.13
-15.00	49.19	49.17	60.16	96.79	130.51
-15.25	30.69	30.75	41.07	76.13	109.19
-15.50	14.41	14.51	23.95	57.24	89.38
-15.75	1.27	1.39	9.92	41.63	72.99
-15.99	-9.11	-8.98	-1.42	28.66	59.13
-16.24	-17.43	-17.29	-10.69	17.78	47.30
-16.49	-23.35	-23.22	-17.52	9.28	37.64
-16.74	-27.57	-27.45	-22.57	2.63	29.89
-16.99	-29.92	-29.80	-25.65	-2.17	23.60
-17.24	-31.00	-30.89	-27.38	-5.61	18.51
-17.49	-30.65	-30.56	-27.60	-7.60	14.61
-17.74	-29.36	-29.29	-26.81	-8.65	11.32
-17.99	-27.13	-27.10	-25.03	-8.70	8.70
-18.24	-24.21	-24.21	-22.49	-8.09	6.10
-18.49	-20.81	-20.83	-19.38	-6.89	3.45
-18.74	-17.14	-17.18	-15.96	-5.44	0.45
-18.99	-13.14	-13.21	-12.18	-3.87	-2.21
-19.24	-9.40	-9.53	-8.72	-2.89	-4.04
-19.49	-5.72	-6.05	-5.63	-2.93	-4.73
-19.74	-2.29	-2.13	-1.49	1.20	3.55
-20.00	0.00	0.00	0.00	0.00	0.01

L. **For D=1.25m**

Depth [m]	Prescribed displacement [Phase_2] [kN m]	0.25Vult [Phase_3] [kN m]	0.5Vult [Phase_4] [kN m]	0.75Vult [Phase_5] [kN m]	1Vult [Phase_6] [kN m]
0.00	0.00	0.00	0.00	0.00	0.00
-0.32	645.71	656.03	664.34	653.59	630.46
-0.64	1233.72	1253.43	1269.03	1246.76	1201.90
-0.95	1856.32	1885.50	1908.05	1870.76	1801.58
-1.26	2404.94	2441.66	2469.01	2413.96	2322.30
-1.57	2949.52	2992.97	3023.91	2946.92	2830.76
-1.88	3447.61	3496.06	3528.65	3426.98	3287.77
-2.20	3923.55	3975.71	4008.49	3879.99	3718.62
-2.51	4353.32	4407.33	4438.27	4281.37	4101.86
-2.82	4757.20	4811.90	4839.70	4653.41	4458.47
-3.13	5115.33	5169.47	5192.81	4977.59	4771.30
-3.44	5448.56	5501.39	5519.47	5275.96	5060.67
-3.76	5735.14	5785.74	5797.97	5529.71	5309.08
-4.07	6004.33	6052.02	6057.77	5766.50	5542.46
-4.38	6217.11	6261.16	6260.23	5951.30	5727.53
-4.69	6419.32	6459.01	6450.70	6125.89	5904.51
-5.00	6559.06	6594.01	6578.58	6244.17	6028.50
-5.31	6687.55	6717.09	6694.01	6352.68	6144.55
-5.63	6765.75	6789.98	6759.97	6417.64	6218.43
-5.94	6812.33	6831.05	6794.39	6455.43	6266.43
-6.25	6816.16	6829.24	6786.44	6456.73	6279.68
-6.56	6807.93	6815.69	6767.32	6449.53	6284.49
-6.87	6754.78	6757.52	6704.36	6404.12	6252.24
-7.19	6676.07	6674.03	6616.46	6336.94	6198.62
-7.50	6562.94	6556.85	6495.73	6239.89	6115.01
-7.81	6434.24	6424.31	6359.75	6130.35	6019.25
-8.12	6275.51	6262.50	6195.30	5993.61	5895.63
-8.43	6098.81	6083.24	6013.67	5840.56	5755.37
-8.75	5882.32	5864.97	5793.48	5650.06	5577.37
-9.06	5685.64	5667.07	5593.97	5477.35	5415.52
-9.37	5438.82	5419.53	5345.79	5256.85	5205.55
-9.69	5215.72	5195.99	5122.09	5056.85	5013.97
-10.00	4943.51	4923.63	4850.39	4808.70	4773.37
-10.32	4680.04	4660.06	4588.21	4566.12	4536.31
-10.63	4398.70	4378.78	4310.47	4303.51	4276.42
-10.94	4112.01	4092.48	4028.98	4034.77	4008.59
-11.25	3826.34	3807.61	3750.08	3765.09	3737.95
-11.57	3541.30	3523.67	3472.78	3495.01	3465.15

-11.88	3264.78	3248.56	3204.29	3230.75	3196.63
-12.19	2998.31	2983.57	2945.74	2974.48	2935.00
-12.50	2730.71	2717.47	2685.72	2714.39	2668.44
-12.81	2479.13	2467.24	2441.03	2468.10	2414.82
-13.12	2251.30	2240.48	2218.79	2242.51	2181.71
-13.44	2023.07	2013.12	1995.61	2014.54	1945.47
-13.75	1807.42	1797.98	1783.93	1796.53	1718.89
-14.06	1611.65	1602.42	1591.16	1596.57	1510.32
-14.37	1426.44	1417.12	1407.88	1405.09	1310.85
-14.68	1256.63	1247.10	1239.24	1227.86	1126.29
-14.99	1096.57	1086.69	1079.45	1058.62	950.40
-15.30	953.01	942.73	935.43	905.17	791.22
-15.62	822.35	811.59	803.34	763.65	645.70
-15.93	700.46	689.15	679.33	630.24	509.62
-16.24	594.07	582.20	570.30	512.85	392.34
-16.55	494.83	482.36	467.94	402.56	284.13
-16.86	410.10	397.08	379.99	308.73	196.08
-17.17	331.34	317.77	297.80	221.91	118.04
-17.49	265.80	251.78	229.05	151.21	59.06
-17.80	205.84	191.38	165.88	88.32	9.92
-18.11	155.71	140.94	113.25	38.84	-25.87
-18.42	113.19	98.32	69.05	-1.95	-56.73
-18.73	76.38	61.75	31.64	-36.96	-87.89
-19.04	47.41	34.31	5.50	-58.06	-105.40
-19.36	23.44	15.53	-6.35	-54.93	-92.49
-19.68	5.54	-3.19	-20.78	-59.36	-95.26
-20.00	0.00	0.00	0.00	0.00	0.00